Riparian Nitrogen Cycling and Stream Evolution: Measuring and Modeling the Effects of Channel Incision on Groundwater Dynamics and Denitrification

by

DANIEL XAVIER BUHR

(Under the Direction of Brian Bledsoe)

ABSTRACT

Nitrogen pollution in groundwater and surface water can cause eutrophication and harmful algal blooms in receiving waterbodies. Riparian zones can effectively reduce nitrogen loading via denitrification, the conversion of nitrate to nitrogen gas under saturated, anoxic conditions with sufficient carbon. Stream incision can reduce denitrification by lowering groundwater below the carbon-rich root zone. Few studies have characterized the interactions between stream incision and riparian processes, which are also often underrepresented in models. The goal of this research is to further investigate the role of incision on riparian groundwater dynamics and nitrogen cycling by analyzing existing models and collecting field data in watersheds with contrasting soil types and land uses, then coupling denitrification and channel evolution models to estimate long-term changes in nitrogen loading.

I evaluated well-known riparian nitrogen models for their robustness in simulating hydrologic processes, vegetation, soils, nutrients, and channel morphodynamics. I performed global, time-varying sensitivity analyses of the Riparian Ecosystem Management Model (REMM) and the Soil and Water Assessment Tool+ (SWAT+) and found that soil and

topographic parameters were most influential for estimating groundwater and nitrogen dynamics. The influence of stream channel depth and incision was underrepresented in all models.

I collected a novel dataset by studying groundwater-surface water interactions and nitrogen dynamics at paired incised and unincised streams at two sites in the southeastern US. Incision lowered the riparian groundwater table and affected the gaining and losing dynamics at each stream. Denitrification was prevalent, removing an estimated 40-95% of available nitrogen. I developed statistical models to predict groundwater depth and denitrification for both the overall dataset and individual sites. I simulated channel morphodynamics over 30 years at each site using the River Erosion Model (REM) and linked the results with the statistical models to estimate the long-term effects of incision on network-scale riparian nitrogen loading. The results of this research indicate that incision can substantially increase long-term nitrate loading in small watersheds, underscore the importance of flow management and stream restoration for water quality improvement, and illustrate the need for fully-coupled channel evolution and riparian nitrogen models to improve estimation of nitrogen loading in evolving stream networks.

INDEX WORDS: Riparian zones, channel incision, nitrogen cycling, groundwater, denitrification

Riparian Nitrogen Cycling and Stream Evolution: Measuring and Modeling the Effects of Channel Incision on Groundwater Dynamics and Denitrification

by

DANIEL XAVIER BUHR

BS, Michigan State University, 2017

A Dissertation Submitted to the Graduate Faculty of The University of Georgia in Partial Fulfillment of the Requirements for the Degree

DOCTOR OF PHILOSOPHY

ATHENS, GEORGIA

2023

Riparian Nitrogen Cycling and Stream Evolution: Measuring and Modeling the Effects of Channel Incision on Groundwater Dynamics and Denitrification

by

DANIEL XAVIER BUHR

Major Professor:	Brian Bledsoe
Committee:	Rhett Jackson
	Ernest Tollner
	Brock Woodson

Electronic Version Approved:

Ron Walcott
Vice Provost for Graduate Education and Dean of the Graduate School
The University of Georgia
May 2023

ACKNOWLEDGEMENTS

I am incredibly grateful for the countless individuals who have supported me throughout this journey. My major professor, Brian Bledsoe, has been an exceptional mentor during my time at UGA. His guidance and breadth of knowledge have honed my personal and professional skills and prepared me for my career. I cannot thank him enough for the opportunities he has given me. My committee members have provided instruction and advice that has enriched my educational experience and strengthened this research. Dean Fletcher at Savannah River Ecology Laboratory garnered financial support for this research and assisted in selecting a field site. Rod Lammers offered valuable mentorship about modeling, coding, and general research ideas. My peers have shared in the triumphs and struggles of graduate school, providing camaraderie and challenging me to think more critically. I appreciate all my colleagues who have assisted with field work, especially Will Mattison, Matthew Thibodeaux, Rod Lammers, and Matt Chambers, who contributed sweat equity in digging groundwater wells. My parents have taught me to value hard work and education, instilled in me a passion for science and the environment, and provided me with opportunities to pursue my dreams. I will be forever indebted to them for this and for their unconditional support. My sisters have been a continuous source of love, motivation, and necessary distractions to keep me focused yet grounded. I am grateful to so many of my other family and friends for their support throughout this process, whether it be notes or treats in the mail, messages of encouragement, or sharing in sports, music, and outdoor adventures. Finally, I would like to thank my fiancée Michelle for her constant love and support that make all the hard work that went into this accomplishment worthwhile.

TABLE OF CONTENTS

LIST OF TABLES

Page

LIST OF FIGURES

Page

CHAPTER 1

INTRODUCTION AND LITERATURE REVIEW

Introduction

Nitrogen (N) pollutant loading is one of the most challenging, widespread, and costly global environmental problems today (Howarth et al., 2011; Howarth, 2008), and improved understanding is needed to inform management strategies. Anthropogenic activities have significantly altered the global nitrogen cycle and increased N loading to terrestrial and aquatic systems, which degrades their ecological integrity and limits provisioning of beneficial services (Mueller et al., 1995; Quinn, 1991; Vitousek et al., 1997). Protection and restoration of riparian areas is a widely-accepted strategy for reducing nitrogen loading to aquatic systems (Naiman et al., 2010), as many studies have confirmed their efficacy for removing nutrients, particularly dissolved nitrate in runoff and groundwater (e.g., Hill, 2019; Mulholland et al., 2008; Peterjohn and Correll, 1984). The primary biological process by which riparian zones remove nitrogen is denitrification, an anoxic process in which microbes convert nitrate to inert dinitrogen gas using organic soil carbon. Therefore, locations where the riparian water table intersects relatively high levels of carbon in the root zone become hotspots for biogeochemical cycling, offering the greatest potential to reduce nitrate loading to streams.

In addition to increased nutrient loading, land development and conversion due to urban and agricultural practices can also generate erosive flows that trigger stream channel instability (Booth, 1990; Jacobson et al., 2001). Disturbed, unstable streams generally exhibit altered morphology that follows one of many paths, deepening (incising) and widening before

transitioning to an entrenched channel with an inset floodplain (Booth and Fischenich, 2015; Schumm et al., 1984). Recent channel evolution models have incorporated biological considerations as a means to quantify changes in ecological conditions such as nutrient loading as a channel incises (Castro and Thorne, 2019; Cluer and Thorne, 2014). The interaction between stream instability and nitrogen pollutant loading is poorly understood and requires further study. Studies have documented lowered riparian water tables adjacent to incised streams (Groffman et al., 2002; Hardison et al., 2009; Schilling et al., 2006), but data showing the influence of incision on nitrogen removal are scarce (Böhlke et al., 2007; Groffman et al., 2002; Mayer et al., 2010; Schilling et al., 2006). Further study of the connections between stream incision and riparian nitrogen cycling is needed to advance scientific understanding of the fluvial ecohydrological and biogeochemical repercussions of human influences.

Several models exist for evaluating the influence of riparian zones on nitrogen loading to streams, ranging from field-scale models specifically for riparian zones to watershed-scale models that include riparian processes (Arnold et al., 1998; Bieger et al., 2017; Lowrance et al., 2000; Wei et al., 2019). A major deficiency in all of these riparian nitrogen models is a lack of adequate coupling among fluvial processes and nitrogen dynamics, particularly interactions among channel evolution, riparian hydrology, and nutrient cycling. Although there are existing tools for simulating channel evolution (Lammers and Bledsoe, 2018; Langendoen and Alonso, 2008; Langendoen and Simon, 2008; Simon et al., 2011, 2000), efforts to integrate them with riparian nitrogen models has omitted nitrogen loading (Langendoen et al., 2005). Accordingly, there is a need for a robust, watershed-scale modeling tool that accurately simulates dynamics between riparian biogeochemistry and stream incision, yet is parsimonious in its complexity and data requirements. Such a tool could assist water resources managers in identifying locations

where channel incision causes a disproportionately large amount of nitrogen to enter stream networks, and guide spatial prioritization of practices for reducing channel erosion, nitrogen loading, and downstream eutrophication.

The goal of this research is to investigate the role of stream incision on riparian groundwater and nitrogen dynamics. I accomplished this by analyzing existing models and collecting field data in small watersheds with contrasting soil types and land uses to inform a novel coupling of denitrification and channel evolution models to estimate long-term changes in nitrogen loading. Three objectives are met to achieve the research goal:

1. Identify and evaluate existing mechanistic riparian nitrogen models, recognizing the strengths and weaknesses of each, and then use a time-varying, global sensitivity analysis to evaluate model structure and function in select models;
2. Collect a novel dataset describing groundwater-surface water interactions and riparian nitrogen cycling at paired incised and unincised streams in two watersheds in the southeast US, and explore variability and relationships within the dataset; and
3. Develop parsimonious statistical models to simulate groundwater depth and denitrification, and couple them with the River Erosion Model (REM) to estimate long-term effects of stream incision on nitrogen loading.

In this and the following section, I introduce the layout of the dissertation and provide a literature review relevant to the goals and objectives. Each of the following three chapters is a journal article that focuses on one of the forgoing objectives, one of which has been published and two that are in the submission process. The first article evaluates well-known riparian nitrogen models and describes global, time-varying sensitivity analyses of two key models, the Riparian Ecosystem Management Model (REMM) and the Soil and Water Assessment Tool+

(SWAT+). The second article details field data collection at two sites with paired incised and unincised streams, highlighting relationships among incision, groundwater-surface water dynamics, and denitrification. The third article describes the development of statistical models to predict groundwater dynamics and denitrification, and couples them to long-term simulations with the River Erosion Model (REM) to estimate changes in nitrogen loading in incising stream networks.

Literature Review

Eutrophication due to anthropogenic nutrient pollution is among the most substantial issues facing society today. Greater than 40% of streams in the United States are unsuitable for drinking and other beneficial uses as a result of nutrient pollution (U.S. EPA, 2016). Furthermore, the functions and services of downstream receiving waterbodies are increasingly degraded by algal blooms and other direct consequences of nutrient pollution (Howarth et al., 2011). Phosphorus and nitrogen are nutrients of particular concern due to their propensity to naturally limit primary production in marine and aquatic environments. Commonly identified point and non-point sources of these nutrients include wastewater treatment plants, urban stormwater, and agricultural runoff, which is considered the most prevalent source of nitrogen and phosphorus to coastal waters (Howarth et al., 2002).

As urban development and human population growth continue, necessitating demand for agricultural commodities, nutrient loading to terrestrial and aquatic systems will likely increase. The amount of reactive nitrogen on Earth has more than doubled, primarily due to food and energy production (Galloway et al., 2004). Most nitrogen exists as nitrogen gas (N_2), an inert gas that composes 78% of the atmosphere. N_2 can be converted to a usable form like organic nitrogen or ammonium (NH_4^+) by nitrogen fixation, a process that occurs both biologically by

soil microbes and industrially through the Haber-Bosch process (Smil, 2001; Stein and Klotz, 2016). Ammonium can also be derived from organic nitrogen via microbial-mediated mineralization, or ammonification (Alexander, 1977). Bacteria such as *Nitrosomonas* and *Nitrobacter* convert ammonium to the more hydrophilic nitrate (NO_3^-) through nitrification (Gee et al., 1990). Nitrate has three major fates in a riparian zone: biological uptake by vegetation and soil organisms, leaching to surface water, or denitrification, if conditions are right (Pinay et al., 2018). These conditions include low oxygen and an organic carbon source – usually from riparian vegetation. This combination encourages denitrification – the reduction of NO_3^- to N_2O or N_2 gas by heterotrophic bacteria (Hill, 1996). Denitrification is a desirable process for pollution control because it permanently removes nitrogen from the aquatic system, transferring it in an inert form to the atmosphere. This process, however, may have detrimental side effects, namely the production of N_2O – a highly potent greenhouse gas (Burgin and Groffman, 2012). Finally, dissimilatory nitrate reduction to ammonium (DNRA) is a method in which nitrate can be converted to ammonium by bacteria and fungi (Stein and Klotz, 2016), then either assimilated by biota or converted to N_2 via anaerobic ammonium oxidation (anammox), which is believed to have a relatively minimal role in soils (Hamilton et al., 2016).

Dissolved nitrate is an especially insidious pollutant because it is rapidly transported through groundwater and surface water and causes a variety of environmental problems – from contaminating drinking water to eutrophication and associated algal blooms. In the U.S., nitrogen pollution is blamed for degraded coastal water quality, including the “dead zone” in the Gulf of Mexico. Nitrogen runoff from agricultural and urban areas is transported through river networks to the coast, where it triggers algal blooms that kill marine life and impair ecosystem function. Still, less nitrogen reaches the coasts than is applied to land surfaces, suggesting that streams and

riparian zones are actually acting as significant nutrient sinks (Peterson et al., 2001). Several large studies (including the Lotic Intersite Nitrogen eXperiment – LINX) have attempted to quantify nutrient retention and uptake in streams (Mulholland et al., 2008, 2004; Webster et al., 2003), finding that nitrate removal can be significant. Furthermore, nitrogen removal in riparian zones has long been an area of research, often with the goal of restoring riparian functions to treat agricultural runoff (e.g., Hill, 1979, 1996; Lowrance, 1992).

Riparian zones can be especially effective nitrate sinks (Mulholland et al., 2008; Orr et al., 2007; Peterson et al., 2001), and may contribute more to nitrogen removal than in-stream processes (Craig et al., 2008; Lammers and Bledsoe, 2017). It is therefore vital to study functioning of riparian systems in smaller watersheds (~1-100 km^2), which likely play a significant role in cumulative nitrogen removal. Under the right conditions for denitrification, riparian buffers can remove greater than 90% of the nitrate in inflowing groundwater (Peterjohn and Correll, 1984; Pinay et al., 1993; Spruill, 2000). Despite the importance of this process, denitrification is notoriously difficult to measure (Groffman et al., 2006), and can occur sporadically in space and time when conditions are favorable (McClain et al., 2003). This makes it difficult to assess just how significant riparian denitrification is in controlling nitrogen export from small watersheds.

Groundwater-surface water interactions at the riparian-stream interface are important to understand because inputs of groundwater, nutrients, organic matter, and other solutes to streams sustain stream baseflow, primary productivity, metabolism, temperature buffering, and ecological and bacterial community composition (Brunke and Gonser, 1997; Holmes, 2000). Conversely, stream inputs to the local aquifer can provide recharge and enhance biogeochemical cycling (Brunke and Gonser, 1997). Groundwater-surface water interactions have been studied

arduously in recent decades, with focus on varying spatial scales and measurement techniques (Jimenez-Fernandez et al., 2022). Improved understanding of the spatiotemporal patterns of groundwater-surface water exchange is useful for assessing in-stream water quality patterns (Covino and McGlynn, 2007; Jimenez-Fernandez et al., 2022; Ranalli and Macalady, 2010). Continuing to evaluate these interactions is critical for water resources management and restoration efforts.

Streams can be classified as gaining or losing, depending on the direction of the groundwater-surface water exchange. Gaining streams receive flow from adjacent groundwater, due to a hydraulic gradient toward the stream, while losing streams have a reversed hydraulic gradient, with water leaving the stream. Gaining and losing conditions can vary spatially and temporally (Cardenas, 2009; Gordon et al., 2004; Wroblicky et al., 1998). Perennial streams are primarily gaining, although analysis of 4.2 million wells in the contiguous USA showed a losing hydraulic gradient for the nearest stream in two-thirds of cases (Jasechko et al., 2021). Both field and modeling studies have observed seasonal variability in gaining and losing conditions (Jimenez-Fernandez et al., 2022; Krause et al., 2007; Zimmer and McGlynn, 2017), with gaining becoming more prevalent when precipitation increases or streamflow decreases (Zhang et al., 2021). Spatially, streams can be net losing or gaining at the watershed scale, yet alternate between gaining and losing reaches (Essaid and Caldwell, 2017). Many stream reaches experience concurrent gains and losses, so only considering the net result is an incomplete representation (Covino et al., 2011; Covino and McGlynn, 2007; Payn et al., 2009).

Gaining and losing conditions have variable effects on the transfer of solutes such as nitrogen between the local aquifer and surface water. Both gaining and losing can be beneficial for nitrogen attenuation in streams, as they allow for dilution from influent groundwater and

efflux into the streambed and riparian zone for denitrification, respectively (Jimenez-Fernandez et al., 2022; Ruehl et al., 2007). However, if a stream has higher nitrogen concentrations than the groundwater, then losing can contaminate the groundwater (Kayabalı et al., 1999; Lasagna et al., 2016). Conversely, where groundwater has more nitrogen than the stream and does not flow through a denitrifying environment, gaining conditions can impair local and downstream water quality (Böhlke and Denver, 1995; Lasagna et al., 2016). Modeling has shown that a losing river can have a larger nitrate removal rate than a gaining river, indicating that conditions that drive losing may create denitrification hot spots (Shuai et al., 2017).

Various controls on groundwater-surface exchange include climate, topography, geology, and watershed position (Sophocleous, 2002; Winter, 1999). Climate affects groundwater flow, as precipitation is the dominant source of recharge. Conceptual models of stream-groundwater interactions have long suggested that water tables mirror surface topography, including recent studies that have specified longitudinal valley gradient as a useful predictor of riparian flow direction (Voltz et al., 2013). Local geology controls the depth and distribution of subsurface flow, while position of a stream within the watershed can affect whether it is losing or gaining, and if it is connected to a local or regional flow system (Winter, 1999). These controls combine to influence the magnitude and direction of surface water-groundwater interactions. For example, losing rivers are more prevalent in drier climates, flatter regions, and areas with considerable groundwater pumping (Jasechko et al., 2021), while gaining streams are more common in wetter areas and in valleys near mountains (de Graaf et al., 2019).

Stream geomorphology can play an important – and largely overlooked – role in groundwater-surface water interactions and riparian denitrification processes. Channel incision, or vertical downcutting via bed erosion, is commonplace (e.g., Booth, 1990; Groffman et al.,

2002; Schilling et al., 2006; Simon and Robbins, 1987), as a result of channel straightening or land use changes (Shields et al., 2010). Riparian denitrification is highest when nitrate-rich groundwater intersects the organic carbon-rich rooting zone of riparian vegetation (Hill, 1996). Streams that incise show subsequently lowered riparian groundwater tables (Hardison et al., 2009; Figure 1.1). This disconnects riparian groundwater from the carbon-rich rooting zone, limiting denitrification and potentially increasing nitrate loading to streams (Groffman et al., 2002; Mayer et al., 2010).

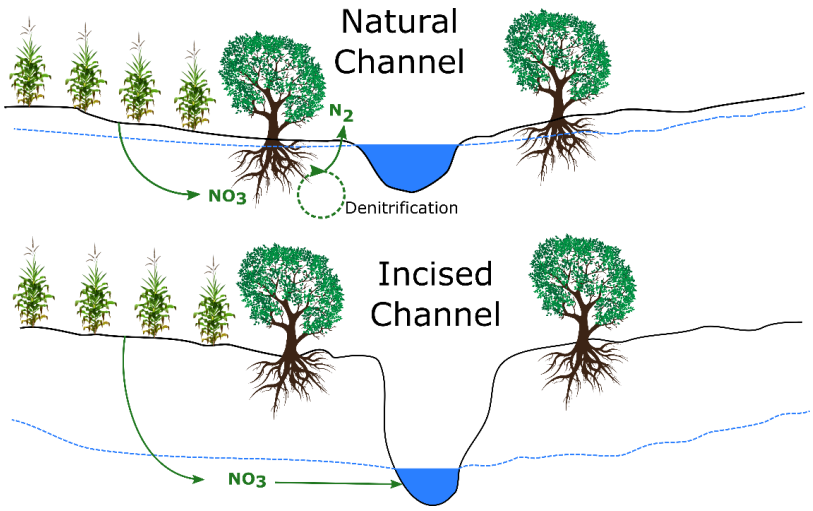

Figure 1.1. Riparian denitrification in a natural riparian zone, with nitrate-rich groundwater intersecting organic carbon-rich surface soils. This connection is lost when the channel incises, lowering groundwater tables below the rooting zone of riparian vegetation. Adapted from Groffman et al. (2003).

Others have made the connection between channel incision and riparian denitrification. Groundwater tables are significantly lower in riparian zones adjacent to incised streams (Hardison et al., 2009; Schilling and Jacobson, 2014). These lower water tables create a larger unsaturated zone, disconnecting groundwater from carbon-rich surface soils, limiting denitrification and increasing nitrate loading to streams (Böhlke et al., 2007; Gift et al., 2010; Groffman et al., 2002; Mayer et al., 2010). Larger unsaturated zones near the stream can also lead to nitrate production via nitrification (Schilling et al., 2006). This means that channel

incision may not only be limiting the ability of the riparian zone to act as a nitrogen sink, it may be converting it to a net nitrate source. While these studies are valuable, they only scratch the surface on the influence of stream incision on riparian denitrification.

Understanding how and why channels evolve morphodynamically is therefore important for understanding how these channel changes impact riparian denitrification. Stream channels can be destabilized by alterations to watershed hydrology and/or sediment supply, both common side effects of land use changes such as urbanization (Poff et al., 2006). These changes (e.g., larger and more frequent high flows) cause channel bed and bank erosion as the stream adjusts to the new hydrologic and sediment regime. This "channel evolution" can follow a generally predictable pattern (Schumm et al., 1984; Simon, 1989). Initially the stream incises (deepens), which increases the height and angle of the banks. These banks become unstable and collapse, leading to channel widening. Eventually, the channel may re-stabilize, although it will be deeper and wider than before, and likely have lost the hydrologic connection to its floodplain. These changes happen through time at an individual channel cross-section, but also occur spatially throughout a drainage network (Figure 1.2). Incision may begin downstream, with this disturbance migrating upstream at a headcut, or abrupt drop in the channel bed.

Although many variations on this conceptual channel evolution model have been developed (Booth and Fischenich, 2015; Cluer and Thorne, 2014; Hawley et al., 2012), the general processes remain the same. Also, while forest clearing and impervious surfaces are common causes of channel degradation (Booth, 1990), other disturbances can destabilize channels as well. For example, channel straightening was a common practice in both urban and agricultural areas to improve drainage efficiency, and led to similar sequences of channel evolution (Simon and Darby, 2002; Simon and Robbins, 1987). Incised stream channels are

therefore widespread (e.g., Booth, 1990; Groffman et al., 2002; Schilling et al., 2006; Simon and Robbins, 1987), but the effects of this channel degradation on nutrient cycling remain unclear.

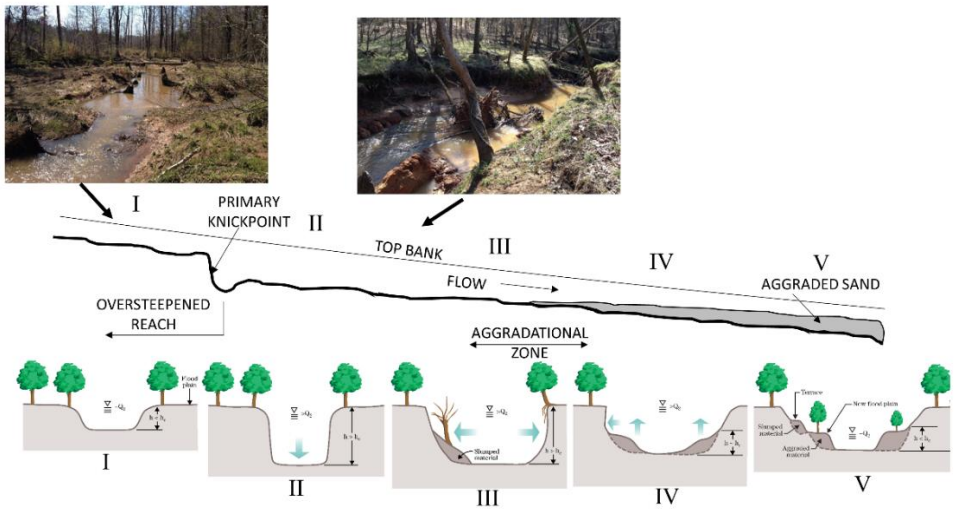

Figure 1.2. Conceptual channel evolution model showing changes at a cross section over time (bottom) and how these changes are distributed upstream to downstream along a channel (middle). Top photos show examples of a Stage I reach (left) and a stage II-III reach immediately downstream. The two reaches are separated by a ~ 1 m tall headcut and illustrate how significantly channel geometry can differ over relatively small spatial scales. Adapted from NRCS (2007) and Schumm et al. (1984).

Studies on the effects of incision on riparian denitrification have largely been limited to urban watersheds in the mid-Atlantic (Groffman et al., 2002; Mayer et al., 2010) and a rural watershed in Iowa (Schilling et al., 2006; Schilling and Jacobson, 2014). Others have shown that soil type and stratigraphy of the riparian zone can significantly control groundwater flow dynamics, and subsequent nitrogen removal (Böhlke et al., 2007; Hill et al., 2004; Schilling et al., 2006). Different soil layers have different hydraulic conductivities, providing areas with rapid groundwater transport that may bypass areas of high denitrification potential (Böhlke et al., 2007). Thus, it is necessary to expand the study of the role of incision on riparian denitrification into other physiographic regions and those with different soil types than previously studied (e.g., clay or sandy soils).

While these effects can be significant, in-channel processes are likely the dominant controls on riparian groundwater dynamics. The depth of incision (a function of stream erodibility) and hydrology of the stream strongly control riparian groundwater levels (Hardison et al., 2009). Near-channel riparian groundwater elevations largely track in-stream water levels, with diminishing influence moving away from the stream (Schilling and Jacobson, 2014). Riparian soils and in-stream hydrology also interact, with high conductivity soils creating more rapid feedbacks between stream and riparian water levels. Therefore, rapid changes in in-stream water levels (e.g., in a "flashy" stream) would result in little change in riparian groundwater elevations in low hydraulic conductivity soil. On the other hand, groundwater levels would be very responsive to changes in in-stream water levels in high hydraulic conductivity soils. Seasonality can also significantly affect riparian denitrification (Hill, 1996); so, the timing of groundwater contributions will likely have a dominant control on nitrate removal (Lowrance, 1992). It is therefore important to consider variability in both riparian soils and erosion susceptibility when analyzing potential controls on riparian denitrification.

Increased nitrate loading from riparian zones adjacent to incised streams is significant at the site-scale (Groffman et al., 2002; Mayer et al., 2010). Although no studies have examined the watershed-scale effects of channel incision on nitrate loading, several factors make it likely that this incision has the potential to significantly increase nitrate loading at this larger spatial scale. Incised channels are widespread, and small, low order streams are especially susceptible to disturbance (Rheinhardt et al., 2009). Furthermore, these low order streams make up the bulk of the total stream length in watersheds, making it likely that incision of these channels will influence nutrient loading and cycling at the watershed scale. The effect of incision on nitrogen loading will depend on the magnitude of nitrate loading to the riparian zone, as well as how

effectively the riparian zone removed nitrate prior to incision. Detailed field data collection at the watershed scale is impractical to quantify these potential impacts; however, modeling can be a useful tool for exploring how many factors either exacerbate or mediate nitrogen loading from incised riparian zones at the watershed scale.

Several models have been developed to simulate nitrogen transport and transformation in the riparian zone. The Riparian Ecosystem Management Model (REMM) is a field-scale model for estimating the influence of riparian ecosystems on nonpoint source pollution (Altier et al., 2001; Lowrance et al., 2000). REMM divides the riparian zone into three zones and balances the water and nutrients routed through each zone using detailed hydrology, soil, and vegetation parameterization. Daily denitrification is calculated through the interaction of temperature, nitrate, soil aeration, and soil organic carbon. The Riparian Nitrogen Model (RNM) is a watershed-scale model for estimating nitrogen removal via denitrification in riparian buffers along low and middle order streams (Rassam et al., 2005). Denitrification is estimated using a depth-integrated exponential decay function with a rate coefficient based on a maximum denitrification rate and rooting depth.

The Soil and Water Assessment Tool (SWAT) is a continuous, physically-based, watershed-scale model capable of estimating nitrogen loading and routing throughout the watershed (Arnold et al., 1998). Several variations of SWAT have been developed to differentiate riparian zones from the uplands for better hydrologic and water quality calculations (Bieger et al., 2017; Hoang et al., 2017; Sun et al., 2016). SWAT+ is the most widely-used, with a more detailed method for routing water and nutrients to different spatial components called landscape units and enhanced management of land use types and water (Bieger et al., 2017). SWAT_LS is another such variation, which incorporates the same denitrification algorithm as

RNM for the riparian zones (Hoang et al., 2017). Efforts have also been made to integrate REMM into SWAT to study the influences of riparian buffers on hydrology and nutrient cycling at a watershed scale (Ryu et al., 2011; Zhang et al., 2017b, 2017a). SWAT-MODFLOW-RT3D is the result of work to couple SWAT with groundwater and reactive transport models for improved simulation of three-dimensional compound movement throughout watersheds (Wei et al., 2019). RT3D is the nitrate transport engine of this model and it uses an advection-dispersion equation to simulate the fate and transport of nitrate. MODFLOW groundwater algorithms have also been integrated into the innovative SWAT+ (Bailey et al., 2020). These models are useful but tend to be complex and data-intensive, and may not adequately represent relevant hydrologic, biogeochemical, and fluvial processes. Most notably, there is little or no accounting for interactions between stream channel evolution and subsurface hydrology and, subsequently, biogeochemical processes such as denitrification in existing models.

There are a number of models that simulate channel erosion processes. The Bank Stability and Toe Erosion Model (BSTEM; Simon et al., 2011, 2000) simulates fluvial bank erosion and mass failure at individual cross-sections. The CONservational Channel Evolution and Pollutant Transport System (CONCEPTS) model simulates detailed changes in cross-section geometry from erosion and deposition processes (Langendoen and Alonso, 2008; Langendoen and Simon, 2008). These models, however, are typically applied at the site-scale, rather than across an entire watershed. A variation of SWAT (SWAT-DEG), incorporates channel erosion processes into a watershed-scale modeling framework (Allen et al., 1999), but it only accounts for relatively simple erosion processes. A new, open-source, model of channel evolution was recently developed that incorporates sufficient complexity of physical processes, but is applicable at the watershed scale. The River Erosion Model (REM) mechanistically simulates

bed and bank erosion processes throughout drainage networks, but with limited data requirements (Lammers and Bledsoe, 2018). The only known attempt to combine channel evolution and riparian nitrogen models was a simple effort to couple CONCEPTS with REMM, which did not include nutrient processes (Langendoen et al., 2005). Thus, there is a need to incorporate riparian hydrologic and biogeochemical processes into a watershed-scale channel evolution model such as REM to explore links between channel erosion and riparian denitrification processes.

CHAPTER 2

GLOBAL SENSITIVITY ANALYSES OF KEY RIPARIAN NITROGEN MODELS[1]

[1] Buhr, D.X., R.L. Lammers, and B.P. Bledsoe. 2022. Environmental Modelling & Software. 158 (2022):105542. Reprinted here with permission of the publisher.

Abstract

Riparian zones can effectively reduce excess nitrogen loading to streams. Modeling nitrogen retention in riparian zones is useful, especially at larger scales. We evaluated select riparian nitrogen models for their robustness in representing hydrology, vegetation, soils, nutrients, and channel morphodynamics. We used global, time-varying sensitivity analyses of REMM (Riparian Ecosystem Management Model) and SWAT+ (Soil and Water Assessment Tool+) to identify the most influential parameters for calculating water table depth and nitrogen processes. Both REMM and SWAT+ were sensitive to topographic and soil parameters such as slope and soil layer thickness, although spatial and temporal scale and hydroclimatic conditions affected parameter sensitivity. Neither model was sensitive to stream channel depth, which is known to affect riparian hydrology and nitrogen cycling. It is necessary to incorporate stream morphodynamics like channel change into both riparian-scale and watershed-scale nitrogen models to provide useful management tools for addressing excessive nitrogen loading in stream networks.

Introduction

Eutrophication resulting from anthropogenic nutrient pollution is among the most substantial issues facing water resources professionals and society today. More than 40% of stream length in the U.S. is impaired by nutrient pollution (U.S. EPA, 2016). Dissolved nitrate is an especially insidious pollutant because it is rapidly transported through groundwater and surface water and causes a variety of environmental problems – from contaminating drinking water to eutrophication and associated algal blooms (Howarth et al., 2011). Nitrogen pollution is a primary driver of water quality degradation in coastal zones globally (Howarth, 2008), including the “dead zone” in the Gulf of Mexico (Große et al., 2019). Nitrogen runoff from

agricultural and urban areas is transported through river networks to the coast; however, less nitrogen reaches the coasts than is applied to land surfaces, indicating that streams and riparian zones act as significant nutrient sinks (Peterson et al., 2001).

The protection and restoration of riparian zones is a cornerstone of effective nutrient management that complements source reductions. Nitrogen removal in riparian zones has long been an area of research, often with the goal of restoring riparian functions to treat agricultural runoff (Hill, 1996, 1979; Lowrance, 1992). Riparian zones effectively remove dissolved nitrate in runoff and groundwater (e.g., Hill, 2019; Mulholland et al., 2008; Newbold et al., 2010), and these areas may contribute more to nitrogen removal than in-stream processes (Craig et al., 2008; Lammers and Bledsoe, 2017). Nitrogen is permanently removed in riparian zones through denitrification, an anoxic process in which microbes use organic soil carbon to reduce nitrate to inert dinitrogen gas (Hill, 1996). Under the right conditions, riparian buffers can remove greater than 90% of the nitrate in inflowing groundwater (Balestrini et al., 2016; Peterjohn and Correll, 1984; Pinay et al., 1993; Spruill, 2000; Wiseman et al., 2014). These conditions include low oxygen and an organic carbon source – usually from riparian vegetation (Mosier et al., 2002). Channel incision (bed erosion) can lower riparian groundwater tables (Hardison et al., 2009), disconnecting nitrate-laden groundwater with soil organic carbon and microbial communities, reducing denitrification potential and increasing nitrate loading to streams (Gift et al., 2010; Groffman et al., 2002). This paper compares the mechanisms relevant to riparian denitrification in existing models via global sensitivity analysis to improve future simulation of nitrogen loading to streams.

Riparian Nitrogen Modeling

Despite the importance of denitrification, the process is notoriously difficult to measure (Groffman et al., 2006), and can occur sporadically in space and time when conditions are favorable (McClain et al., 2003). Riparian nitrogen models are therefore valuable for providing quantitative estimates of riparian denitrification and nutrient sequestration, and guiding management activities in cases where direct measurement of these processes is not feasible. Several models exist for evaluating the influence of riparian zones on nitrogen loading to streams, ranging from field-scale models specifically for riparian zones to watershed-scale models that include riparian processes (Arnold et al., 1998; Bieger et al., 2017; Lowrance et al., 2000; Sun et al., 2018). Typical processes included in a riparian nitrogen model are shown in Figure 2.1. The Riparian Ecosystem Management Model (REMM) is a field-scale model for estimating the influence of riparian ecosystems on nonpoint source pollution (Altier et al., 2002; Lowrance et al., 2000). Daily denitrification is calculated through the interaction of temperature, nitrate, soil aeration, and soil organic carbon. The Riparian Nitrogen Model (RNM) is a watershed-scale model for estimating nitrogen removal via denitrification in riparian buffers along low and middle order streams (Rassam et al., 2005). Denitrification is estimated using a depth-integrated exponential decay function with a rate coefficient based on a maximum denitrification rate and rooting depth.

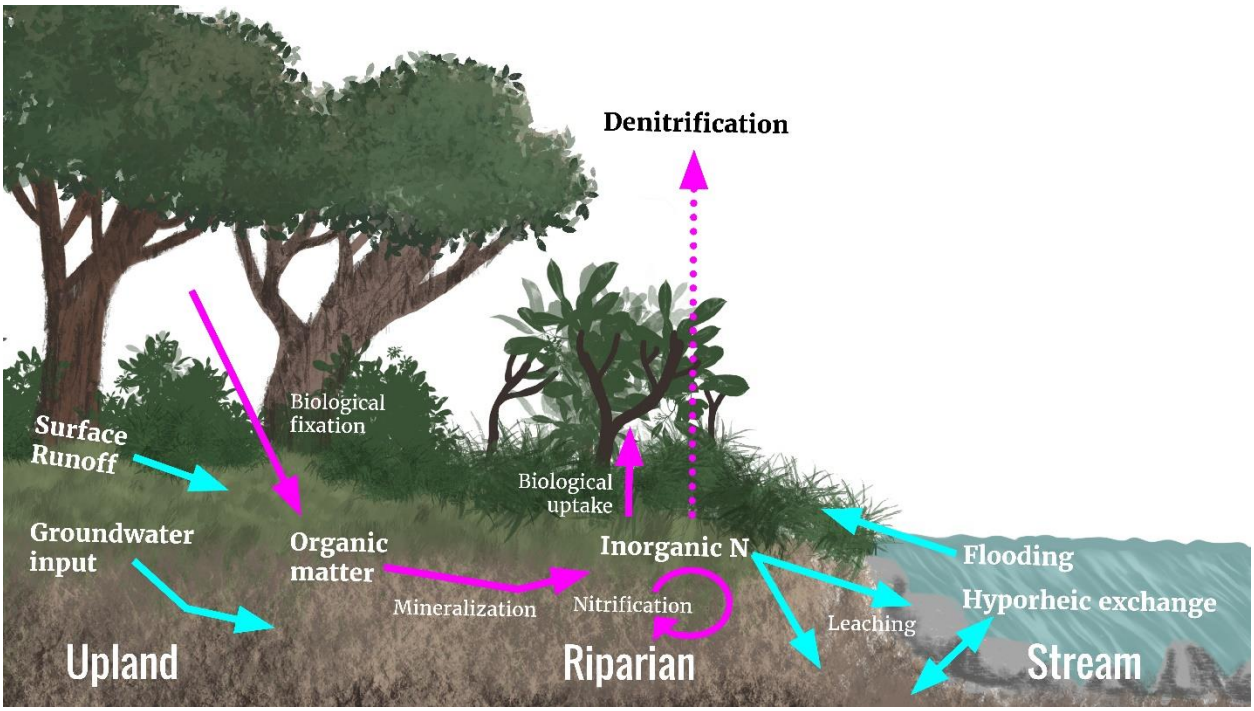

Figure 2.1. Schematic of the major processes typically simulated in a riparian nitrogen model.

The Soil and Water Assessment Tool (SWAT) is a watershed-scale model capable of estimating nitrogen loading and routing throughout the watershed (Arnold et al., 1998). Several variations of SWAT have been developed to differentiate riparian zones from the uplands for better hydrologic and water quality calculations (Bieger et al., 2017; Hoang et al., 2017; Sun et al., 2016), including an integrated SWAT-REMM to study the influences of riparian buffers on hydrology and nutrient cycling at a watershed scale (Ryu et al., 2011; Zhang et al., 2017b, 2017a). SWAT+ is one of the newest and more commonly-used variations, but denitrification is modeled the same as previous SWAT versions, with an exponential decay equation of denitrification rate, temperature, saturation, and organic carbon (Bieger et al., 2017; Neitsch et al., 2011). SWAT-MODFLOW-RT3D is the result of recent work to couple SWAT with groundwater and reactive transport models for improved simulation of three-dimensional solute movement throughout watersheds (Wei et al., 2019). RT3D is the nitrate transport engine of this

model and it uses an advection-dispersion equation to simulate the fate and transport of nitrate. MODFLOW groundwater algorithms have also been integrated separately into the new SWAT+ (Bailey et al., 2020). The trend toward increasing model complexity may allow for more realistic simulation of hydrologic and biogeochemical processes, but also at a cost of increased data requirements, computational power, and uncertainty, potentially making these models less useful for managers. Quantification of model sensitivity and uncertainty can help users interpret results and strike a balance between model complexity and utility.

Uncertainty and Sensitivity Analyses

Uncertainty is typically present in environmental modeling, and quantifying this uncertainty is essential for assessing the accuracy and reliability of model outputs and better understanding model structure (Byrd and Melching, 2005; Melching and Bauwens, 2001; Pappenberger and Beven, 2006). An effective approach to uncertainty analysis is Monte Carlo simulations. Essentially, a model is run hundreds or thousands of times, with each model run using a slightly different set of model inputs. This provides a distribution of model outputs, directly accounting for the uncertainty in model inputs. Sensitivity analyses apportion the uncertainty in this distribution of model output to different input variables, identifying which inputs most influence model results (Saltelli et al., 2004). Sensitivity analyses can be local or global (Saltelli et al., 2004). Local, or one-at-a-time, sensitivity analyses focus on quantifying parameter influence while changing a single parameter from the base case and fixing the remaining parameters, whereas global sensitivity analyses select across the entire parameter space for all inputs of interest (Tian, 2013).

In general, global sensitivity analyses are preferable to local due to their ability to account for parameter influences across the entire range of reasonable values and compatibility

with non-linear models, making results more generalizable and less influenced by modeler bias (Song et al., 2015). Nearly half of published sensitivity analyses in science-related fields use global methods (Saltelli et al., 2019), with a positive trend in prevalence of global sensitivity analyses in recent years (Ferretti et al., 2016). Global sensitivity analyses can belong to one of several sub-classes: regression-based, variance-based, and density-based, among others. Regression-based global sensitivity analyses are one of the most common due to the moderate computing power required and easily understandable outputs (i.e., regression coefficients and R^2), but generally require a linear relationship between parameter and model output (Ferretti et al., 2016; Song et al., 2015). Variance-based approaches use a variance ratio to determine both first-order and total effects, which can be advantageous because it works with models of varying type and complexity, including those with significant parameter interactions. However, variance-based methods can be computationally intensive or require strict sampling design (Saltelli et al., 2010, 1999; Song et al., 2015). Density-based methods provide a suite of probability density curves for each parameter across its selected range, but sensitivity values are only informative for relative comparisons (Plischke et al., 2013). The density-based methods of Plischke et al. (2013) can be advantageous over other methods because they are less computationally-intensive, can be used with log-transformed outputs, and have been applied to various water resources-related studies (Borgonovo et al., 2017; Herman et al., 2015; Lammers et al., 2017).

Most sensitivity analyses determine parameter sensitivity aggregated across the entire time series, which leads to incomplete information. Recent studies have investigated time-varying sensitivity at preset intervals to determine how input importance changes under variable conditions (Ghoreishi et al., 2021; Herman et al., 2013a, 2013b; Pianosi and Wagener, 2016; Reusser et al., 2011; Reusser and Zehe, 2011; Wagener et al., 2003; Wu et al., 2022). These

studies have found that parameter sensitivities change in response to dominant real-world processes that control hydrologic transport during wet and dry conditions, such as interflow and snowmelt (Reusser et al., 2011; Reusser and Zehe, 2011; Wu et al., 2022). Time-varying sensitivity analyses improve understanding of how these different processes control model outputs and how well a model incorporates these processes.

Sensitivity and uncertainty analyses on terrestrial nitrogen models have shown that soil and hydrologic parameters and processes are most important for simulating nitrogen transport (McIntyre et al., 2005; Rankinen et al., 2013); however, modeled denitrification rates were, perhaps unsurprisingly, influenced by factors that are known to directly control denitrification, such as temperature and nitrate concentration (Bouwman et al., 2013). Denitrification estimates are also sensitive to parameters influencing soil moisture, including groundwater table depth (Heinen, 2006). Stream channel characteristics such as streamflow and depth can also influence simulated denitrification via their connection to the riparian groundwater table (Dukes and Evans, 2003; Tilak, 2012). Using streamflow data to calibrate a denitrification model can constrain and reduce the uncertainty in values for soil parameters, and thus the denitrification estimates, emphasizing the inherent interplay between the two (Tague, 2009). Despite these results, to our knowledge there are no comparative analyses of global sensitivity results for riparian nitrogen models. Many aspects of the models are complex and prohibitively data-intensive to parameterize. Therefore, there is a need for a comprehensive summary and comparison of riparian nitrogen models and investigation of uncertainty and sensitivity of model outputs. A rigorous comparison of processes incorporated into these models can identify what is lacking and how that affects model utility. Furthermore, this can help inform future research and

model development, as well as provide guidance for model users on which parameters should be most carefully quantified to reduce model uncertainty.

Objectives

The objectives of this research are to: 1) compare the mechanisms incorporated in existing riparian denitrification models, and 2) conduct a global, time-varying sensitivity analysis of two of these models, REMM and SWAT+. Comparing current tools for modeling riparian nitrogen processes, including the specific model algorithms that are present, inadequate, or omitted, provides insight into the state of riparian nitrogen modeling and pinpoints research directions that are most needed for improvement. The global sensitivity analyses will allow for a critical evaluation of existing models to determine which parameters are most influential for hydrologic and nitrogen processes in those models. Time-varying sensitivity analysis methods will show how these influential parameters change with variable hydroclimatic conditions. While REMM and SWAT+ operate at different spatial scales, we can use our findings to draw general conclusions about processes that are either ubiquitously underrepresented in riparian nitrogen models or lacking at different scales. The results from this study can be used to improve existing models and provide a basis for building a parsimonious riparian nitrogen model with the most relevant parameters and processes.

Methods

We identified four riparian nitrogen models (REMM, RNM, SWAT+, and SWAT-MODFLOW-RT3D) to analyze for their mechanistic complexity – number of parameters, spatial and temporal resolution, data requirements, and fidelity to scientific processes. We assigned a qualitative score from zero to three to model algorithms related to hydrology, nutrients, soils, vegetation, and stream connectivity (see Table 2.3). Scores were representative of the data

requirements and physical robustness of the equation, with zero meaning the process was completely omitted, one indicating low complexity, and three indicating high complexity. Complexity was scored based on the required parameterization to calculate that process, relative to other known calculation methods. Hydrologic processes that were evaluated were surface runoff and infiltration, evapotranspiration, and subsurface flow. The only nutrient process that we considered in this analysis was denitrification. For soils, we evaluated the number of soil layers and relationship between organic matter and depth, along with the types and general parameterization of vegetation. Finally, we assessed geomorphic, bank storage, and overbank flow algorithms to determine the ability of the models to connect the stream with the riparian zone.

Although other riparian nitrogen models exist, these four models were selected because they are prevalent in literature and representative of the spectrum of spatial scales, regional applications, complexity, and the advances in riparian process modeling in the last few decades. REMM is a field-scale model that was developed by the USDA-ARS in Georgia, USA (Altier et al., 2002), and has been applied in a variety of landscapes across the United States (Tamanna, 2021) and internationally when coupled as SWAT-REMM (Ryu et al., 2011; Zhang et al., 2017a). RNM is a catchment-scale model developed for low and middle order streams in Australia, with capabilities of estimating denitrification for ephemeral and perennial channels (Rassam et al., 2005). SWAT+ is a recent adaptation of the watershed-scale SWAT to better represent watershed spatial connections, including floodplain and upland flow and pollutant routing (Bieger et al., 2017). Similar to REMM, SWAT+ was initially tested at the Little River Experimental Watershed in Georgia. SWAT-MODFLOW-RT3D couples SWAT with MODFLOW for improved groundwater process representation and RT3D for solute transport at

the catchment scale (Wei et al., 2019). This model was initially tested in a large watershed (4100 km^2) in Oregon, USA. Comparing the mechanistic complexity of these models is useful because they are representative of the diversity in scale and landscape application of riparian nitrogen models.

We performed a global sensitivity analysis of REMM and SWAT+ to identify model parameters that most affected model output, and to identify processes that may not be adequately represented. These two models were chosen due to their ease to implement and their intermediate-complexity, as determined in the prior assessment. REMM was selected due to its specificity to field-scale riparian systems and detailed hydrology and vegetation models. Many past applications of REMM have included a local sensitivity analysis (Dukes and Evans, 2003; Graff et al., 2005; Kim et al., 2007; Lowrance et al., 2000; Tilak, 2012), but only one attempted to use a global sensitivity analysis (Tamanna et al., 2021). We analyzed SWAT+ because it is a recent improvement of the widely-applied, watershed-scale SWAT model that explicitly differentiates riparian zones from uplands. Furthermore, we chose to analyze these models that simulate at various spatial scales to investigate generalizable strengths and shortcomings in riparian nitrogen modeling. The Monte Carlo and sensitivity analysis procedures for each of these models followed an identical structure: 1) selection of parameters to test; 2) identification of valid ranges for each parameter based on literature, model documentation, and expert judgement; 3) random sampling of parameter values from a representative statistical distribution; 4) simulations of the model using unique parameter sets (500 for SWAT+, 1000 for REMM); and 5) global, density-based sensitivity analysis using methods of Plischke et al. (2013). Sensitivity analyses were performed for the entire simulation and repeated with annual, seasonal, and 30-day, non-moving time windows to investigate how parameter sensitivity varied across

temporal scales. Seasonal time windows were initiated at the associated solstice or equinox, while 30-day time windows were initiated on the first day of the simulation and segmented every 30 days. Only time windows that were completely encompassed in the simulation timeframe were used. Results using the Plischke et al. method for the full simulation were compared to a more recent approach (Baroni and Francke, 2020) that combines variance- and distribution-based (CVD) methods and estimates main effect and interactions separately. Since results using these two methods were similar, only the Plischke et al. method was used for the time-varying analysis. For shorter time scales, the CVD method failed because some outputs did not change sufficiently over a month or season.

REMM Sensitivity Analysis

The Riparian Ecosystem Management Model is a continuous field-scale model that performs daily balances on water, sediment, and nutrients in riparian buffers (Altier et al., 2002). The model code was edited to accommodate this sensitivity analysis. Parameter modifications were made relative to an example dataset from the Gibbs Farm in the Little River Watershed near Tifton, Georgia, USA. We selected 47 of the more than 150 REMM parameters for this sensitivity analysis (Table 2.1), focusing on those that we hypothesized would influence riparian hydrology and nitrogen cycling. Parameters describing the buffer, soil, vegetation, and rate coefficients were varied, while time-series data (i.e., weather and field inputs) were not adjusted because we assumed that they were inherently influential on the studied outputs and must be specified in future modeling regardless. We chose distributions and ranges for each parameter based on literature. If data were not found in literature, then we based distributions and ranges on REMM documentation or ± 50-100% variations of REMM example data. Many soil parameters were treated as uniform distributions across their common ranges so that all soil types could be

reasonably tested. Log-normal distributions used the natural logarithm. We defined means and standard deviations for selection of random values from each distribution. Mean values were assumed to be either: middle of the chosen range, a literature value, assumed based on expert judgement, or the value used in the default Gibbs Farm REMM model. Standard deviations, when not found, were specified as one-fourth the range (Hozo et al., 2005). Complete tables of distributions and statistics for these parameters can be found in Appendix A (Tables A1, A2, A3, and A4).

We accounted for several simple correlations among parameters to ensure that the parameter sets represented realistic conditions (e.g., soil bulk density was based off of clay content). Additionally, we checked logical relationships between parameters and adjusted them accordingly (e.g., field capacity could not exceed porosity). See Appendix A for more details.

Table 2.1. List of REMM parameters selected for the sensitivity analysis based on literature and perceived importance to hydrology and N cycling. *Correlated with drainage area. **Correlated with percent clay.

Buffer Characteristics	Vegetation	Rate Coefficients
Drainage area	Rainfall interception	Residue metabolic release
Stream depth	N max concentration, buds	Residue structural release
Soil temperature	N max concentration, leaves	Humus active release
Zone width	N max concentration, stems	Humus slow release
Surface slope*	N max concentration, branches	Humus passive release
Deep seepage	N max concentration, coarse roots	Denitrification
Overland Manning's n	N max concentration, fine roots	
Ammonium	N min concentration, buds	
Nitrate	N min concentration, leaves	
Depth to bedrock	N min concentration, stems	
Pore size distribution index	N min concentration, branches	
Layer thickness	N min concentration, coarse roots	
Wilting point	N min concentration, fine roots	
Field capacity	Maximum rooting depth	
Porosity	Rooting depth	
Volumetric water content		
Permeability**		
Percent clay		
Bulk density**		
pH		
Structural carbon pool		
Metabolic carbon pool		
Active humus carbon pool		
Slow humus carbon pool		
Passive humus carbon pool		
Lignin carbon pool		

Parameter values in each of the three riparian zones (Figure 2.2) were changed identically, meaning that the only differences among the zones were in the parameters that remained as defaults of the Gibbs Farm model. Excluding the correlation for clay content, we changed each of the three soil layers homogeneously. We performed more than 1000 REMM simulations, each driven by the four years of daily time-series data collected at Gibbs Farm representing wet, dry, and average amounts of precipitation. Precipitation was above average for

the first and third years, approximately average in the second year, and drier than average in the final year. Only the first 1000 model results with outputs that were greater than zero and did not include any "N/A" values were included in the sensitivity analysis. We analyzed the following model outputs: near-stream water table depth, subsurface dissolved nitrogen load to stream, total denitrification, and total nitrogen balanced in the near-stream zone (Zone 1 in Figure 2.2). For each model run, we used the standard deviation of the four years (or whichever time window was used) of daily values for water table depth and the sum of the four years of daily values for nitrogen outputs in the density-based sensitivity analysis (Plischke et al., 2013). In this method, probability distributions of model output were conditioned on different modeled inputs. We then compared these distributions to the total unconditioned probability distribution of all modeled output. Larger differences between conditioned and unconditioned probability distributions indicated that input variable had a larger effect on model output. We performed 500 bootstrapping iterations to minimize bias (and calculate confidence intervals) and used natural logarithm transformations when output distributions were skewed. A dummy variable, a purely random set of numbers not used in REMM, was included as a baseline to account for noise in the sensitivity method. Highly sensitive input parameters are those with a minimum sensitivity index value larger than the maximum sensitivity of the dummy variable. All Monte Carlo simulations and sensitivity analyses were conducted in R (R Core Team, 2021) using the following packages: *KernSmooth* (Wand, 2021), *EnvStats* (Millard, 2013), *dplyr* (Wickham et al., 2020), *Rcpp* (Eddelbuettel, 2013; Eddelbuettel and Balamuta, 2018; Eddelbuettel and Francois, 2011), *RColorBrewer* (Neuwirth, 2014), *ks* (Duong, 2021), *randtoolbox* (Dutang and Savicky, 2021), *plyr* (Wickham, 2011), *lattice* (Sarkar, 2008), and *Matrix* (Bates and Maechler, 2021).

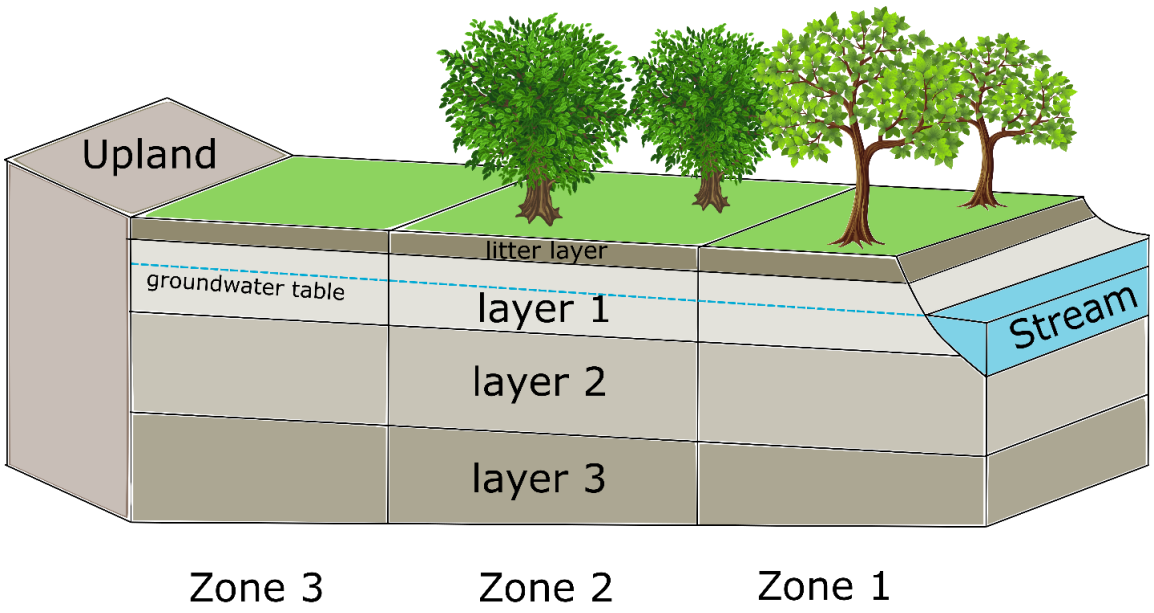

Figure 2.2. Schematic of REMM. Water and nutrients are routed through the three soil layers and three zones from the upland to the stream. Image adapted from Lowrance et al. (2000).

SWAT+ Sensitivity Analysis

SWAT+ (rev. 59.3), an updated version of SWAT, is a semi-distributed, continuous, watershed-scale model which differentiates riparian zone processes from both channel and upland processes. Of the hundreds of available parameters in SWAT+, we selected 19 for this analysis (Table 2.2), including those hypothesized to influence riparian hydrology and nitrogen cycling and focusing on ones that can be reasonably quantified by a user. The default model, like REMM, was a simulation in the Little River Experimental Watershed in southern Georgia, a model that was used to test SWAT+ during its development (Bieger et al., 2017). We ran the model at a daily time step for four years representing wet, dry, and average amounts of precipitation, with three years of model warmup. The first two simulation years had above average precipitation, followed by a drier than average third year and an average fourth year of precipitation. We defined distributions, ranges, means, and standard deviations using the same procedures as outlined for REMM, maintaining similarities for parameters that were identical

between the two models. SWAT+-recommended minima and maxima were set as parameter range boundaries, when reasonable. The most notable difference for SWAT+ was that most parameters were spatially distributed in hydrologic response units (HRUs), rather than given as a single value. We modified these spatial parameters based on percent changes to the base value. This ensured that all parameters were changed directionally and proportionally while maintaining the spatial relations. Values for spatially-invariable defaults were changed using the same selection procedure as for REMM. A complete table of parameters, distributions, and statistics can be found in Appendix A (Table A5). We also used correlations similar to those in REMM, which are discussed in Appendix A.

SWATplusR, an R package for automating SWAT+ simulations (Schürz, 2019), was used to perform Monte Carlo simulations, along with the same R packages from the REMM analysis. We conducted 500 error-free simulations due to high computational time. The same density-based sensitivity analysis methods were performed using standard deviations of daily water table depth and sums of daily nitrogen outputs. Outputs selected for analysis were basin-averaged water table depth and denitrification, plus basin output riverine nitrate load.

Table 2.2. List of SWAT+ parameters selected for the sensitivity analysis based on literature and perceived importance to hydrology and N cycling. Italicized parameters are those that were adjusted by percentage. *Correlated with clay content. **Correlated with slope length.

Basin	**Soil**	**Aquifer and Routing**	**HRU**
Nitrate percolation	*Layer thickness*	*Stream depth*	*Slope***
Denitrification rate	*Bulk density**	Aquifer bottom depth	Slope length
Denitrification saturation threshold	*Available water capacity*	Minimum water table depth for return flow	*Lateral length***
	*Hydraulic conductivity**	Maximum baseflow	Field length
	Carbon		Field width
	Clay content		
	pH		

Results

Model Comparison

We analyzed four innovative and representative riparian nitrogen models (REMM, RNM, SWAT+, and SWAT-MODFLOW-RT3D) for their completeness and complexity of algorithms for hydrology, nutrients, soils, vegetation, and stream connections (Table 2.3). All four models had similar methods for performing hydrologic calculations, using either or both of the Curve Number (Hawkins, 1980) and Green-Ampt (Green and Ampt, 1911) equations for infiltration. Evapotranspiration in all four models was highly complex since each was capable of applying the data-intensive Penman-Monteith equation. Groundwater was represented at low complexity in all models except SWAT-MODFLOW-RT3D, which used the complex groundwater algorithms from MODFLOW. REMM utilized the most detailed approach for estimating denitrification, with a first-order decay equation that incorporated multiplicative factors based on pH, saturation, carbon, available nitrate, and temperature. This was much more complex than the simple first order decay equations in RNM and SWAT+ or the advection-dispersion equation used in SWAT-MODFLOW-RT3D. The designation of soil layers was most complex in SWAT+ and SWAT-MODFLOW-RT3D, which allowed up to 25 layers. Estimation of organic matter with depth was most complex in REMM, which performed a carbon balance in every soil layer.

Vegetation algorithms were also most intricate in REMM, with specification of one of a dozen types of vegetation for each zone of the riparian buffer and detailed calculations of vegetative growth. The only model that included a geomorphic connection between the stream and riparian water table was REMM, which used the thalweg elevation of the stream to set the hydraulic gradient for the water table depth in the near-stream riparian zone. However, there was no bank storage calculation in REMM despite all other models including it. SWAT+ was the

only model of those selected that accounted for overbank flows, which was done by defining a floodplain landscape unit and routing water onto it when a known or calculated bankfull discharge was exceeded (Bieger et al., 2017). Detailed information on each of these models can be found in their respective documentation (Altier et al., 2002; Rassam et al., 2005; Texas A&M University, 2022; Wei et al., 2019).

Table 2.3. Major features of select riparian nitrogen models and their complexity. (✓ - low complexity to ✓✓✓ - high complexity; x – process not included).

Components		**REMM**	**RNM**	**SWAT+**	**SWAT-MODFLOW-RT3D**
Hydrology	Surface runoff and infiltration	✓✓	✓✓	✓✓	✓✓
	Evapotranspiration	✓✓✓	✓✓✓	✓✓✓	✓✓✓
	Groundwater flow	✓	✓	✓	✓✓✓
Nutrients	Denitrification	✓✓✓	✓	✓	✓✓
Soils	Number of layers	✓✓	✓	✓✓✓	✓✓✓
	Organic matter - depth	✓✓✓	✓✓	✓✓	✓✓
Vegetation	Types	✓✓	✓	✓✓	✓✓
	Parameters	✓✓✓	✓	✓✓	✓✓
Stream connection	Geomorphic	✓	x	x	x
	Bank storage	x	✓	✓	✓
	Overbank flows	x	x	✓	x

REMM Sensitivity Analysis Results

Select results of the REMM sensitivity analysis using the methods of Plischke et al. (2013) for the full simulation are displayed in Figure 2.3, showing only sensitive parameters and those of most interest. Complete results can be found in Appendix A (Figure A1). We

determined 1000 simulations to be adequate by visually verifying parameter sensitivity values stabilized for each output as simulations increased in increments of 50 (Figure A2). Parameters were considered highly sensitive if there was no overlap with the dummy variable. Parameters were considered slightly sensitive if there was only slight overlap (but no overlap in interquartile range).

Water table depth was highly sensitive to soil layer thickness and slightly sensitive to drainage area, surface slope, and field capacity for the Plischke et al. method (Figure 2.3a). Subsurface dissolved nitrate loading to the stream was highly sensitive to permeability and percent clay (Figure 2.3b). Slope and bulk density showed slight sensitivity despite the overlap of the error bars and mean dummy sensitivity in the plot. Denitrification was highly sensitive to the denitrification rate coefficient K and soil layer thickness (Figure 2.3c). Slope, drainage area, permeability, stream depth, and various carbon and nitrogen concentrations slightly influenced denitrification. Total nitrogen was highly sensitive to drainage area and surface slope, and slightly sensitive to permeability, field capacity, and soil layer thickness (Figure 2.3d). Each output was overall sensitive to only a few parameters, aligning with the Pareto principle that the majority of the consequences (in this case, sensitivity) result from the vital few causes.

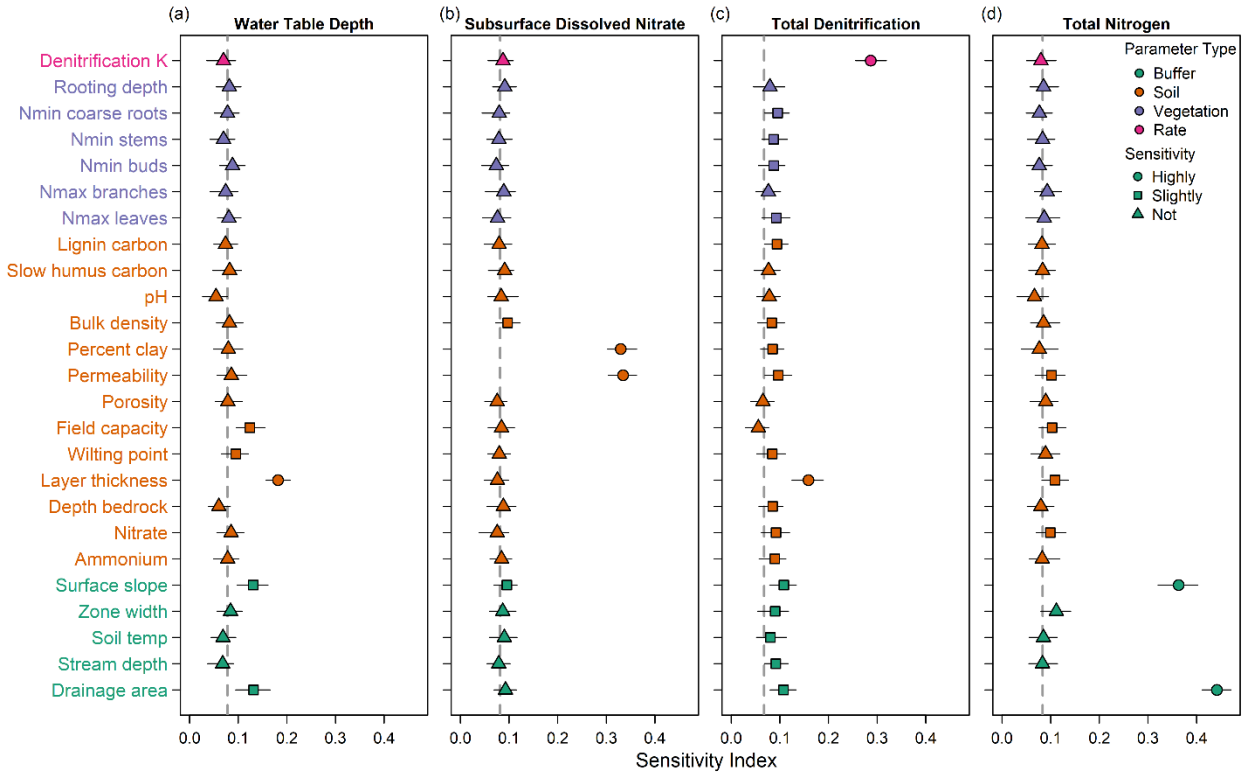

Figure 2.3. Sensitivity of the four chosen REMM outputs to the most sensitive or interesting input parameters. The dashed vertical line is the mean sensitivity of that output to a dummy variable. Error bars represent the minimum and maximum sensitivity across all simulations with bootstrapping.

Results for the full simulation using the Baroni and Francke (2020) combined variance- and distribution-based (CVD) method are shown in Figure 2.4. The most influential parameters were similar between the two methods, with total nitrogen showing additional sensitivity to riparian zone width for the CVD method (Figure 2.4d). High interaction effects for subsurface dissolved nitrate (Figure 2.4b) signified that although most parameters were not individually sensitive, they had substantial interactions with other parameters. Interaction effects were relatively low for the other outputs.

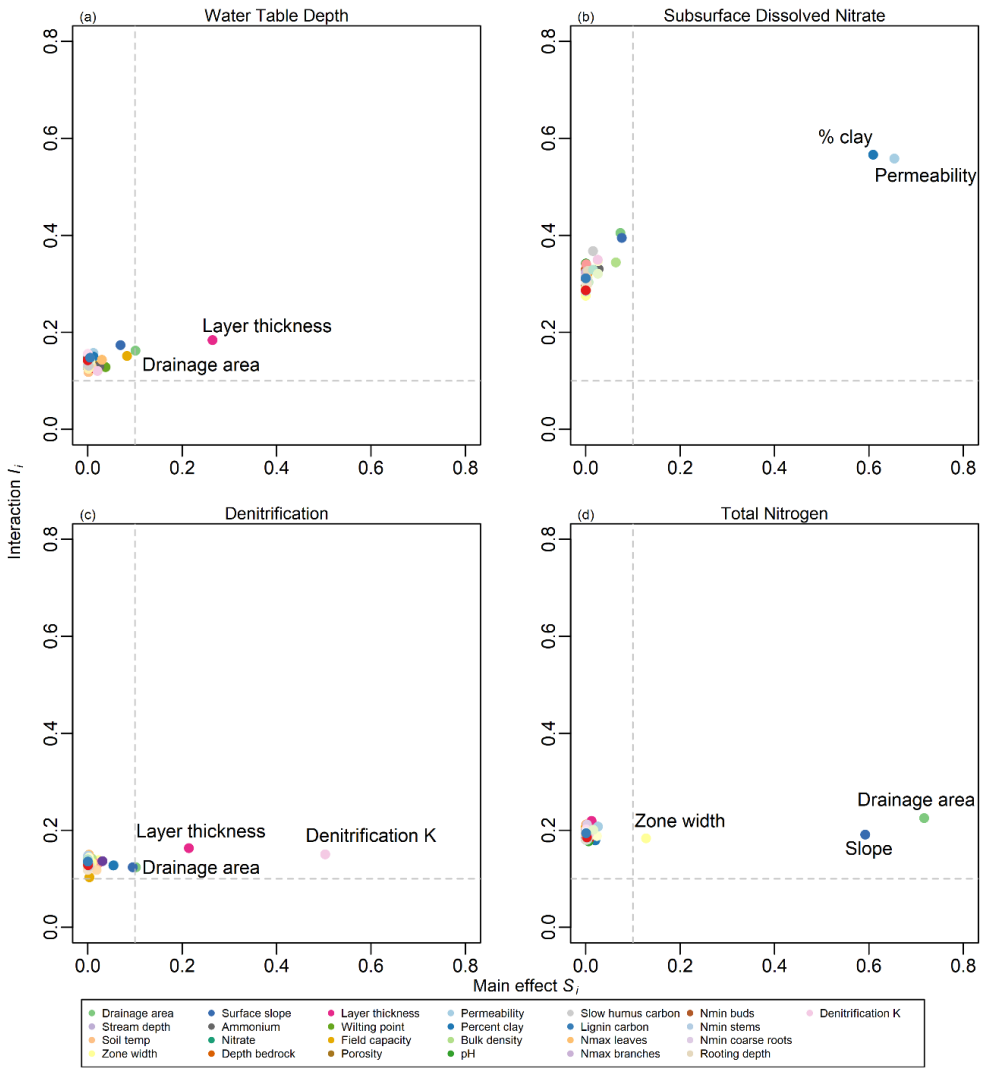

Figure 2.4. Sensitivity of the four chosen REMM outputs to a subset of the selected input parameters using the CVD method (Baroni and Francke, 2020). Plots are arbitrarily divided the same as Baroni and Francke (2020; dashed line) to highlight the lowest values for the indices.

Results for the REMM time-varying water table depth sensitivity analyses are shown in Figure 2.5. Only parameters that were influential at multiple window sizes are shown – drainage area, surface slope, field capacity, permeability, and percent clay. Drainage area and surface slope had the most consistent sensitivity across time periods, with the highest sensitivity occurring during spring of years 2 and 4. The importance of other variables was sporadic but most substantial during year 4. Water table depth was not sensitive to layer thickness at finer

time scales, despite it being the most influential parameter across the full simulation. Similar figures for the other outputs are shown in Appendix A (Figures A3, A4). Subsurface dissolved nitrate did not change enough across the shorter time scales to provide reliable sensitivity outputs, and was therefore excluded from the time-varying analysis. Denitrification was most sensitive to the denitrification rate coefficient and soil layer thickness for all or most of the simulation, but sensitive to surface slope and drainage area only when denitrification was high (Figure A3). Volumetric water content, permeability, percent clay, and rooting depth became influential at several 30-day time windows, but not during any longer periods. Total nitrogen was consistently sensitive to drainage area and slope, and sporadically sensitive to permeability and rainfall interception (Figure A4). Percent clay and maximum rooting depth were influential only during a few 30-day time windows.

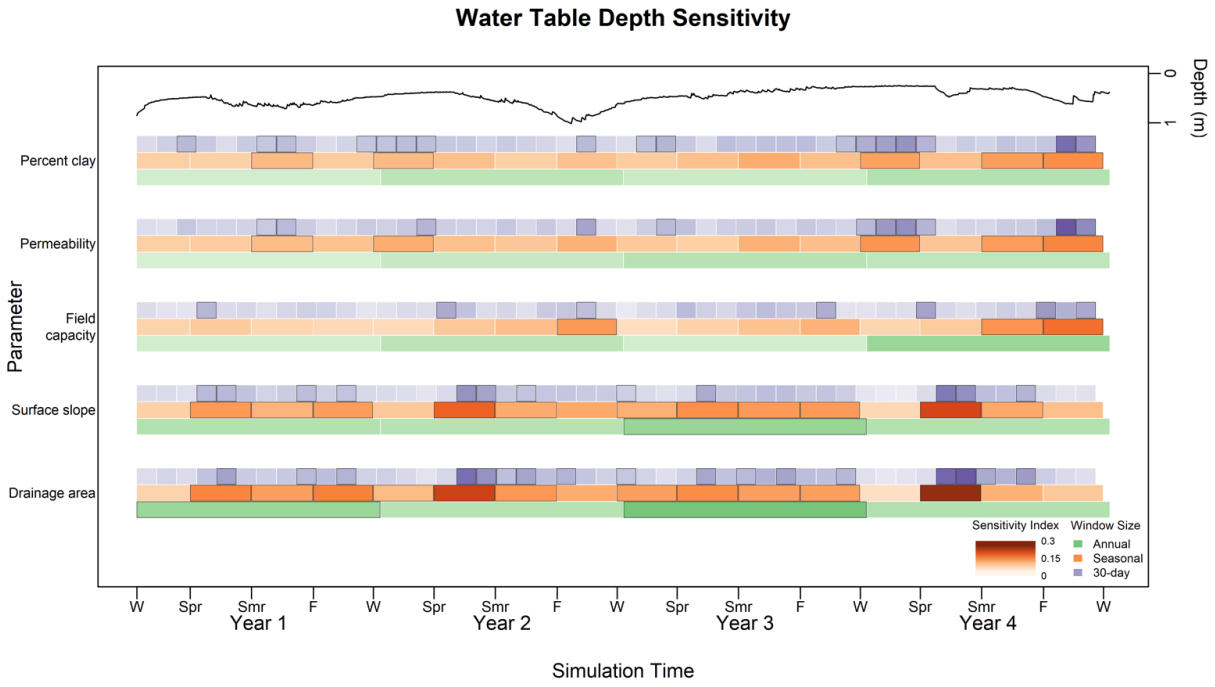

Figure 2.5. Time-varying sensitivity of the water table depth output in REMM to the most influential parameters. Time windows are shaded according to the value of the sensitivity index. Times when parameters were highly sensitive (no overlap with the dummy variable sensitivity) are outlined. The average daily water table depth across all model runs is shown at the top.

SWAT+ Sensitivity Analysis Results

SWAT+ sensitivity analysis results (using the Plischke et al. method) are displayed in Figure 2.6. Results showed only a few inputs exerting most of the influence on the outputs, which again agreed with the Pareto principle. Water table depth was highly sensitive to field parameters such as lateral length and slope (Figure 2.6a). Soil properties such as clay content, hydraulic conductivity, bulk density, and soil layer thickness also highly influenced water table depth. Water table depth was slightly sensitive to slope length and soil layer thickness, among others. Nitrate export from the watershed and total denitrification were only highly sensitive to the denitrification saturation threshold (Figure 2.6b, 2.6c). We considered 500 simulations to be adequate by plotting and visually inspecting that the change in cumulative output sensitivity stabilized near zero as the number of simulations increased in increments of 50 (Figure A5).

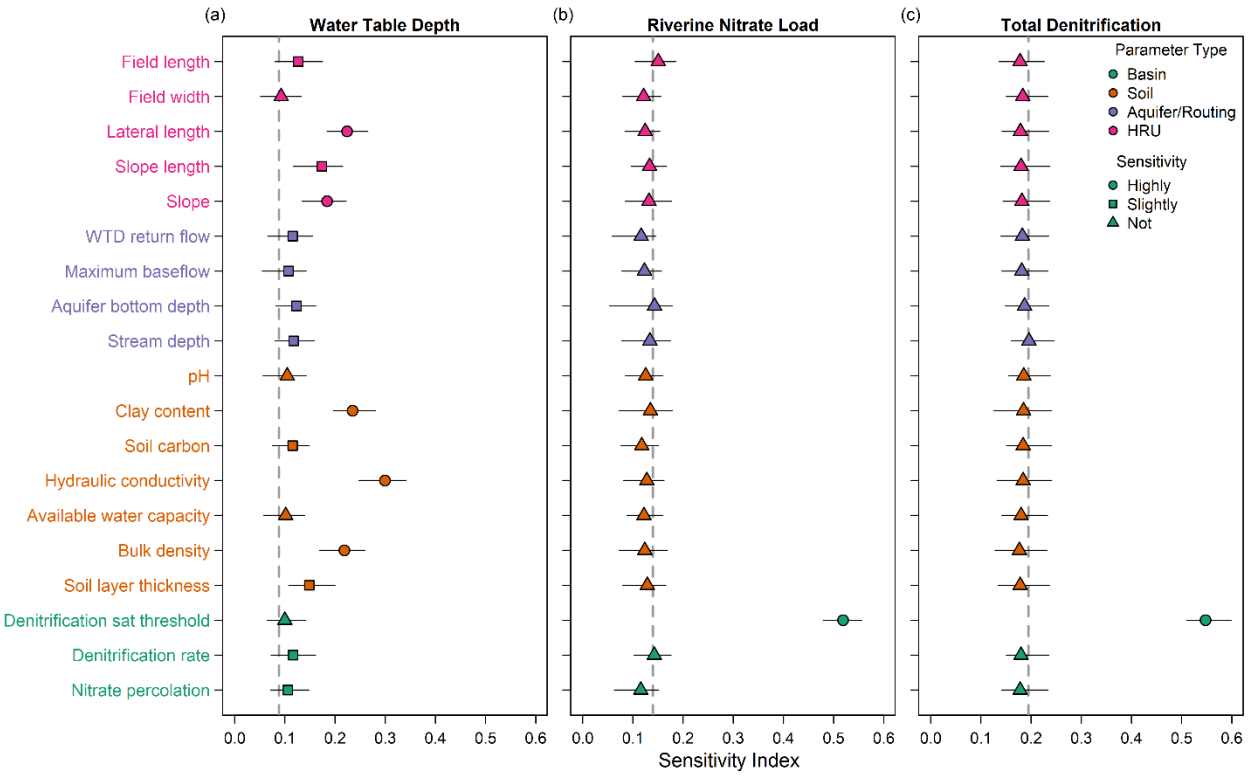

Figure 2.6. Sensitivity of the three chosen SWAT+ outputs to each of the selected 19 input parameters. The dashed vertical line is the mean sensitivity of that output to a dummy variable. Error bars represent the minimum and maximum sensitivity across all simulations with bootstrapping.

Like our REMM analysis, we also used CVD sensitivity analysis methods for the full SWAT+ simulation (Figure 2.7). Largely similar parameters were identified as important as from the Plischke et al. method, with more sensitivity of water table depth to slope length. Riverine nitrate load (Figure 2.7b) and denitrification (Figure 2.7c) had parameters with high interaction effects, which again showed the interconnectedness of these parameters that were not individually influential. Denitrification saturation threshold had high interaction and total effects for those outputs, showing its overwhelming importance to those processes despite having interactions with other factors.

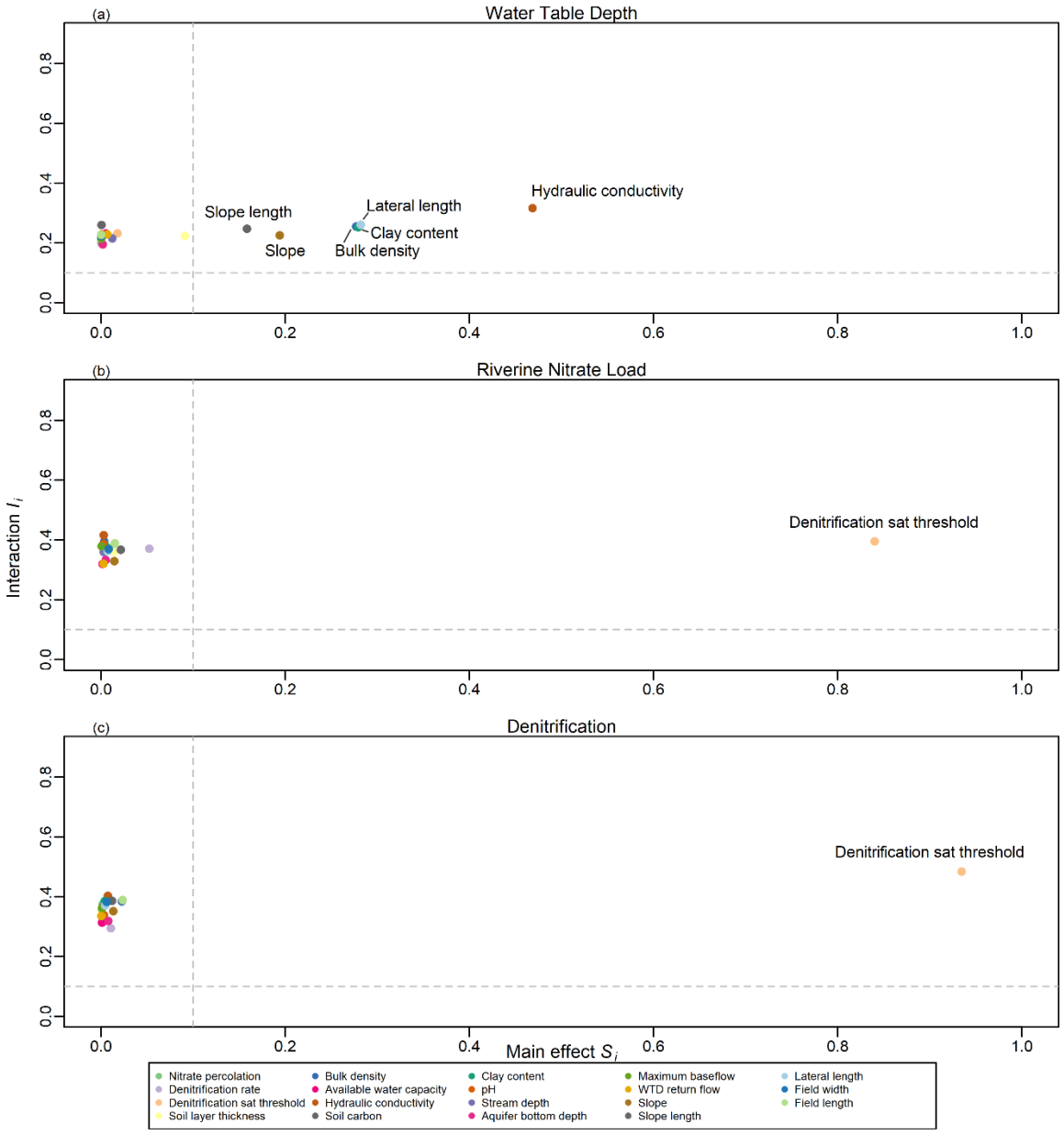

Figure 2.7. Sensitivity of the three chosen SWAT+ outputs to a subset of the selected input parameters using the CVD method (Baroni and Francke, 2020). Plots are arbitrarily divided the same as Baroni and Francke (2020; dashed line) to highlight the lowest values for the indices.

Results for the SWAT+ time-varying water table depth sensitivity analyses are shown in Figure 2.8. Water table depth was sensitive to hydraulic conductivity, clay, lateral length, bulk density, and slope at all time scales, including the full simulation. Soil layer thickness was not influential for the overall simulation but was for each of the finer time scales, with particular

importance during the final year of the simulation. Similarly, slope and slope length were influential at only the finer time scales, especially during the first and third years. Denitrification was only sensitive to the denitrification saturation threshold across all window sizes, but not during all time windows (Figure A6). No figure was necessary for riverine nitrate load because the only influential parameter was denitrification saturation threshold, which was influential during every time window.

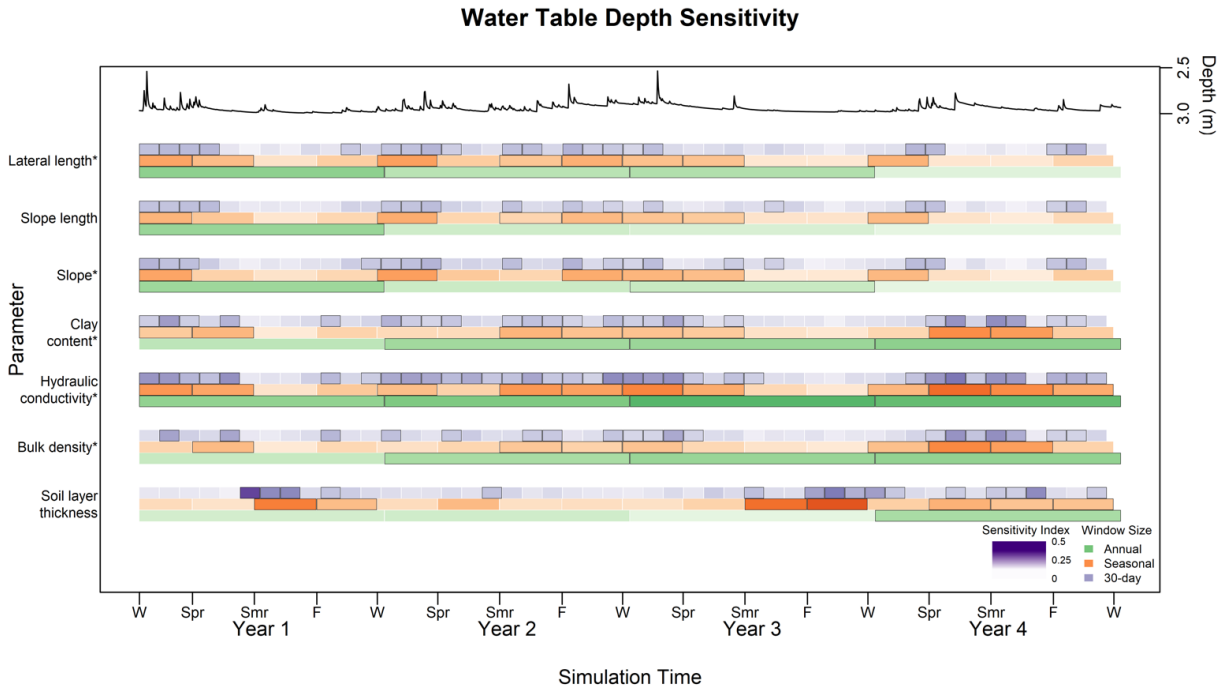

Figure 2.8. Time-varying sensitivity of the water table depth output in SWAT+ to the most influential parameters. Time windows are shaded according to the value of the sensitivity index. Times when parameters were highly sensitive (no overlap with the dummy variable sensitivity) are outlined. Parameters that were highly sensitive across the entire simulation length are denoted with an *. The average daily water table depth across all model runs is shown at the top.

Discussion

Riparian Nitrogen Model Comparison

Among the four models selected for evaluation of process inclusion and complexity, none simultaneously balanced complexity, broad utility, and presence of the most important processes

for riparian denitrification. We recognize that these models were not developed specifically for riparian denitrification, so this finding is not a criticism of each model's general utility, but an evaluation of its representation of this process. All of the models contained specific processes that required extensive input data that may not be feasible for users to provide. REMM provides detailed soils and vegetation parameterization but lacks in both groundwater and stream connections. RNM simplifies representations of nutrients, vegetation, and some aspects of hydrology. SWAT+ also simplifies nutrient cycling and groundwater flow, but its algorithms for connecting the stream to the riparian zone are the most robust of the four models analyzed. Finally, SWAT-MODFLOW-RT3D includes highly complex hydrology algorithms but also omits the necessary fluvial connections that influence water table dynamics. While these models are valuable tools for simulating riparian processes, they all lack robust representation of the influence of channel morphology on riparian nitrogen removal. These results suggest the need for an intermediate-complexity riparian denitrification model to integrate hydrology and riparian nitrogen cycling with stream channel processes.

REMM Expectations and Findings

Many of the highly sensitive parameters in REMM were unsurprising; however, there were several parameters that were not influential but were expected to be based on model structure, past sensitivity analyses, and physical understanding. Many past REMM sensitivity analyses used local methods, which are not directly comparable to our results but can be used to explore if certain outputs show sensitivity only at specific input values or across the entire range. Furthermore, those results are broadly comparable because several past studies used data from the same location (Gibbs Farm in Tifton, Georgia, USA; Graff et al., 2005; Kim et al., 2007; Lowrance et al., 2000) or physiographic region (coastal plain, Dukes and Evans, 2003; Tilak,

2012) as our analyses. It makes physical sense that water table depth was controlled by soil layer thickness, field capacity, and topographic parameters that influence water delivery (drainage area and surface slope), and past sensitivity analyses mostly corroborate these findings (Dukes and Evans, 2003; Graff et al., 2005; Tamanna et al., 2021; Tilak, 2012). Both physical understanding and past analyses suggested that depth to bedrock and stream depth influence water table depth (Altier et al., 2002; Dukes and Evans, 2003; Tilak, 2012); however, neither of these parameters were identified as highly important in our results. This discrepancy between our results and past local sensitivity analyses could be because we tested across the entire parameter space instead of only varying a single parameter by ± 10-100%. Since our results also do not align with our physical understanding, another reason for this disagreement could be due to how REMM represents these physical processes. For example, stream depth is based on thalweg elevation and is used to set the Zone 1 hydraulic gradient, limiting its effect to the near-stream zone.

For subsurface dissolved nitrate load, the sensitivity to permeability and slope coincided with previous analyses (Graff et al., 2005; Kim et al., 2007), but we expected higher sensitivity to parameters such as root depth and nitrate concentration. Tamanna et al. (2021) found that both water table depth and groundwater nitrate concentration were globally sensitive to soil porosity, yet we found porosity to be unimportant to those outputs. The sensitivity of dissolved nitrate to other influential parameters including percent clay and drainage area had not been studied in past sensitivity analyses. The importance of the rate coefficient K and soil layer thickness to denitrification made physical sense and aligned with past model studies (Lowrance et al., 2000; Tilak, 2012). However, more sensitivity was expected from other parameters such as rooting depth, carbon pools, pH, nitrate concentration, and soil temperature, which are used to calculate denitrification in the model (Altier et al., 2002) and have been shown to control denitrification in

field studies (Hefting et al., 2006; Hill et al., 2000; Šimek and Cooper, 2002; Waters et al., 2014). Soil hydraulic conductivity and clay content, which influence anoxic conditions by controlling soil saturation (Balestrini et al., 2016; Vidon and Hill, 2006, 2004), were also expected to be more influential. While denitrification showed slight sensitivity to some of these parameters (nitrate, permeability, soil temperature, clay percentage), the reduced importance of these indicates that the rate coefficient is the most substantial driver of the way REMM specifies denitrification. This diminished sensitivity to pH, rooting depth, and carbon pools could also suggest that our parameter modifications did not substantially limit the conditions for denitrification. Finally, for total nitrogen, drainage area and slope may have been most influential because they control water and nitrogen import and export, but previous local sensitivity analyses of total nitrogen either did not test these parameters or did not find them influential when varying them by ±50% (Kim et al., 2007; Lowrance et al., 2000).

SWAT+ Expectations and Findings

Given the novelty of SWAT+, we are not aware of any global sensitivity analyses that are comparable with these results. Although many major algorithms remained unchanged between SWAT and SWAT+, previous SWAT results were not used for comparison with these SWAT+ results due to the differences in hydrologic routing (Bieger et al., 2017). Most of the SWAT studies also analyzed different hydrologic and nutrient outputs such as streamflow and total nitrogen. Water table depth was most sensitive to topographic and soil parameters, which are both used directly to simulate water tables. Nitrate export and denitrification were only influenced by denitrification saturation threshold – different from literature regarding biogeochemical mechanisms in riparian zones. Both nitrate and denitrification should have been sensitive to changes in parameters that explicitly control nitrogen amounts such as nitrate

percolation and denitrification rate (Neitsch et al., 2011). We expected typical controls of denitrification such as soil carbon, pH, and stream depth to be influential (Mosier et al., 2002; Qiong et al., 2020), but they were not. Our physical understanding also suggests that aquifer properties should have showed greater control of nitrate transport to streams by affecting groundwater movement throughout the watershed. However, a review of field nitrate studies found that denitrification was primarily controlled by factors indicative of redox conditions such as saturation and that other environmental variables including nutrient availability and pH were much less influential (Rivett et al., 2008), findings that agree with our SWAT+ results. The overwhelming importance of the denitrification saturation threshold indicates that SWAT+ emphasizes when denitrification can occur more than how much denitrification can occur (e.g., denitrification rate), which aligns with the concept of biogeochemical "hot spots" and "hot moments" (McClain et al., 2003).

Time-varying Sensitivity Analyses

The time-varying results for both REMM and SWAT+ corresponded well with trends in outputs and hydroclimatic conditions, which aligned with previous time-varying sensitivity analyses (Herman et al., 2013b; Wu et al., 2022; Xie et al., 2017). For REMM, water table depth was most sensitive to drainage area and surface slope in wetter years, while most of the influence of field capacity was during drier years when the water table was suppressed. These relationships make physical sense because drainage area and slope control the volume of water reaching the subsurface when groundwater tables are rising, while field capacity controls water draining from soil pores when the water table is falling. Percent clay and permeability were most frequently influential at fine time scales during winter. In SWAT+, water table depth was most sensitive to soil layer thickness when water table depth was low, which coincided with drier periods.

Conversely, the importance of the other soil and topographic parameters generally decreased during these drier times. Denitrification in REMM was sensitive to drainage area and surface slope only at seasonal and 30-day time windows and during summer and fall of the first two years, when denitrification peaked. Soil layer thickness was most important at annual and seasonal time windows, also during the peak periods of denitrification. This correspondence to peak denitrification suggests the importance of saturation in calculating denitrification in REMM, especially since these parameters also controlled water table depth at varying scales. The sporadic sensitivity of total nitrogen to permeability and rainfall interception during the summers of Years 2 and 3, respectively, was surprising, but these were wet periods, indicating the importance of total water export in controlling nitrogen loads. The consistent sensitivity of denitrification and riverine nitrate load to denitrification saturation threshold in SWAT+ showed the overwhelming importance of that parameter, regardless of output magnitude or hydroclimatic condition. Again, this suggests that whether the soil is wet enough for denitrification is more important than the rate of denitrification in SWAT+. Periods when denitrification was not sensitive to anything did not correspond to specific climatic conditions.

These time-varying analyses also allowed us to identify parameters that are influential regardless of time scale, output magnitude, or hydroclimatic condition (e.g., denitrification rate coefficient for denitrification in REMM; denitrification saturation threshold for riverine nitrate load in SWAT+). Furthermore, we identified parameters with increased prevalence of sensitivity as window size decreased, a relationship that has previously been shown to depend on output process time scale (Pianosi and Wagener, 2016; Xie et al., 2017). For example, in REMM, water table depth may have been more sensitive to percent clay at finer time windows because clay affects soil water movement at the daily and sub-daily time scale, an effect that can appear less

influential when aggregated to larger time periods. Topographic parameters such as drainage area and slope showed more influence at coarser time scales, indicating a greater influence in the long-term than the day-to-day hydrologic and nitrogen cycles.

Comparing REMM and SWAT+

Global sensitivity analyses on riparian nitrogen models are rare in literature, making these detailed evaluations of REMM and SWAT+ a novel contribution. Results from both global sensitivity analyses somewhat agreed with each other and with previous findings. Both sensitivity analyses showed water table depth was influenced by topographic parameters such as slope and slope length, which corroborated past research (Burt et al., 2002, 1999; Vidon and Hill, 2004). Water table depth was also controlled by soil properties including hydraulic conductivity, soil texture, and soil thickness, consistent with previous studies (Amatya et al., 1997; Burt et al., 1999; Hinton et al., 1993; van Meerveld et al., 2015). However, the two models did not have similar findings for the nitrogen cycling outputs. SWAT+ nitrate and denitrification outputs did not show sensitivity to soil and topographic parameters, particularly those that were influential in REMM. SWAT+ was highly sensitive to changes in denitrification saturation threshold, a value hardwired in REMM (Altier et al., 2002).

One possible factor contributing to differences between the model results is spatial scale – REMM operates at the field scale and SWAT+ at the watershed scale. Similar topographic and soil parameters influenced water table depth between the models, indicating that this process has similar controls at both the field and watershed scale. The slight (or high) sensitivity of nitrogen cycling in REMM to soil parameters suggests that soil characteristics are more important for estimating nitrogen cycling at a riparian scale than at larger, watershed scales, where soil characteristics may be more variable and the effect of a unique characteristic could be

diminished. Denitrification may also have been more sensitive to the rate coefficient in REMM than in SWAT+ because the riparian zone is consistently wetter relative to the saturation threshold than across an entire watershed. This suggests that denitrification at the watershed scale may be more controlled by the timing of when denitrification can occur but that the rate of denitrification is more important at the field scale where denitrification can occur more regularly. These results align with recent findings that spatial sensitivity patterns in nitrogen modeling depend on nitrogen inputs and hydrological transport capacity (Wu et al., 2022). Whatever difference in model results that can be attributed to spatial scale has implications for model users who can focus parameterization efforts on the processes and parameters that dominate at the scale of interest.

The discrepancies between these results and expectations based on past findings could also be due to model purpose and structure. Model developers come from various disciplines, often including and emphasizing the processes that best achieve the purpose of the model. Riparian denitrification was not a main focus of the selected models, possibly causing results to differ from expectations. REMM was developed to estimate the water quality benefits of riparian buffers for pesticides and nutrients, while SWAT+ was developed to improve water and pollutant routing for watershed-scale water resources modeling and management. Furthermore, the complexity required for a calculation or simplifying assumptions made can influence the sensitivity analysis results. In REMM, denitrification relies on seven factors, including four multipliers that each vary with their own unique factors. Having so many factors that affect a single output can diminish the sensitivity of that output to expected inputs, particularly if one is inherently more heavily weighted than the others or is hard-coded in the model and cannot be changed. One reason that stream depth may not have been influential in REMM is that the model

only uses stream depth for setting the hydraulic gradient in the near-stream zone (Altier et al., 2002), underrepresenting its importance in hydrologic and nutrient cycling calculations. In SWAT+, stream depth is classified as a routing parameter and may be more intended for in-channel processes than those in the floodplain. Nutrient calculations in this version of SWAT+ have not been extensively tested (R. Srinivasan, pers. comm.), so further testing and refinement could yield more expected results. Several input variables that are often important for nitrate and denitrification calculations – hydraulic conductivity and soil texture, for example – are not directly involved in model code for those processes (Neitsch et al., 2011), although they can still indirectly influence denitrification by controlling soil water movement. Other denitrification controls including nitrate concentration, initial water table depth, and soil temperature have been influential in past studies (Batlle-Aguilar et al., 2012; Bouwman et al., 2013), but SWAT+ structure currently precludes Monte Carlo analysis of these parameters. Regardless, both denitrification rate and soil organic carbon are explicitly used in SWAT+ denitrification calculations (Neitsch et al., 2011) and therefore should have shown more influence in our results.

Comparing Sensitivity Analysis Methods

Another possible explanation for disagreement between the results and expectations could be due to the global sensitivity analysis methods. SWAT+ does not have a published global sensitivity analysis, and the only one published for REMM used integrated local-global methods with limited parameters (Tamanna et al., 2021). Testing REMM across the entire parameter space simultaneously instead of with a local sensitivity analysis may have been responsible for different results (Blasone et al., 2007).

Different global sensitivity methods can yield different results. While we found slight differences in parameter importance using the Plischke et al. and CVD methods, the fact that the

two approaches largely agreed increases confidence in our findings. Another benefit of including the CVD method for the full simulation was the calculation of main and total (main plus interaction) effects to assess parameter importance and identifiability. We define identifiability as the ability to constrain a vector of parameter values to reduce model uncertainty (Ghasemizade et al., 2017; Guillaume et al., 2019). Parameters with high main effect and low interaction effect are important and identifiable, while those with high interaction effects are not identifiable (Baroni and Francke, 2020; Ghasemizade et al., 2017). Important and identifiable parameters in REMM were drainage area and slope for total nitrogen (Figure 2.4d) and denitrification K for denitrification (Figure 2.4c). Layer thickness was the most important and identifiable parameter for water table depth, although there was less disparity in main effect size than for other outputs (Figure 2.4a). Hydraulic conductivity was the most important parameter for determining water table depth in SWAT+, but had the highest interaction effect size. In general, the CVD method estimated higher interaction effects, and thus fewer identifiable parameters, for subsurface dissolved nitrate in REMM (Figure 2.4b) and riverine nitrate load and denitrification in SWAT+ (Figure 2.7b and 2.7c, respectively), which indicate model complexities that could explain why these outputs were highly sensitive to only one or two inputs and insensitive to others we expected.

Future Research

The initial evaluation of riparian nitrogen models determined that, while they are valuable tools under many landscape settings, they include overly complex methods for some processes, while omitting or incompletely modeling others. This finding was substantiated with sensitivity analyses that showed both water table depth and several nitrogen outputs were not sensitive to a majority of model inputs. A critical parameter with minimal influence in the

models was stream depth, which represents the connection between channel and riparian processes. Due to the prevalence of stream erosion and incision as a result of land use change (Booth, 1990; Rheinhardt et al., 2009; Schilling et al., 2006; Shields et al., 2010; Simon and Robbins, 1987) and its known effect on both riparian hydrology (Groffman et al., 2003, 2002; Hardison et al., 2009; Jung et al., 2004; Omar et al., 2014; Schilling et al., 2004) and nitrogen cycling (Böhlke et al., 2007; Gift et al., 2010; Groffman et al., 2002; Korol et al., 2019; Schilling et al., 2006; Schilling and Jacobson, 2008), this relationship requires improved model specification. This research gap can be addressed by developing a parsimonious riparian nitrogen cycling model that includes the most sensitive parameters from REMM and SWAT+, plus necessary parameters and algorithms for estimating the interplay between riparian nitrogen cycling, hydrology, and stream processes. As identified in our sensitivity analysis, major inputs should include topographic parameters (slope, slope length, drainage area), soil parameters (soil texture, layer thickness, hydraulic conductivity), and nutrient parameters (carbon pool sizes, denitrification rate coefficient and saturation threshold). This model should incorporate many of the features in Table 2.3 at sufficient complexity to represent the necessary processes across various physiographic settings, but not so complex that it cannot be used and understood by watershed managers and modelers.

Incorporating stream connections into model specification will be a challenging yet necessary step for improving the state of riparian nitrogen modeling. Notably, this connection was made when REMM was coupled with CONservational Channel Evolution and Pollutant Transport System (CONCEPTS) to investigate the role of riparian water and vegetation on streambank erosion (Langendoen et al., 2009). While the coupled model did not include nitrogen cycling, it was an important initial step in modeling the riparian-stream morphodynamic

interaction. Including this interaction in future modeling efforts will require accounting for dynamic stream processes in response to changes throughout the watershed and stream network. Geometry and geomorphology of streams evolve along various trajectories, and a subsequent model must be capable of simulating stream conditions in different stages of channel evolution (Booth and Fischenich, 2015; Cluer and Thorne, 2014; Hawley et al., 2012; Schumm et al., 1984). Stream depth can be modeled by accounting for in-channel erosion and deposition, which can then be applied to riparian calculations for estimating water table depth and denitrification.

Hydrodynamic connections at the surface water-groundwater interface should also be incorporated. Since nitrogen cycling can vary in response to losing and gaining stream conditions (Shuai et al., 2017; Trauth et al., 2018), a model should be capable of simulating the bidirectional transfer of water and nitrogen between streams and riparian zones. Determination of the hydraulic gradient based on stream depth and stage, as well as riparian hydrology, will be necessary for accurately estimating two-way fluxes of water and nutrients. Incorporating these stream-riparian connections is essential, and should be done in the simplest way possible, while still including sufficient mechanistic rigor, to reduce the number of required model inputs. In this way, a robust yet intermediately-complex model can be developed for studying the role of riparian zones for mitigating nitrogen loading.

This improved riparian nitrogen modeling tool will be valuable for more comprehensively addressing nitrogen loading in incised stream networks. Riparian zones are an effective strategy for retaining and removing nitrogen, but these capabilities can be compromised by stream incision. Thus, management strategies to mitigate nitrogen loading should prioritize both riparian and stream condition, emphasizing the hydrologic connection between the two. Global sensitivity analyses, like those in this study, improve understanding of model

performance and limitations across a more encompassing range of parameter values and time scales, which can be supplemented with knowledge of various real-world systems to ultimately provide beneficial insights that inform action. The coupled riparian-stream approach is currently overlooked in management practices, but the development of a parsimonious riparian nitrogen and channel morphodynamic model will be a significant enhancement to the toolbox for watershed managers looking to identify locations for and benefits of stream and riparian restoration.

Conclusions

Four standard riparian nitrogen models – REMM, RNM, SWAT+, and SWAT-MODFLOW-RT3D – were evaluated for their completeness and complexity of algorithms related to hydrologic processes, vegetation, soils, nutrients, and channel morphodynamic influences. This was coupled with a global sensitivity analysis of REMM and SWAT+ to identify the most influential parameters for determining water table depth and nitrogen cycling outputs. The four models exhibited varying degrees of complexity for different components, but a common finding was that the connection between riparian zones and stream morphodynamics was missing or minimal. Drainage area, slope, and soil layer thickness were the most commonly sensitive parameters across the chosen outputs in REMM. Other nutrient and soil parameters including denitrification rate coefficient, permeability, and soil moisture controls like field capacity were also influential for certain outputs. In SWAT+, water table depth was most sensitive to soil parameters such as hydraulic conductivity, clay content, and bulk density, and the topographic parameters of lateral length, slope, and slope length. Nitrate export and denitrification were only sensitive to denitrification saturation threshold, which might suggest the importance of defining when nitrogen removal can occur and not just the rate of removal. Time-

varying analyses of both models found a relationship between output sensitivity and hydroclimatic conditions that affected output magnitude. Greater sensitivity of nitrate and denitrification to soil properties such as hydraulic conductivity, carbon, and pH was expected based on past research. Our sensitivity results also confirm the need for an increased influence of stream depth on water table depth and riparian nitrogen cycling.

These analyses illustrate the need for improving riparian nitrogen modeling by striving for parsimony in the processes that are included and how extensively each is parameterized. Improved models that combine the best features of existing tools, make appropriate simplifying assumptions, and expand processes that are predominantly omitted are needed to improve model fidelity to physical understanding and support management applications across dynamic channel networks. Ultimately, the finding that all models underrepresented stream connections and that none of the select model outputs were sensitive to stream channel depth, which could result from incision and other factors, verified the need for further study, and specifically modeling, of riparian nitrogen-channel morphology interactions. Field studies have shown the influence of channel dynamics on riparian hydrology and nitrogen cycling, making this modeling gap an important one to address. Development of intermediate-complexity riparian nitrogen models using both the most influential parameters and important missing parameters shown in this analysis will provide water resources managers and researchers with improved tools for estimating the role of riparian zones in mitigating nitrate loading to streams, and how these benefits are impacted by channel morphodynamics.

CHAPTER 3

EFFECTS OF STREAM INCISION ON GROUNDWATER-SURFACE WATER INTERACTIONS AND RIPARIAN DENITRIFICATION[2]

[2] Buhr, D.X., and B.P. Bledsoe. To be submitted to *Hydrological Processes.*

Abstract

Riparian zones can create biogeochemical conditions promoting denitrification, reducing excess nitrogen loading to aquatic systems. Groundwater-surface water interactions in riparian areas control the exchange of organic matter, nutrients, and other constituents among streams, aquifers, and adjacent land uses. An understudied control on groundwater-surface water interactions and nitrogen cycling is stream channel incision, which can lower groundwater tables and reduce nitrogen removal in riparian zones. We studied groundwater-surface water and nitrogen dynamics at paired incised and unincised stream reaches at two locations in the southeast US with varying soils, land use, and physiography. Channel incision lowered the riparian groundwater table and influenced groundwater-surface water gradients and dynamics. Both incised stream reaches were largely gaining groundwater, while unincised reaches were mainly losing water to the riparian zone over 16 months of sampling, despite the adjacency of these reaches. This relationship varied with groundwater fluctuations due to storm events and seasonal changes in evapotranspiration. Riparian zones removed an estimated 40-95% of available nitrogen via groundwater denitrification. Total denitrification gases (N_2O and excess N_2) were similar for all transects and composed of nearly 50% N_2O, an indicator of incomplete denitrification. In near-stream wells, a predominantly losing, unincised reach removed ~20% more available nitrogen than its paired incised reach, which, combined with the marked effects of incision on groundwater levels, indicates that incision may substantially alter near-stream nitrogen dynamics in certain settings. We recommend that future studies consider interactions between incision and gaining and losing stream conditions to better understand potential differences in riparian denitrification and pollutant loading associated with channel change. This research provides a unique dataset spanning contrasting stream morphologies and can inform

future research to understand the effects of channel incision on nitrogen loading in disturbed drainage networks.

Introduction

Groundwater-surface Water Interactions

Groundwater-surface water interactions are important to understand because inputs of groundwater, nutrients, organic matter, and other solutes to streams sustain stream baseflow, primary productivity, metabolism, temperature buffering, and ecological and bacterial community composition (Brunke and Gonser, 1997; Holmes, 2000). Conversely, stream inputs to the local aquifer can provide recharge and enhance biogeochemical cycling (Brunke and Gonser, 1997). Groundwater-surface water interactions have been studied arduously in recent decades, with focus on varying spatial scales and measurement techniques (Jimenez-Fernandez et al., 2022). Improved understanding of the spatiotemporal patterns of groundwater-surface water exchange is useful for assessing in-stream water quality patterns (Covino et al., 2011; Jimenez-Fernandez et al., 2022; Ranalli and Macalady, 2010). Continuing to evaluate these interactions is critical for water resources management and restoration efforts.

Streams can be classified as gaining or losing, depending on the direction of the groundwater-surface water exchange. Gaining streams receive flow from adjacent groundwater, due to a hydraulic gradient toward the stream, while losing streams have a reversed hydraulic gradient, with water leaving the stream. Gaining and losing conditions can vary spatially and temporally (Cardenas, 2009; Gordon et al., 2004; Wroblicky et al., 1998), which can have variable effects on the transfer of solutes such as nitrogen between the local aquifer and surface water. Various controls on groundwater-surface exchange include climate, topography, geology, and watershed position (Sophocleous, 2002; Winter et al., 1999). These controls combine to

influence the magnitude and direction of surface water-groundwater interactions (de Graaf et al., 2019; Jasechko et al., 2021).

Stream geomorphological processes are another major, yet less studied, control on groundwater-surface water exchange (Larkin and Sharp, 1992). Channel incision, or vertical downcutting via bed erosion, is commonplace (e.g., Booth, 1990; Groffman et al., 2002; Schilling et al., 2006; Simon and Robbins, 1987) as a result of channel straightening or land use changes (Shields et al., 2010). Groundwater tables are significantly lower in riparian zones adjacent to incised streams compared to unincised channels with well-connected floodplains (Hardison et al., 2009; Schilling and Jacobson, 2014).

Riparian Zones and Nitrogen Cycling

Riparian zones are critical areas of biogeochemical cycling of many pollutants, particularly nitrogen (Vidon et al., 2010). Nitrogen is an important pollutant to study because it causes a variety of environmental problems, including drinking water contamination and eutrophication (Howarth et al., 2011). Under ideal conditions, riparian buffers can remove greater than 90% of groundwater nitrate (Peterjohn and Correll, 1984; Pinay et al., 1993; Spruill, 2000), contributing more removal than in-stream processes (Craig et al., 2008; Lammers and Bledsoe, 2017). These conditions include low oxygen and an organic carbon source, which encourage denitrification – the anoxic reduction of NO_3- to N_2O or N_2 gas by heterotrophic bacteria (Hill, 1996). Denitrification is a desirable process for pollution control because it permanently removes nitrogen from the aquatic system, transferring it in an inert form to the atmosphere.

In addition to its role in altering groundwater-surface water exchange, stream geomorphology can play an important – and largely overlooked – role in riparian nitrogen

cycling. The lower riparian water tables resulting from stream incision create a larger unsaturated zone, disconnecting groundwater from vegetation (Petralia, 2022) and carbon-rich surface soils, potentially limiting denitrification and increasing nitrate loading to streams (Böhlke et al., 2007; Groffman et al., 2002; Mayer et al., 2010). While field studies have demonstrated that channel incision can reduce riparian denitrification, these have been limited to a few urban watersheds in the mid-Atlantic (Groffman et al., 2002; Mayer et al., 2010) and a rural watershed in Iowa (Schilling et al., 2006; Schilling and Jacobson, 2014).

It is important to study the dynamics among stream geomorphology, groundwater-surface water exchange, and riparian nitrogen cycling to improve understanding of the effects of channel incision on nitrogen loading to streams. Addressing this knowledge gap can improve numerical accuracy of models for estimating nitrogen loading at the watershed scale, which can be used for spatial prioritization of watershed restoration. Enhanced understanding of incision-related changes in nitrogen loading can highlight the importance of flow management and stream restoration for water quality improvement.

To our knowledge, no datasets are available that link continuous monitoring of riparian and stream hydrology and nitrogen cycling with variable stream geomorphology. In addition to addressing this gap, the objectives of this research are to: 1) investigate continuous groundwater-surface water interactions at southeast US streams with different physiographic context, soil type, and land use, and 2) measure nitrogen transport and transformation in riparian zones of disturbed streams. Continuous monitoring of groundwater and streamflow levels is useful for examining patterns in hydrologic connections at seasonal and event-based temporal scales. Comparing locations with intra-site variability in stream morphology can improve understanding

of the effects of channel change on groundwater-surface water interactions and riparian nitrogen cycling, which can inform estimation and management of nutrient loading.

Methods

Study Sites

We examined riparian groundwater and stream elevations and riparian nitrogen dynamics at two stream study sites, Dairy Farm and McQueen Branch, with paired incised and unincised reaches (Table 3.1). The first study site is located in the piedmont physiographic region at the University of Georgia Teaching Dairy Farm, southeast of Athens, GA, USA (Figure 3.1). The study stream is a perennial unnamed tributary to Big Creek, a channel that was straightened prior to 1938 (based on available aerial imagery). This channel straightening induced incision, which caused a headcut to form on the tributary stream. We placed our paired incised and unincised reaches approximately 40 m apart, downstream and upstream of this headcut, respectively. Historic and current land use contribute to ongoing channel evolution of piedmont streams, inputting significant loads of fine sediment to watersheds (Mukundan et al., 2011; Schoonover, 2005). A forested riparian buffer of at least 10 m separates the tributary from surrounding agricultural fields. The soil type at our study transects is predominantly sandy clay loam.

Table 3.1. Summary characteristics of the two study sites. *Watershed area draining to the headcut between reaches.

	Dairy Farm	**McQueen Branch**
Location	Piedmont region, GA	Sand hills region, SC
Watershed Area*	0.4 km^2	2.0 km^2
Soils	Sandy clay loam	Sand
Land Use	Active dairy farm	Primarily forested
Stream Incision	Incision caused by straightening of main channel.	High runoff from developed areas leading to incision.

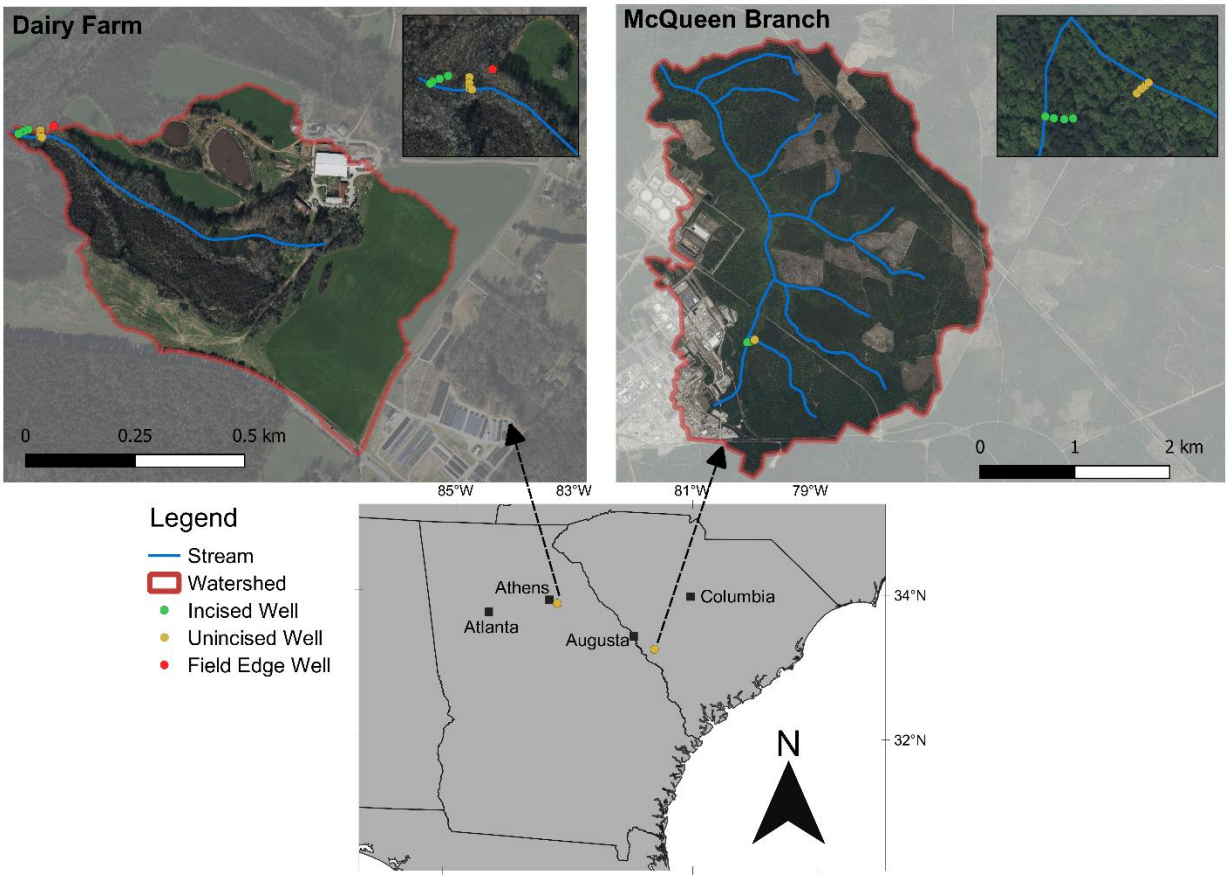

Figure 3.1. Maps of the two study watersheds with sampling points indicated by yellow, green, and red dots. Sampling locations are upstream and downstream of the headcut at the Dairy Farm (top left), respectively, and upstream on the mainstem and tributary at McQueen Branch (top right).

The McQueen Branch site is located on the US Department of Energy (DOE) Savannah River Site (SRS; Figure 3.1). The SRS lies in the Sand Hills ecoregion on the southeast coastal plain, where surface and subsurface sand deposits are prevalent (Siple, 1967). The high porosity of these sand deposits means that most natural streams receive water, and therefore dissolved nitrate, via groundwater flow (Dosskey and Bertsch, 2016). Stream channels in drainage areas influenced by industrial facilities (like our study stream) are susceptible to incision as a result of amplified, erosive overland flows from impervious surfaces imposed on fine-grained, non-cohesive bed materials such as erodible sand deposits (Magilligan and Stamp, 1997). Prior to

becoming a DOE site, the area was primarily row crop agriculture, which likely left some legacy nitrogen.

McQueen Branch, like the dairy farm site, consists of an unincised, perennial tributary flowing into an incised main channel. This forms a headcut at the channel junction, which provides a direct comparison between incised and unincised channels. Each reach is approximately 100 m upstream of the junction on its respective stream. Both channels are perennial, but the mainstem receives runoff from a large industrial area to the west, which is likely responsible for increased flows and ongoing channel incision (D. Fletcher, Savannah River Ecology Laboratory, personal communication). The tributary drains primarily forested land.

Field Methods

We established transects of monitoring well nests perpendicular to the stream channel at both incised and unincised reaches at each location. At the dairy farm, these transects were upstream and downstream of a headcut on the same tributary, while at McQueen Branch the unincised transect was on a tributary of the incised mainstem. Each transect contained three nests with three wells each. Nests were installed adjacent to the stream, midway through the riparian zone, and at the upland-riparian interface, with specific distances dependent on the width and geometry of the riparian zone. At each nest, three wells were installed to different depths. One was screened to collect water from the plant rooting zone (up to 1 m below ground surface), one to collect water from the intermediate zone (1 – 2 m below ground surface), and the final well to collect water from deeper flow paths (>2 m below ground surface). These depths were site-specific, depending on vegetation characteristics, geologic controls, and expected low water table elevation. Wells were 5.1 cm diameter PVC pipe and backfilled with well sand to approximately 10 cm below the ground surface and sealed with bentonite. Stream monitoring wells were also

installed and vented to allow flow to pass through. An additional well was installed near the field edge at the dairy farm to approximate groundwater conditions upland of the riparian zone.

During groundwater well installation, soil samples were collected from each screened depth and analyzed for texture with a hydrometer (Gee and Bauder, 1979). Organic matter content was quantified from loss on ignition and used to estimate soil organic carbon (Dean, 1974). We surveyed well elevations and channel cross-section geometry annually at each transect using a total station. We also surveyed a longitudinal profile annually using a laser level. These repeated measurements allowed us to quantify the extent of incision and how it changed over the monitoring period.

Continuous, 5-minute groundwater elevations were monitored by installing a pressure transducer in the deep well of each nest. Depth to groundwater was measured monthly to calibrate measured groundwater elevations. Pressure transducers also recorded stream elevation at 5-minute intervals. Precipitation data were collected at 5-minute intervals using an Onset HOBO tipping rain gauge installed in an open area near the stream (within 0.5 km).

Grab samples were collected monthly from streams and all groundwater wells with sufficient water. An extra sample was collected on the McQueen Branch mainstem below the confluence with the unincised tributary. Wells were purged one day in advance to ensure collection of fresh groundwater. Groundwater samples were collected using a peristaltic pump with a low pumping rate of about 100 mL/min. Samples were vacuum filtered through a 0.45 μm Supor ® filter (Pall, shop.pall.com) within 24 hours of collection and analyzed for dissolved nutrients: nitrate + nitrite, ammonia, total nitrogen, and organic carbon. Chloride was quantified as a conservative tracer to account for effects of dilution on reducing nitrate concentrations. Samples for total nitrogen and organic carbon were stored at 3°C, while all other samples were

frozen at -5°C. Analysis was performed by the Phillips Water and Soil Laboratory at the University of Georgia using the cadmium reduction method (Clesceri et al., 1998) on an Astoria Pacific flow analyzer for nitrate, the phenate method (Clesceri et al., 1998) and fluorometry (Aoki et al., 1983) on an Astoria Pacific flow analyzer for ammonia, high temperature combustion on a Shimadzu TOC-L analyzer for dissolved organic carbon, chemiluminescence on a Shimadzu TNM-L analyzer for total nitrogen, and ion chromatography on a Dionex ICS-2100 for chloride. Additional groundwater samples were collected from deep wells and sent to the Cary Institute of Ecosystem Studies for analysis of headspace gases— N_2:Ar gas ratios using membrane-inlet mass spectrometry as described in Kana et al. (1994) and N_2O concentration using automated gas chromatography (GC) on a Shimadzu GC-14 GC system for greenhouse gas analysis. Calculations to estimate excess N_2 and convert these dissolved gas measurements into denitrification estimates are in Appendix B. Water chemistry data (temperature, pH, dissolved oxygen, specific conductance) were collected in the field using a YSI multiparameter probe.

Nitrous Oxide Fluxes

N_2O flux (kg N_2O-N/ha/yr) from groundwater was estimated using Equation 3.1, adapted from Vilain et al. (2012). We assumed that all N_2O was released into the atmosphere from input to the stream or diffusion from the water table to the unsaturated zone. We assumed a constant N_2O concentration and groundwater discharge between each sampling event.

$$Flux = \frac{\Sigma(C_i Q_i n_i)}{\Sigma(n_i)A} * 365 \qquad \text{[Eq. 3.1]}$$

Where C_i is the groundwater concentration of N_2O-N in the near-stream well (kg/L), Q_i is instantaneous groundwater discharge (L/day), n_i is the number of days between sampling events, and A is riparian zone surface area (ha). Groundwater discharge was calculated with Darcy's Law using the hydraulic gradient at sampling, cross-sectional area at the riparian-stream

interface, and hydraulic conductivity (Soil Survey Staff, 2022). We only estimated N_2O flux within the first 3 m from the stream on each side because that was the maximum distance between the stream and our near-stream well, where we observed the most pronounced effects of incision. N_2O flux was converted to CO_2eq by assuming that 1 kg N_2O equals 298 kg CO_2eq.

We estimated potential greenhouse gas emissions within 3 m adjacent to low-order streams in the United States. There are 5.195 million km of stream length in the NHDPlus V2 dataset for the conterminous United States at 1:100k resolution (McManamay and DeRolph, 2019). We assumed that approximately 80% of that stream length was low-order streams and multiplied the average greenhouse gas emission rate between our two sites by the surface area within 3 m on each side of this stream length. Finally, we compared this estimate to annual, energy-based global greenhouse gas emissions (40.8 Gt CO_2eq in 2021; International Energy Agency, 2022) and annual US nitrous oxide emissions (265.72 Mt CO_2eq in 2019; Climate Watch, 2022). We estimated a range of emissions by repeating these calculations for scenarios where incised streams composed 0% and 100% of low-order streams.

Statistical Analyses

We compared differences in water chemistry parameters, nutrient concentrations, and denitrification by site (dairy farm and McQueen), transect (incised and unincised), depth, and proximity to stream. Denitrification data were also analyzed for differences between gaining and losing conditions. Data were tested for normality using the Shapiro-Wilks test, and any data that violated the normality assumption required non-parametric analyses. Nearly all data violated normality and were analyzed using a Kruskal-Wallis H test. When we found a statistically significant difference, we further analyzed relationships with a Dunn test for multiple comparisons. Data that did not violate normality were analyzed using analysis of variance

(ANOVA). Additionally, two-sample t-tests assuming unequal variances were used to compare nitrate and ammonia concentrations at each transect. Significance level was set at $p = 0.1$. All analyses and plotting were conducted in R (R Core Team, 2021) using the following packages: *rstatix* (Kassambara, 2023), *FSA* (Ogle et al., 2023), *dplyr* (Wickham et al., 2020), *RColorBrewer* (Neuwirth, 2014), and *vioplot* (Adler et al., 2022).

Results

We observed that stream incision lowered the riparian groundwater table and affected gaining and losing conditions, with seasonal and event-based switching. Stratifying the water quality data based on groundwater-surface water gradient, incision, and proximity to stream were important for analyzing controls on nitrogen dynamics. In this section, we present our groundwater-surface water observations at each site, followed by site-specific trends in water chemistry and nitrogen concentrations, before showing denitrification gas results combined across both sites. Annual survey results, which showed minor variations in bankfull width and slope within our measurement uncertainty, are summarized in Appendix B (Table B1).

Hydrology

Dairy Farm

At the incised transect at the dairy farm, groundwater was often more than one meter below the ground surface and became closer to the surface moving away from the stream (Figure 3.2a). Groundwater at the unincised transect followed an opposite trend, with upland groundwater around one meter below the surface and near-stream and intermediate groundwater typically within 0.5 meter of the ground surface (Figure 3.2b). The distribution of groundwater elevations was more variable at the incised transect than the unincised transect. Seasonal trends in groundwater elevation occurred at both transects, with groundwater levels elevating in winter

then receding from May-October 2021 and 2022, with periodic groundwater rises due to precipitation (Figure 3.2c-d). This recession switched the incised stream reach from gaining to losing during the driest periods in summer 2021 and 2022 (Figure 3.2c). The unincised stream reach was losing during the entire monitoring period (Figure 3.2d).

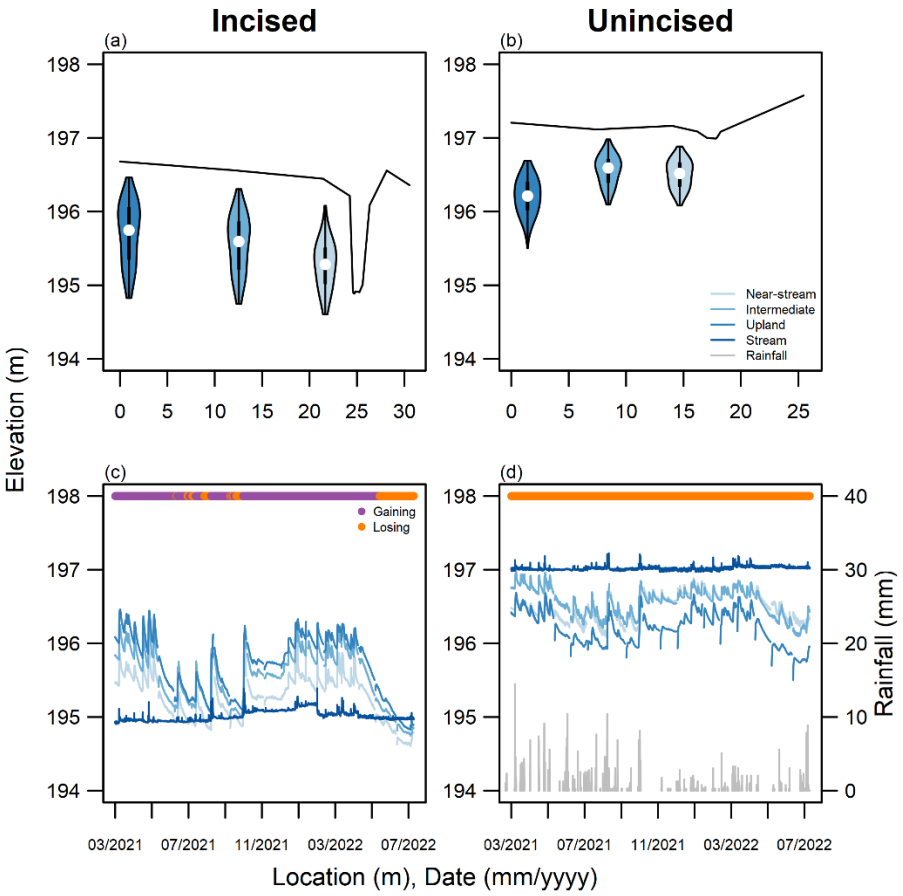

Figure 3.2. Groundwater monitoring results from the dairy farm, with distributions of elevations in the deep wells relative to the ground surface (a-b) and time-series of elevations relative to the stream elevation (c-d). Rainfall collected at 5-minute intervals is shown with gray bars (d). Gaining and losing conditions are denoted by color bars in (c) and (d). Gaps in the time series indicate data removed on sampling dates.

McQueen Branch

At the incised transect at McQueen Branch, groundwater was often approximately two meters below the ground surface and became closer to the surface moving away from the stream (Figure 3.3a). Groundwater at the unincised transect followed an opposite trend, with upland

groundwater around 0.5 meter below the surface and near-stream groundwater occasionally above the ground surface (Figure 3.3b). The distribution of groundwater elevations was more variable at the incised transect than the unincised transect. Seasonal trends in groundwater elevation occurred at both transects, with groundwater levels elevating in winter then receding from May-October 2021 and 2022, with periodic groundwater rises due to precipitation (Figure 3.3c-d). This seasonal variation was sufficient to switch the unincised stream reach from predominantly losing during dry periods of the summer to gaining when the groundwater table elevated in the winter (Figure 3.3d). The incised stream reach was gaining nearly the entire monitoring period except for several stormflows when the stream elevation rose above the adjacent groundwater elevation (Figure 3.3c).

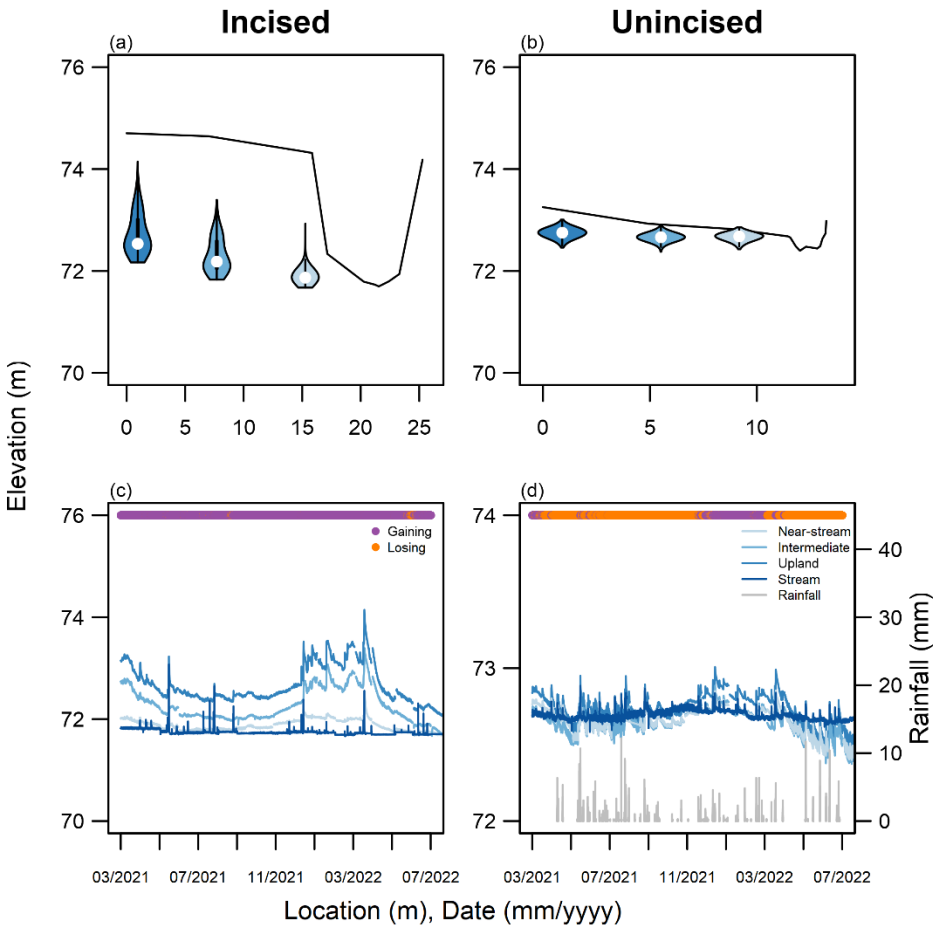

Figure 3.3. Groundwater monitoring results McQueen Branch, with distributions of elevations in the deep wells relative to the ground surface (a-b) and time-series of elevations relative to the stream elevation (c-d). Rainfall collected at 5-minute intervals is shown with gray bars (d). Gaining and losing conditions are denoted by the color bars in (c) and (d). Gaps in the groundwater time series indicate data removed on sampling dates.

Water Quality

Dairy Farm

Stream and groundwater temperature ranged from 6.2 to 23.8°C (Figure 3.4a) and was significantly higher at the unincised transect ($\chi^2 = 4.97$, $p = 0.03$). Temperature did not vary across nests ($\chi^2 = 1.49$, $p = 0.47$) and depths ($\chi^2 = 0.86$, $p = 0.65$). Dissolved oxygen was higher at the incised transect compared to the unincised ($\chi^2 = 52.7$, $p < 0.001$) and varied with depth ($\chi^2 = 12.8$, $p = 0.002$), peaking in the intermediate wells (Figure 3.4b). Specific conductance was

greater than 100 μS/cm everywhere except in the field-edge well (Figure 3.4c). Specific conductance and pH (Figure 3.4d) were significantly higher at the unincised transect and decreased with depth and distance from the stream (all $p < 0.001$). Dissolved organic carbon (Figure 3.4e) was higher at the unincised transect and decreased with depth and distance from stream (all $p < 0.001$). Chloride was higher at the unincised transect ($\chi^2 = 11.1$, $p < 0.001$) and decreased with distance from the stream ($\chi^2 = 54.1$, $p < 0.001$) but did not vary with depth ($\chi^2 = 0.78$, $p = 0.68$; Figure 3.4f). Stream measurements were typically higher and more variable than those in the corresponding groundwater, except for chloride.

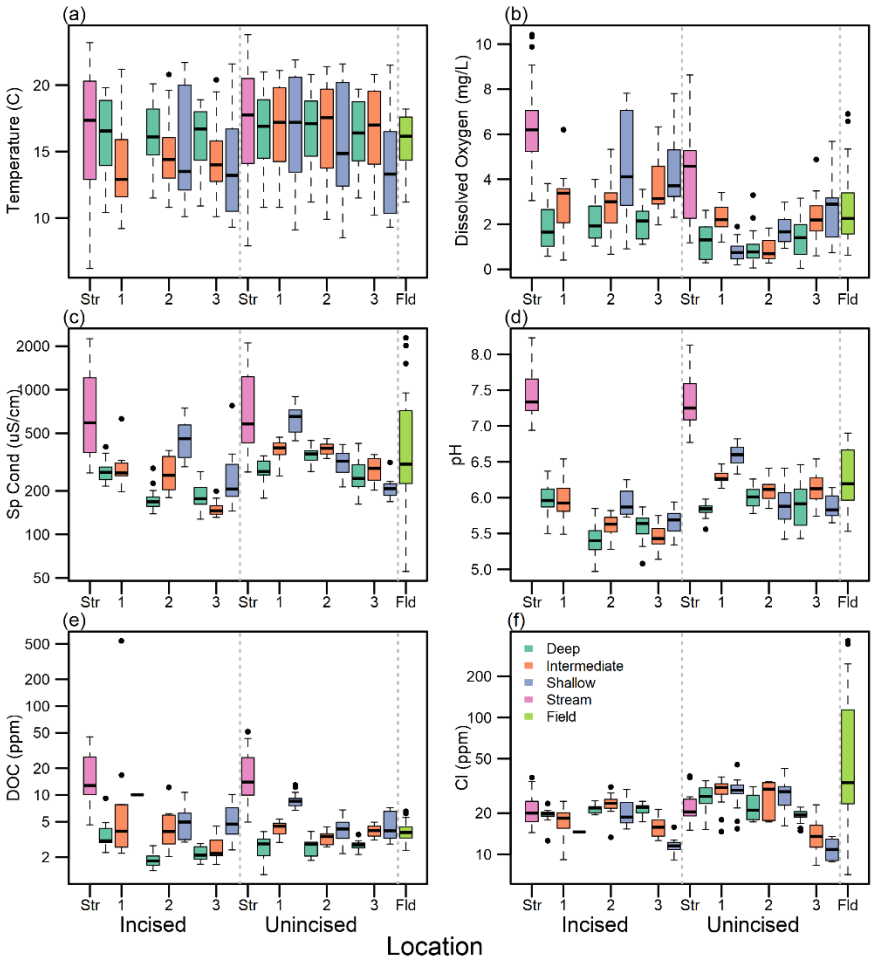

Figure 3.4. Distributions of physicochemical parameters from each well at the dairy farm. Temperature (a), dissolved oxygen (b), specific conductance (c), and pH (d) were measured *in situ* with a YSI, while dissolved organic carbon (e) and chloride (f) were analyzed from grab samples. Vertical axes in some panels (c, e, and f) are logarithmic to aid visualization of distributions. Locations are abbreviated for the stream (Str), well nest (1 to 3, with 1 being nearest the stream), and field edge (Fld). Boxes are the quartiles and median, and whiskers show the non-outlier maximum and minimum.

Stream nitrate and ammonia concentrations ranged from 0.51 to 8.58 ppm and 3.84 to 53.0 ppm, respectively (Figure 3.5). Groundwater nitrate (Figure 3.5a) and ammonia (Figure 3.5b) ranged from 0.0004 to 20.3 ppm and 0.007 to 13.7 ppm, respectively. Groundwater nitrate concentrations exceeded the EPA drinking water standard (10 mg/L) in two shallow wells at the incised transect, although samples were only collected from these wells during wet periods with elevated groundwater. Nitrate was higher at the incised transect than the unincised transect (χ^2 =

28.3, $p < 0.001$) and decreased with depth ($\chi^2 = 22.6$, $p < 0.001$) but did not vary with distance from the stream ($\chi^2 = 0.13$, $p = 0.94$). Ammonia was higher at the unincised transect than the incised transect ($\chi^2 = 50.4$, $p < 0.001$) and decreased with distance from the stream ($\chi^2 = 25.1$, $p < 0.001$) but did not vary with depth ($\chi^2 = 1.59$, $p = 0.45$). At the incised transect, nitrate was more abundant than ammonia ($t = 3.34$, $p = 0.001$), while the reverse was true at the unincised transect ($t = -8.3$, $p < 0.001$).

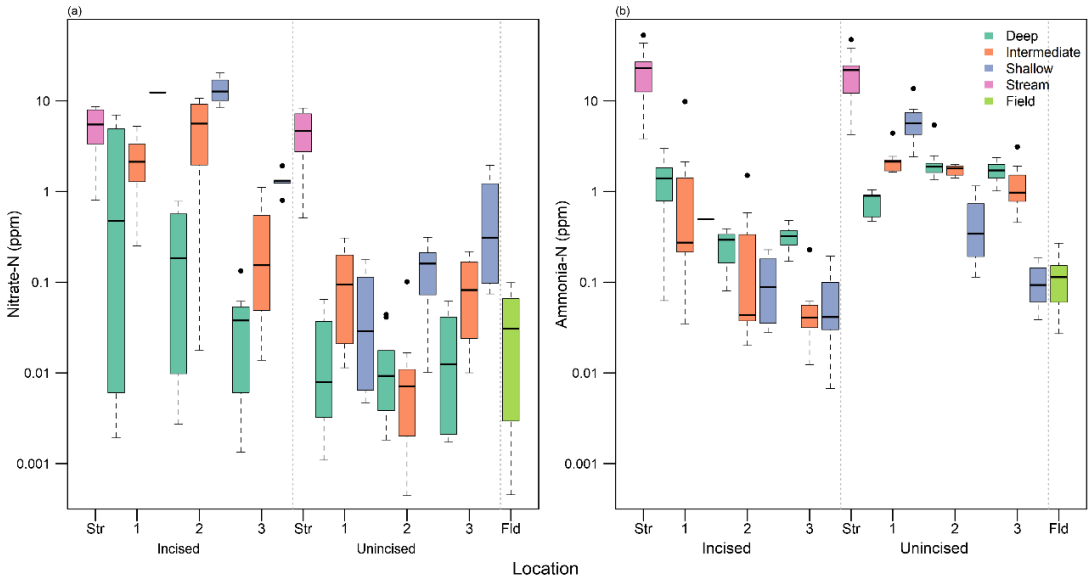

Figure 3.5. Distributions of nitrate and ammonia concentrations from each stream and groundwater well at the dairy farm. Vertical axes are logarithmic to aid visualization of distributions. Locations are abbreviated for the stream (Str), well nest (1 to 3, with 1 being nearest the stream), and field edge (Fld). Boxes are the quartiles and median, and whiskers show the non-outlier maximum and minimum.

Nitrate varied significantly with month ($p < 0.001$). Nitrate concentrations were lowest in summer (May-July) and typically higher in the incised transect than the unincised transect (Figure 3.6a). Higher nitrate was measured at the incised transect during wetter and cooler months when the groundwater table was closer to the ground surface. Ammonia concentrations at the unincised transect were similar across all months and greater than at the incised transect, where ammonia peaked in summer and declined over time (Figure 3.6b). Total nitrogen was

similar across months at the unincised transect, while TN was reduced to less than 1 ppm at the incised transect during dry summer months (Figure B1a). TN concentrations were higher at the unincised transect than the incised transect during those dry months but reversed when conditions were wetter. Dissolved organic carbon varied with month (χ^2 = 18.9, p = 0.06). Concentrations of DOC were typically 2-5 ppm at the unincised transect (Figure B1b) and often higher than the incised transect, with exceptions during late summer 2021 and spring 2022. Median DOC peaked at 10 ppm at the incised transect in August 2021, which coincided with a high groundwater table. All parameters were often more variable within the incised transect than unincised transect.

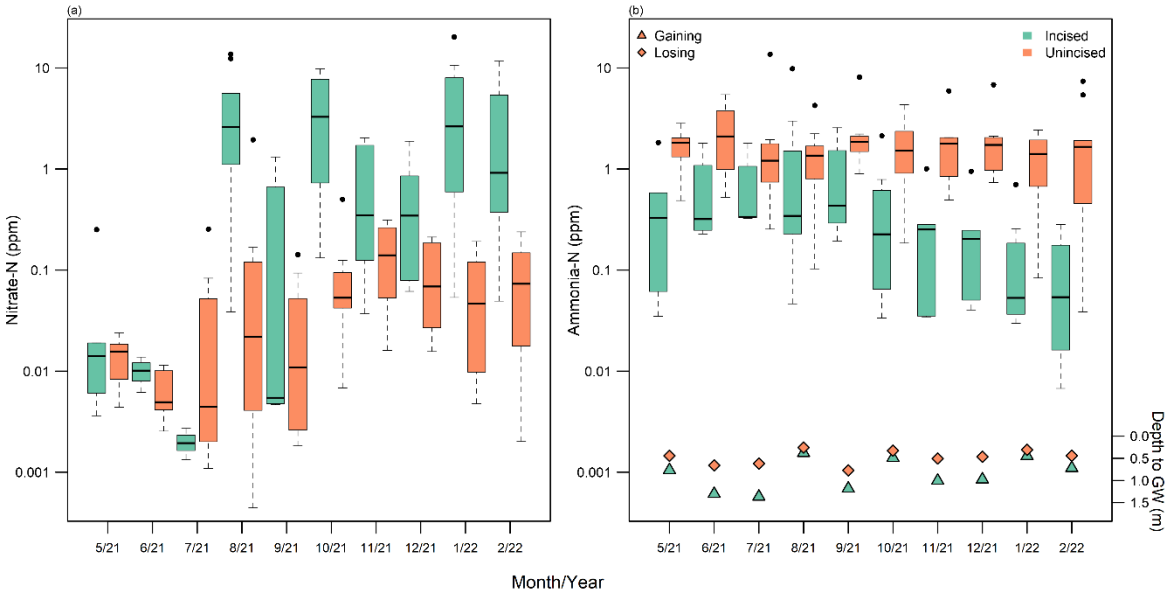

Figure 3.6. Distribution of monthly groundwater nitrate-N (a) and ammonia-N (b) for the incised and unincised transects at the dairy farm. Transect-averaged groundwater depths are noted with triangles for gaining conditions and diamonds for losing conditions (b). Vertical axes are logarithmic to aid visualization of distributions. Boxes are the quartiles and median, and whiskers show the non-outlier maximum and minimum.

McQueen Branch

None of the shallow wells or the near-stream intermediate well at the incised transect at McQueen ever had sufficient groundwater to sample. Temperature ranged from 9.3 to 24.9°C

and did not significantly vary across transect ($\chi^2 = 2.08$, $p = 0.15$), depth ($\chi^2 = 0.48$, $p = 0.79$), or distance from stream ($\chi^2 = 1.66$, $p = 0.44$; Figure 3.7a). Dissolved oxygen was higher at the incised transect compared to the unincised and was greatest at intermediate depths and distance from the stream (Figure 3.7b; all $p < 0.001$). Specific conductance was lower at the unincised transect, highest in the shallow wells, and increased with distance from the stream (Figure 3.7c; all $p < 0.001$). The pH was low everywhere (< 6) and was more basic at the unincised transect ($\chi^2 = 54.9$, $p < 0.001$; Figure 3.7d). pH varied with depth ($\chi^2 = 14.1$, $p < 0.001$), peaking in the intermediate wells, but did not change with distance from the stream ($\chi^2 = 1.34$, $p = 0.51$). Dissolved organic carbon did not vary between transects ($\chi^2 = 1.28$, $p = 0.26$) but decreased with depth ($\chi^2 =113$, $p < 0.001$) and distance from the stream ($\chi^2 = 7.95$, $p = 0.019$; Figure 3.7e). Intra-nest variability in DOC was greatest at the unincised transect, where concentrations in the shallow wells were above 10 ppm. Chloride was higher at the incised transect ($\chi^2 = 31.8$, $p < 0.001$) and decreased with distance from the stream ($\chi^2 = 6.08$, $p = 0.048$) but did not significantly vary with depth ($\chi^2 = 1.81$, $p < 0.4$; Figure 3.7f). Intermediate stream measurements at the confluence reflected mixing of the incised mainstem water and unincised tributary.

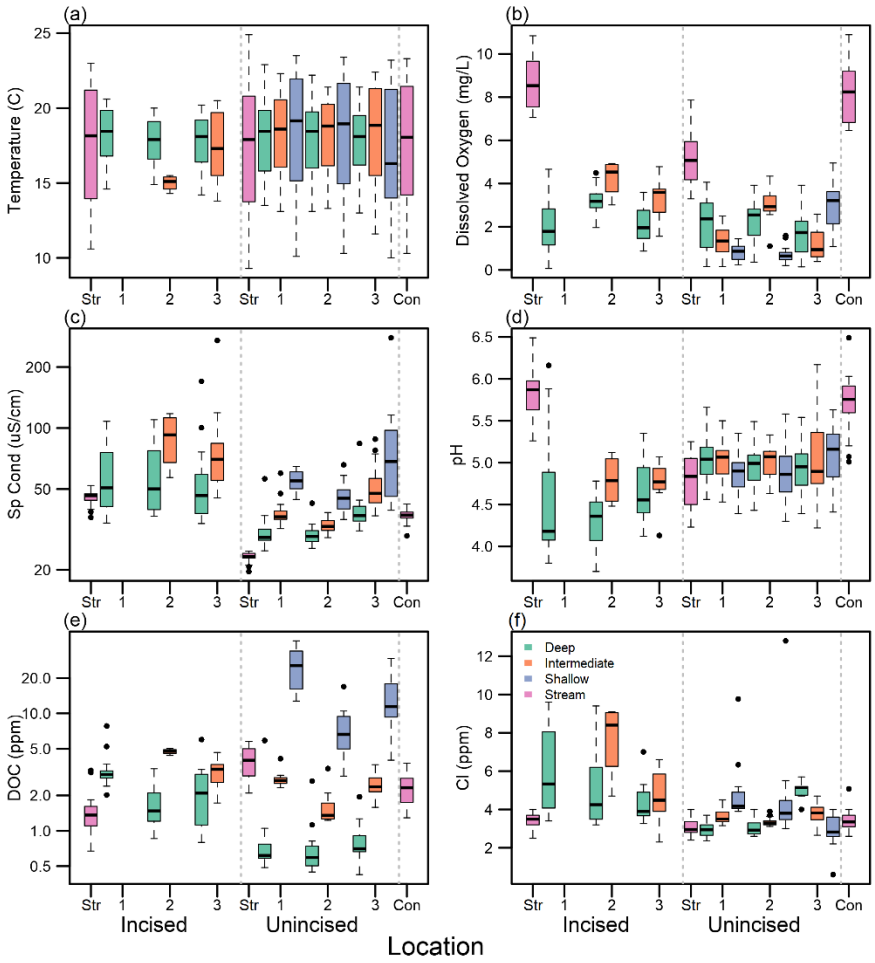

Figure 3.7. Distributions of physicochemical parameters from each well at McQueen Branch. Temperature (a), dissolved oxygen (b), specific conductance (c), and pH (d) were measured *in situ* with a YSI, while dissolved organic carbon (e) and chloride (f) were analyzed from grab samples. Vertical axes in panels (c) and (e) are logarithmic to aid visualization of distributions. Locations are abbreviated for the streams (Str), well nests (1 to 3, with 1 being nearest the stream), and confluence (Con). Boxes are the quartiles and median, and whiskers show the non-outlier maximum and minimum.

Stream nitrate and ammonia concentrations ranged from 0.03 to 1.22 ppm and 0.0003 to 0.087 ppm, respectively (Figure 3.8). Groundwater nitrate and ammonia concentrations ranged from 0.0006 to 1.10 ppm and 0.0014 to 0.52 ppm, respectively. Nitrate was higher at the unincised transect than the incised transect ($\chi^2 = 8.70$, $p = 0.003$) and increased with depth ($\chi^2 = 26.9$, $p < 0.001$; Figure 3.8a). Nitrate did not vary with distance from the stream ($\chi^2 = 1.99$, $p = 0.37$). Ammonia did not differ between transects ($\chi^2 = 1.3$, $p = 0.25$), but varied significantly

with depth (χ^2 = 12.7, p = 0.002) and distance from the stream (χ^2 = 24.1, p < 0.001; Figure 3.8b). Near-stream wells and shallow wells had more ammonia than wells in other nests and depths, respectively. At the incised transect, ammonia was more abundant than nitrate (t = -6.14, p < 0.001), while no difference between nitrate and ammonia was detected at the unincised transect (t = 1.11, p = 0.27).

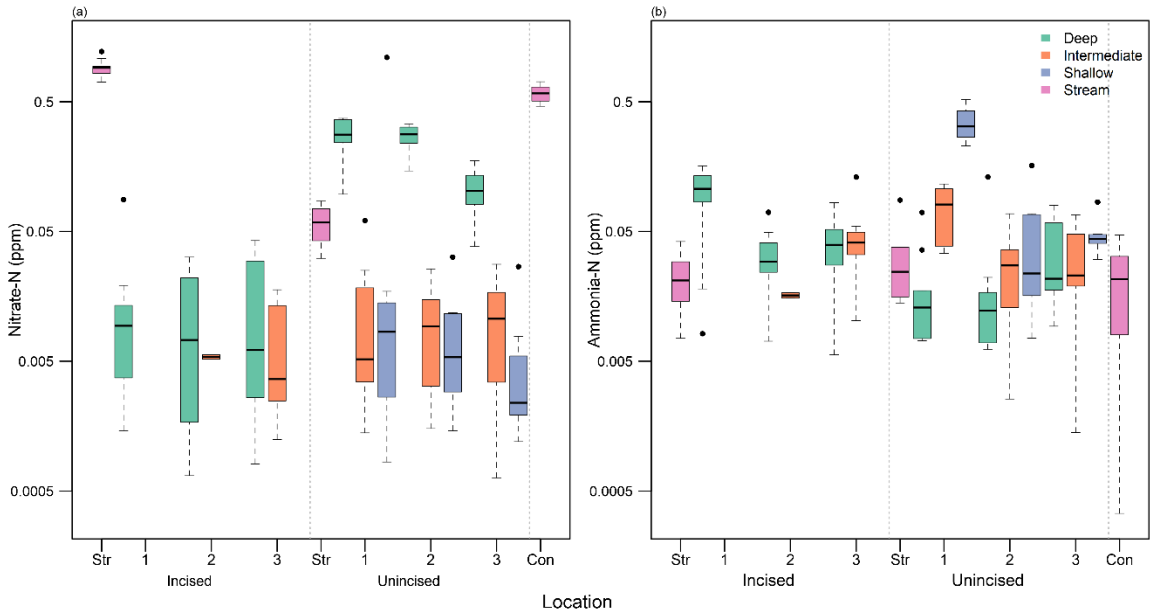

Figure 3.8. Distributions of nitrate and ammonia concentrations from each well at McQueen Branch. Vertical axes are logarithmic to aid visualization of distributions. Locations are abbreviated for the streams (Str), well nests (1 to 3, with 1 being nearest the stream), and confluence (Con). Boxes are the quartiles and median, and whiskers show the non-outlier maximum and minimum.

Total nitrogen, nitrate, and ammonia all varied significantly by month (p < 0.001). Nitrate concentrations were typically lower in the incised transect than the unincised transect, with differences more pronounced during summer (Figure 3.9a). Incised groundwater nitrate declined in summer, rose in the fall, and declined during winter. A similar trend occurred at the unincised transect, although less pronounced due to greater variability during each month. Ammonia concentrations declined over time at both transects, although the decline slowed at the incised transect during fall, yielding higher ammonia concentrations than at the unincised transect

(Figure 3.9b). Total nitrogen was low (less than 1 ppm) at both transects, rising each summer and decreasing throughout fall and winter (Figure B2a). Median TN concentrations were higher at the unincised transect than the incised transect during every month except January and February 2022. Dissolved organic carbon did not vary between months (χ^2 = 2.95, p = 0.99), but peaked at the incised transect in Jan-May 2022, when the water table was highest (Figure B2b).

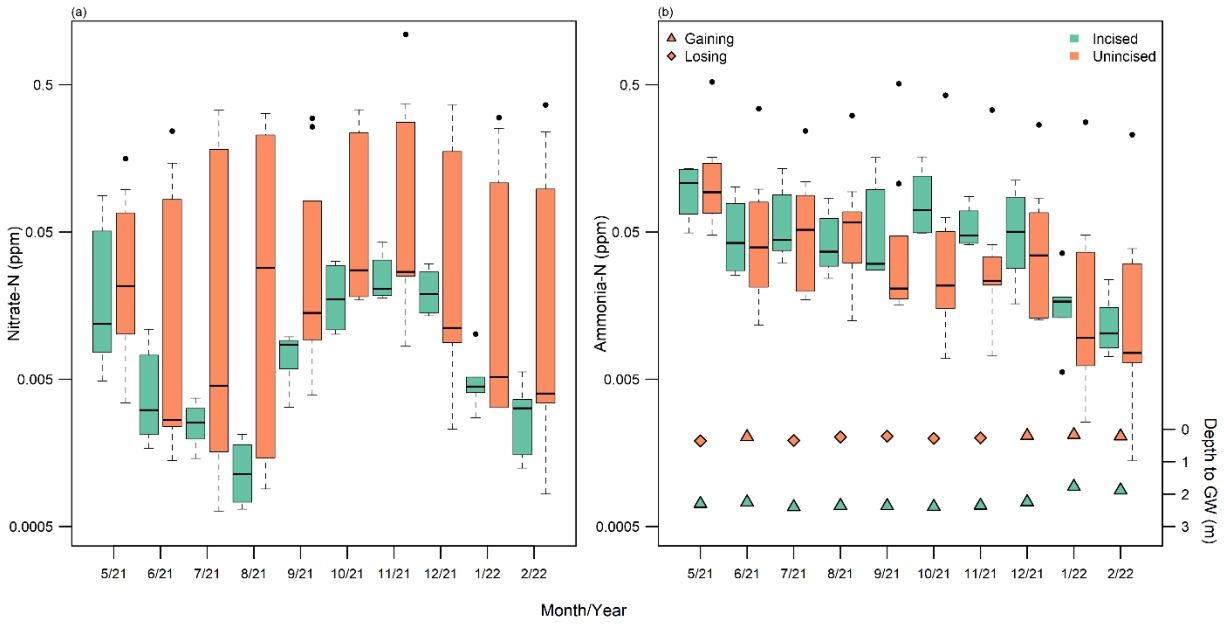

Figure 3.9. Distribution of monthly nitrate-N (a) and ammonia-N (b) for the incised and unincised transects at McQueen Branch. Transect-averaged groundwater depths are noted with triangles for gaining conditions and diamonds for losing conditions (b). Vertical axes are logarithmic to aid visualization of distributions. Boxes are the quartiles and median, and whiskers show the non-outlier maximum and minimum.

Combined Results

Compared to McQueen Branch, groundwater at the dairy farm was higher in specific conductance, pH, chloride, total nitrogen, nitrate, and ammonia, and lower in temperature. When combining the data from each site by incision, incised transects were higher in nitrate (χ^2 = 4.62, p = 0.03), dissolved oxygen, and chloride (χ^2 = 4.03, p = 0.045). Unincised transects had higher temperature, pH, DOC, and ammonia (χ^2 = 6.19, p = 0.013). All p values were less than 0.001 unless noted.

Median total denitrification (excess N_2-N + N_2O-N) across all sites was generally less than 2 mg/L (Figure 3.10). The extent of denitrification was estimated using reaction progress (RP) and the proportion of incomplete denitrification was estimated using the fraction of N_2O in total denitrification. Across both sites, the average RP and incomplete denitrification were 0.71 and 0.52, respectively (Table 3.2). RP was the only variable that showed a significant difference with incision when combined across both sites, with higher RP at incised transects ($\chi^2 = 4.01$, $p = 0.045$). Reaction progress ($\chi^2 = 18.0$, $p < 0.001$) and incomplete denitrification ($\chi^2 = 3.34$, $p = 0.068$) were higher during gaining conditions, while increased excess N_2-N during losing conditions was only slightly insignificant ($\chi^2 = 2.65$, $p = 0.103$). Denitrification was higher at the dairy farm than McQueen Branch ($\chi^2 = 13.2$, $p < 0.001$). McQueen Branch had higher N_2O-N ($\chi^2 = 12$, $p < 0.001$), RP ($\chi^2 = 31.7$, $p < 0.001$), and incomplete denitrification ($\chi^2 = 33.1$, $p < 0.001$), but lower excess N_2-N ($\chi^2 = 74.5$, $p < 0.001$) than the dairy farm. At the dairy farm, total denitrification ranged from 0.6 to 6.0 mg/L (Figure 3.10) but did not vary significantly between transect ($\chi^2 = 0.87$, $p = 0.35$). Total denitrification ($\chi^2 = 15.5$, $p = < 0.001$) and excess N_2-N ($\chi^2 = 23.5$, $p < 0.001$) were highest near the stream, while incomplete denitrification decreased with distance from the stream ($\chi^2 = 7.76$, $p = 0.02$). RP was higher at the incised transect ($\chi^2 = 7.71$, $p = 0.005$). The highest denitrification ($\chi^2 = 3.87$, $p = 0.049$) and RP ($\chi^2 = 7.71$, $p = 0.005$) coincided with gaining conditions. Total denitrification at McQueen Branch ranged from 0.4 to 5.9 mg/L (Figure 3.10) and did not vary significantly between transect ($\chi^2 = 2.64$, $p = 0.104$) or distance from the stream ($\chi^2 = 1.33$, $p = 0.51$). Both N_2O-N ($\chi^2 = 3.18$, $p = 0.075$) and excess N_2-N ($\chi^2 = 12.2$, $p < 0.001$) were higher at the unincised transect, but there were no significant trends with distance from the stream or in reaction progress or incomplete denitrification. Reaction progress was higher during gaining conditions than losing ($\chi^2 = 7.74$, $p = 0.005$).

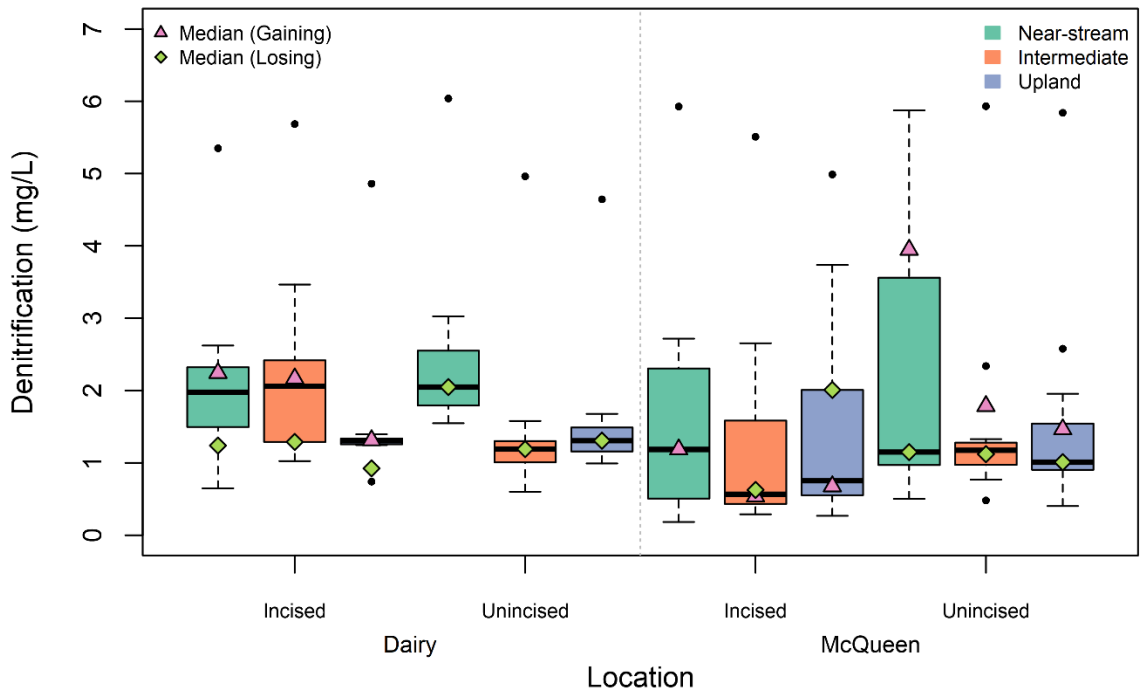

Figure 3.10. Distribution of denitrification from each deep well at both locations. Median denitrification during gaining and losing conditions are shown with triangles and diamonds, respectively. No gaining samples were collected at dairy unincised or losing at the near-stream well at McQueen incised. Boxes are the quartiles and median, and whiskers show the non-outlier maximum and minimum.

Table 3.2. Summary of the dissolved gases that are denitrification end products, denitrification reaction progress (RP), and the fraction of N_2O for each well nest.

Stream	Incision	Location	Excess N_2-N (mg/L)			N_2O-N (mg/L)			RP			Frac N_2O		
			Median	*Min*	*Max*	*Median*	*Min*	*Max*	*Median*	*Min*	*Max*	*Median*	*Min*	*Max*
Dairy	Inc	Near-stream	1.33	0.32	2.36	0.40	0.26	4.42	0.53	0.07	0.57	0.29	0.10	0.83
		Intermediate	1.16	0.48	2.16	0.38	0.24	4.33	0.81	0.51	0.88	0.30	0.11	0.77
		Upland	0.87	0.28	1.11	0.38	0.24	4.24	0.72	0.67	0.95	0.33	0.18	0.87
	Uninc	Near-stream	1.53	1.23	2.78	0.30	0.23	4.68	0.71	0.66	0.88	0.14	0.08	0.78
		Intermediate	0.74	0.26	1.26	0.40	0.27	4.59	0.40	0.26	0.77	0.35	0.20	0.93
		Upland	0.83	0.14	1.33	0.39	0.29	4.50	0.48	0.37	0.81	0.34	0.20	0.97
McQueen	Inc	Near-stream	0.12	0.02	0.86	0.43	0.15	5.48	0.92	0.59	0.98	0.93	0.27	0.99
		Intermediate	0.05	0.03	0.33	0.42	0.17	5.39	0.95	0.79	0.97	0.92	0.44	0.98
		Upland	0.17	0.03	0.47	0.35	0.17	4.96	0.94	0.81	0.97	0.83	0.38	0.99
	Uninc	Near-stream	0.39	0.02	0.91	0.73	0.33	5.77	0.92	0.67	0.96	0.72	0.27	0.99
		Intermediate	0.32	0.21	0.74	0.69	0.46	5.67	0.85	0.66	0.96	0.65	0.39	0.96
		Upland	0.32	0.06	0.85	0.60	0.28	5.58	0.87	0.80	0.98	0.65	0.25	0.95

We further subset our data into only near-stream wells, where we expected the greatest effect of incision. Reaction progress was the only variable with a significant relationship to incision across both locations, with higher reaction progress at the unincised transect ($\chi^2 = 6.37$, $p = 0.012$), the opposite from when all wells were considered. At the dairy farm, both excess N_2 ($F = 4.32$ $p = 0.049$) and RP ($\chi^2 = 12.6$, $p < 0.001$) were higher at the unincised transect, while N_2O was greater at the incised transect ($\chi^2 = 3.33$, $p = 0.068$; Figure 3.11). No statistically significant relationships with incision were found at the near-stream only wells at McQueen, which showed greater variability in denitrification than other wells (Figure 3.10).

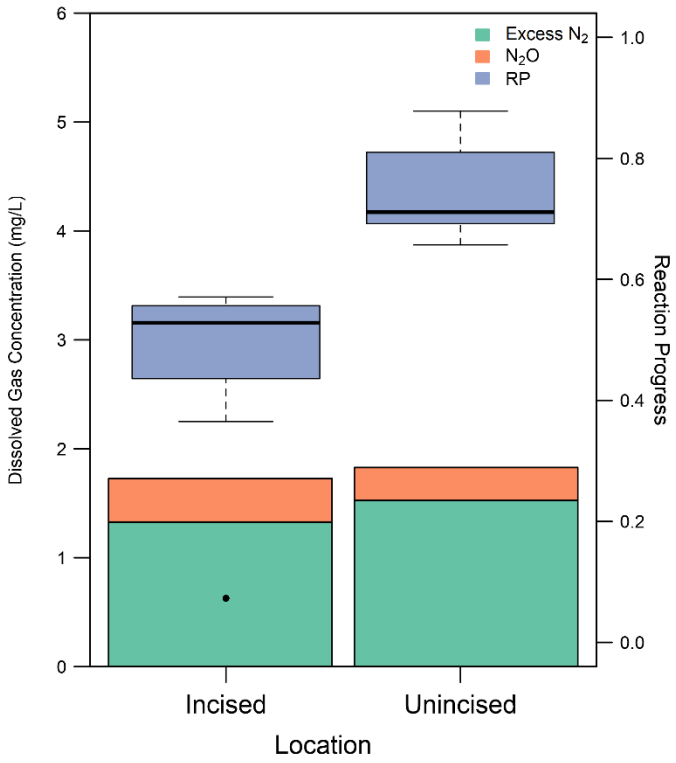

Figure 3.11. Median denitrification gases (N_2 and N_2O) and the distribution of denitrification reaction progress in the near-stream deep wells at both transects at the dairy farm. Boxes for RP are the quartiles and median, and whiskers show the non-outlier maximum and minimum.

Nitrous Oxide Emissions

N_2O flux was higher at incised transects than at unincised transects (Table 3.3). More N_2O was emitted from near-stream groundwater at McQueen Branch than at the dairy farm. Approximately 5-6 times more greenhouse gas equivalents were emitted from incised transects than unincised transects, with a proportionally higher increase at the dairy farm, where N_2O concentrations were lower. Using the average of these values between sites, we estimated that annual greenhouse gas emissions from groundwater adjacent to low-order streams in the US ranged from 13 to 70 Mt/year for scenarios of completely unincised and incised stream length, respectively. These estimates were approximately 0.03% to 0.17% of global, annual energy-based greenhouse gas emissions and 4.9% to 26.3% of annual nitrous oxide emissions in the US.

Table 3.3. Comparison of estimated N_2O flux and greenhouse gas emissions as CO_2 equivalents from the near-stream wells.

Stream	Incision	N_2O Flux (kg N_2O-N/ha/yr)	CO_2 eq (kg CO_2/ha/yr)
Dairy	Inc	42.5	20,000
	Uninc	7.3	3,400
McQueen	Inc	76.1	36,000
	Uninc	14.9	7,000

Discussion

Gaining and Losing Variability

We found that hydroclimatic conditions drove seasonal and event-based switching in gaining and losing conditions at most of our transects. Catchment storage and hydrogeomorphic processes have been shown to drive temporary shifts in seasonal or event-based switching of groundwater-surface water magnitudes and directions (Jencso et al., 2009; Nippgen et al., 2009; Rodhe and Seibert, 2011). Both incised transects switched from gaining to losing during summer and fall storm events, which aligns with other research that found exacerbated losing conditions

during storms (McCallum et al., 2009). The rapid rise in stream elevation during storm events can temporarily reverse the hydraulic gradient (Barrie et al., 2022), driving flow into the bank and riparian zone until either the streamflow recedes or the groundwater table rises sufficiently to restore gaining conditions.

The incised transect at the dairy farm also switched from gaining to losing during a prolonged dry period in summer 2022. Drier climates generally promote losing conditions due to drier soils and increased transpiration (Jasechko et al., 2021; Leuthold et al., 2021). Sub-seasonal and seasonal transitions to losing during drier periods in summer have been observed across various catchments and physiographic settings (Jimenez-Fernandez et al., 2022; Payn et al., 2009; Voltz et al., 2013), including the southeast piedmont (Zimmer and McGlynn, 2017) and coastal plain (Barrie et al., 2022). The unincised transect at McQueen showed an inverse trend, switching from losing to gaining during the winter of 2021-2022 as groundwater elevations rose, likely in response to decreased evapotranspiration (Zimmer and McGlynn, 2017). The unincised transect at the dairy farm was losing during our entire monitoring period, which may have been driven by its proximity to the incised reach. The abrupt drop in groundwater elevation along the stream due to the headcut could have sufficiently drawn down the water table in the unincised reach to create losing conditions. Additionally, the combination of hydroclimatic conditions, stream channel geometry, and riparian soil type at the unincised transect may have maintained a groundwater elevation below the adjacent stream elevation. Groundwater elevation at this transect also dropped sharply in the upland well nest relative to the other two nests, an observation that warrants more detailed investigation of surface topography and groundwater flow paths to better understand this unexpected behavior.

Groundwater at both sites showed expected seasonal variability throughout the study period, with the water table declining farther below the surface in summer and rising during winter (Harden and Spruill, 2008; Hardison et al., 2009). We attributed these trends to changes in evapotranspiration and precipitation which led to water table declines in the growing season and rising water tables during dormancy. Similar groundwater response to changes in evapotranspiration and soil water storage state have been observed in another southeast piedmont watershed (Zimmer and McGlynn, 2017). We also observed effects of channel incision on groundwater-surface water exchange at both study sites, with stream incision causing deeper, more variable groundwater with distinct summer lows and winter highs in disturbed catchments (Groffman et al., 2002; Hardison et al., 2009; Schilling and Jacobson, 2014).

While these groundwater-surface water trends appear connected to stream incision, it is important to note that these are only singular transects at each stream reach. We are studying additional streams near McQueen Branch and have found reciprocal trends (incised stream is losing, unincised stream is gaining). However, these other streams experience variable boundary controls (e.g., clay aquiclude underlying the streambed, topographic depressions in floodplain) that make direct comparisons difficult. While stream incision may play a role in altering groundwater-surface water interactions in some contexts, this finding is not ubiquitous and still depends on overlying controls such as climate, topography, and geology.

Riparian Denitrification Controls

We observed an average of 40-95% removal of available nitrogen based on denitrification reaction progress. While it is difficult to compare these estimates to other studies due to methodological differences, our values for denitrification reaction progress were similar in magnitude and variability to other *in situ* denitrification studies (Jahangir et al., 2013; Jeffers,

2018; McAleer et al., 2017). Excess N_2-N was comparable to literature values, including at catchments of similar land use, physiography, and geographic location (Böhlke et al., 2007; Jeffers, 2018; McAleer et al., 2017). N_2O-N measurements were higher than other *in situ* denitrification studies, which averaged less than 0.1 mg/L N_2O-N (Jahangir et al., 2013; Kim et al., 2009; McAleer et al., 2017; Weymann et al., 2008). We observed a substantial amount of incomplete denitrification, with an estimated 52% of total denitrification as N_2O-N, which is usually below 20% (Jahangir et al., 2013; McAleer et al., 2017), but has reached over 70% in past studies (Bouwman et al., 2013; Hefting et al., 2003). One reason for the prevalence of N_2O-N could be the acidic pH, which inhibits complete denitrification and increases N_2O production (Nägele and Conrad, 1990; Šimek and Cooper, 2002; Van Den Heuvel et al., 2011; Weymann et al., 2008). High nitrate concentrations, such as those at the dairy farm, can also inhibit complete denitrification and exacerbate N_2O production (Weymann et al., 2008). Additionally, N_2O can be produced during nitrification and DNRA, so quantification of nitrogen cycling processes may distinguish actual contributions of N_2O results from denitrification. If other nitrogen cycling processes are responsible for this N_2O generation, then we may be overestimating the effect of riparian denitrification in these systems.

Denitrification was likely greater at the dairy farm than at McQueen due to higher available nitrogen and dissolved organic carbon (Mayer et al., 2010). Significantly higher reaction progress at McQueen Branch corresponded to greater N_2O-N production and lower excess N_2-N compared to the dairy farm, which may be evidence that incomplete denitrification is dominant there. We were surprised to observe similar denitrification between incised and unincised transects because incised transects had a lowered water table that was disconnected from the carbon-rich root zone (Groffman et al., 2002; Schilling et al., 2006). The unincised

transects also had higher dissolved organic carbon, pH, and temperature, and lower dissolved oxygen, all conditions that may be favorable for denitrification (Gift et al., 2010; Heinen, 2006; Mayer et al., 2010; Rivett et al., 2008; Schilling et al., 2018; Schipper et al., 1993; Šimek and Cooper, 2002). Lower pH and higher DO at the incised transects likely produced N_2O due to inhibition of complete denitrification (Jurado et al., 2017; Nägele and Conrad, 1990; Šimek and Cooper, 2002; Van Den Heuvel et al., 2011; Weymann et al., 2008), making denitrification estimates at the two transects comparable.

Relationships between reaction progress and incision were driven by high RP that did not vary with incision at McQueen and inverse trends in RP with proximity to the stream at the dairy farm. Across all data points, denitrification reaction progress was higher at the incised transects and during gaining conditions, which coincided with higher nitrate concentrations (but lower TN), corroborating previous findings that nitrate availability is an important control on nitrogen removal via denitrification (Barton et al., 1999a; Gift et al., 2010; Schipper et al., 1993). However, when focusing on near-stream wells where the effects of incision would be most pronounced, we found that nearly 20% more available nitrogen could be removed via denitrification in the unincised losing reach at the dairy farm than at the incised reach. Higher excess N_2 and lower N_2O are additional evidence for removal of this nitrogen via complete denitrification at the unincised transect. Two-dimensional modeling has shown that losing reaches can have higher nitrate removal rates than gaining reaches (Shuai et al., 2017). Since the unincised reach was losing, remaining nitrogen could be further processed in the riparian zone, while gaining groundwater at the incised reach flowed into the stream with less effective nitrogen removal. We did not observe this near-stream effect on RP at McQueen, likely due to lower denitrification than the dairy farm, high RP (> 0.9) driven by lower excess N_2 and greater

incomplete denitrification, and lower available nitrogen. These findings show the potential for incision to increase nitrogen loading in certain contexts and stress the need to consider the direction of the groundwater-surface water gradient and the localized effects of stream incision on riparian nitrogen cycling.

Nitrogen and Water Chemistry Comparisons

Nitrogen was more concentrated in surface water and groundwater at the dairy farm than at McQueen Branch, likely due to land use. Groundwater nitrate was on the low end of the range of concentrations measured in other agricultural catchments (Duncan et al., 2015; Harden and Spruill, 2008; McAleer et al., 2017; Williams et al., 2014). Differences in these concentrations among transects could be due to sources of nitrogen or dominant nitrogen cycling processes. The unincised transect at the dairy farm had more ammonia than nitrate and likely received some ammonia from the ammonia-rich, predominantly losing unincised stream reach that had not yet nitrified. Independently, elevated ammonia can result from increased ammonification of atmospheric or organic nitrogen, while decreased nitrate can be due to plant uptake or denitrification. Plant uptake is generally not a significant source of nitrate decrease (Hill, 2019) but may have played a role here since the elevated groundwater table was able to interact with the plant rooting zone. Conditions were good for denitrification, yet denitrification end products were similar to our other locations. Another possible explanation for this difference in available forms of nitrogen is dissimilatory nitrate reduction to ammonia (DNRA), the anaerobic conversion of nitrate to ammonia (Burgin and Hamilton, 2007; Burt et al., 2010; Hill, 2019; Rütting et al., 2011). Studies have documented DNRA as a significant source of nitrate decrease (Davis et al., 2008; Jahangir et al., 2017; McPhillips et al., 2015). Lower nitrate than ammonia was also observed at the McQueen incised transect, although concentrations were overall lower.

However, the water table was much lower and disconnected from its rooting zone, making it unlikely that plant uptake of nitrate caused this trend. Dissolved oxygen was generally greater than 2 mg/L here, meaning anoxic conditions for denitrification and DNRA were sub-optimal (Jahangir et al., 2013). This combination of a deeper water table and aerated soils indicated that ammonification may have been most responsible for the higher ammonia at McQueen incised. Adequate nitrogen supply, aerobic conditions (DO mainly above 2 mg/L), and a larger unsaturated vadose zone due to reduced groundwater elevation may have favored conversion of ammonia to nitrate via nitrification at the incised dairy transect (Groffman et al., 2002; Hanson et al., 1994; Hinkle et al., 2001). No difference was detected between nitrate and ammonia at McQueen unincised, but the deep wells appeared to have more nitrate than ammonia. This could have also been due to nitrification since nitrate remained low in the shallower wells.

Nitrate did not decrease closer to the channel as expected through a riparian zone (Fennessy and Cronk, 1997; Hill, 2019, 1996). Since the two shallowest near-stream incised wells were frequently dry, these results could be disproportionately affected by near-stream groundwater at the unincised transect mixing with water from the nitrogen-rich, predominantly losing stream. Ammonia increased closer to the stream at both locations, which again could be influenced by most near-stream samples being collected at the unincised transect, which had higher ammonia. These results for both locations could additionally be due to mixing with groundwater from a different flow path with elevated nitrogen. Nitrate decreased with depth at the dairy farm, similar to other riparian groundwater findings (Böhlke et al., 2007; Groffman et al., 2002). This could represent dilution or nitrate transformation via denitrification or DNRA. At McQueen, nitrate increased with depth and ammonia decreased, indicating that nitrification may have been prevalent.

Other studies have also observed seasonal fluctuations in nitrogen cycling (Duncan et al., 2015; Pinardi et al., 2022; Ranalli and Macalady, 2010). Our findings of lower nitrate in summer, with a lower water table, indicate that nitrate may be reduced by disconnection from higher soil nitrate concentrations near the surface. Lower monthly nitrate concentrations coinciding with the growing season could mean that plant uptake of nitrate may be important, particularly at the unincised transect where the water table was still elevated enough to interact with the root zone. Lower ammonia in winter could be due to dilution as the groundwater table rose or temperature or saturation-induced changes in nitrogen cycling, like reduced ammonification.

Specific conductance, pH, DOC, and chloride were higher at the dairy farm than McQueen and near typical concentrations for riparian groundwater (e.g., Blicher-Mathiesen and Hoffmann, 1999; Jencso et al., 2010; Sherman et al., 2022; Spruill, 2000). Our water chemistry measurements at McQueen Branch closely aligned with a study in a nearby watershed (Jeffers, 2018). Comparatively higher values for these parameters at the dairy farm are reasonable due to differences in land use and soil type. The dairy farm watershed has been disturbed by agriculture activity that reduced forest cover, which is typically correlated with higher specific conductance and pH (Conway, 2007; Roy et al., 2003). Groundwater pH at the dairy farm may also have been higher because the dominant soil type, Chewacla soils, are less acidic (pH = 5.9) than the Troup and Pinckney sands at McQueen Branch (pH of 5.2 and 4.7, respectively; Soil Survey Staff, 2022). Groundwater affected by animal waste typically has elevated chloride, although effects are most prominent for shallow groundwater (Israel et al., 2005; Karr et al., 2003, 2001; Showers et al., 2008). Average dissolved oxygen concentrations between 2 and 4 mg/L were similar to other riparian groundwater studies (Anderson et al., 2014; Mulholland, 1992; Nogueira et al., 2021; Spruill, 2000), including near incised streams (Schilling et al., 2006). Lower

concentrations of DO can be associated with frequent saturation (Pfeiffer et al., 2006), explaining why we observed a decrease in DO with depth and at both unincised transects, which were frequently saturated. Most average DOC concentrations were less than 5 mg/L, consistent with riparian groundwater literature (Israel et al., 2005; Mayer et al., 2010; McGlynn and McDonnell, 2003; Rutlidge et al., 2021; Spruill, 2000).

The decrease in specific conductance with depth may be explained by deep groundwater flow paths that have more influence than surface water exchange (Wallace and Soltanian, 2021). This also could result from dilution. We observed a decrease of DOC with depth likely because DOC is often processed along flow paths through the subsurface (Chasar et al., 2000; Goni and Gardner, 2003; Rutlidge et al., 2021) and generally correlates to soil organic matter, which is higher near the surface in riparian soils (Blanco-Canqui et al., 2006; Blazejewski et al., 2009; Omonode and Vyn, 2006; Sterte et al., 2022). No clear depth profile of chloride was a reasonable finding since chloride varies with proximity to source (including animal waste applications), dilution, soil type, and rainfall chloride concentrations (Altman and Parizek, 1995; Duff et al., 2007; Hill et al., 2014; Williams et al., 2014).

Greenhouse Gas Contributions

Channel incision corresponded to increased greenhouse gas emissions from near-stream groundwater at both sites. Shallow groundwater in riparian zones releases N_2O to the unsaturated zone and atmosphere (Jurado et al., 2017), yet to our knowledge, no studies have connected stream morphodynamics to emissions of this potent greenhouse gas in CO_2 equivalents. Our estimates of N_2O flux were higher than in previous studies (Kim et al., 2009; Minamikawa et al., 2010; Vilain et al., 2012; Well et al., 2005), likely due to similarly higher N_2O-N concentrations. Comparisons to annual greenhouse gas emissions for both global energy-based emissions and US

nitrous oxide emissions indicated that low-order streams can be substantial sources of greenhouse gas emissions due to N_2O production, particularly when incision is prevalent. Actual greenhouse gas contributions from these near-stream areas may be closer to the mean of our estimated ranges, after accounting for the proportion of low-order streams that are incised and recognizing that our estimates may be inflated by relatively high N_2O concentrations. We also focused on a smaller area, where effects of incision on groundwater and denitrification were most pronounced. Had we expanded our analysis to the entire width of the riparian zone, the areal N_2O flux and corresponding effect of incision on greenhouse gas emissions would likely be dampened. Nonetheless, our findings indicated that riparian groundwater has the potential to be a substantial source of greenhouse gas emissions, which can be exacerbated by channel incision.

Implications and Future Work

Our findings are relevant to water resources management in the context of broader anthropogenic disturbance. Groundwater recharge is declining due to altered precipitation patterns and increased evapotranspiration related to climate nonstationarity, causing a reversal of groundwater-surface water interactions in gaining streams, substantially altering the water balance and having repercussions for water quality and biota (Uhl et al., 2022). Given the prevalence of incision, particularly in agricultural watersheds, a depressed riparian water table that reaches its lowest in summer could reduce available water needed for irrigation during the growing season. Where incision generates favorable gaining conditions, the groundwater entering the stream may not have undergone adequate biogeochemical processing (e.g., denitrification) and could represent a source of pollution. In some contexts, floodplain reconnection to counteract incision could raise the water table and reverse the hydraulic gradient to make the stream losing more frequently, similar to our unincised streams (Hester et al., 2016).

Based on our analysis of near-stream wells, it is reasonable to believe this can enhance biogeochemical processing by increasing interaction between nutrients in the water and the plant root zone.

Another important implication of this research is the potential greenhouse gas emissions from riparian zones. Riparian zones are a substantial source of N_2O (Bouwman et al., 2013; Groffman et al., 1998), a harmful greenhouse gas, that is exacerbated at high nitrate and low pH. Our findings corroborate this conclusion and estimate potential increases in emissions due to channel incision, which underscores the need to consider these systems in assessing greenhouse gas emissions globally. Targeted restoration of riparian zones near incised streams or those with low pH or elevated nitrate concentrations could be a viable strategy for reducing total emissions.

To our knowledge, this is the first study to assemble a dataset of riparian zone hydrology, nitrogen cycling, and stream geomorphology. We hope these preliminary findings from individual transects will provide motivation for additional spatially-distributed studies in disturbed riverscapes. Since gaining and losing dynamics are spatially and temporally variable (Gordon et al., 2004), expanding the scope of hydrologic measurements longitudinally can investigate if our observed patterns of gaining and losing in relation to incision indicate a broader trend or simply represent variability. Instrumenting additional streams can identify varying controls on the riparian hydrologic responses to channel incision (e.g., soil type, stratigraphy, topography, degree of incision, etc.). Tracer studies at the existing study sites can explore the effects of variable groundwater flow paths and dilution of solutes such as nitrate.

Enhanced water quality sampling is necessary to quantify effects of incision on riparian nitrogen cycling. Stable isotope studies could track water and nitrogen transport and uptake throughout the riparian zone and stream (Hinkle et al., 2001). Denitrification assays would be

valuable to directly determine denitrification and would be comparable to literature denitrification rates that are often expressed per unit soil mass and time (Groffman et al., 2006). Quantification of nitrification, DNRA, or other nitrogen cycle components would provide insight into major processes responsible for the variable trends in nitrogen species. Finally, measuring discharge to develop a rating curve for these streams would allow us to quantify nitrogen loads and explore how channel incision affects nitrogen loading.

Expanding and replicating this dataset in other landscape settings is important for discerning the effects of channel incision on nitrogen loading to streams. Given the lack of data connecting channel incision with riparian nitrogen processes, datasets like this one can be used to improve numerical estimates of watershed-scale nitrogen loading by incorporating channel incision and groundwater-surface water dynamics into models. These improved models are important tools for prioritizing watershed restoration to maximize stream water quality and morphological benefits. Overall, our results highlight the importance of combining flow management and stream restoration for water quality improvement.

Conclusions

Channel incision significantly lowered the riparian groundwater elevation and affected groundwater-surface water gradients. Incised stream reaches were predominantly gaining groundwater, while unincised streams were mainly losing water to the riparian zone. We observed reversal in these gradients during storm events and seasonally due to evapotranspiration demand. The results of this study show that channel incision, in some contexts, plays a role in the interactions between disturbed streams and riparian zones. Expanded research is needed to investigate spatial variability in this pattern and to identify what conditions control the relationship between incision and groundwater-surface water exchange.

Water quality monitoring results yielded several key findings about riparian denitrification adjacent to incised streams. We observed estimated removal of 40-95% of the available nitrogen in riparian groundwater by denitrification. We expected greater denitrification at unincised transects due to more favorable conditions: a higher groundwater table that could interact with the carbon-rich rooting zone, and higher pH, temperature, DOC, and nitrogen availability than the incised transect. However, total riparian denitrification was not significantly different between incised and unincised stream reaches. We hypothesize that this was due to conditions like acidic pH that inhibited complete denitrification, producing N_2O that comprised 52% of our estimated denitrification. When considering near-stream wells where the effects of incision were most immediate, we found that the losing, unincised reach at the dairy farm could remove nearly 20% more available nitrogen than the incised reach. We also found evidence for nitrification, DNRA, or other nitrogen cycling components that require more specific sampling to differentiate the dominant processes in these systems.

The results of this study provide a novel dataset that considers stream morphology when assessing riparian nitrogen cycling. Our findings demonstrate the importance of analyzing near-stream effects and the groundwater-surface water gradient when studying how incision affects nitrogen loading to streams. Enhancing this unique dataset and building similar ones in different regional and hydrogeomorphic settings is important for improving understanding about the effects of channel incision on groundwater-surface water interactions and nitrogen loading. These datasets can subsequently be used to improve models that inform scientists and water resources managers about the role of hydromodification and flow management for water quality improvement.

CHAPTER 4

COUPLED MODELING OF THE EFFECTS OF STREAM INCISION AND GROUNDWATER-SURFACE WATER INTERACTIONS ON NETWORK-SCALE NITROGEN LOADING[3]

[3] Buhr, D.X., and B.P. Bledsoe. To be submitted to *Journal of Environmental Management.*

Abstract

Excess nitrogen loading to waterbodies is a global challenge that has resulted in widespread eutrophication and degradation of water quality. Denitrification processes in riparian zones can significantly reduce nitrogen pollution, but stream channel incision can impair this function by disconnecting the adjacent groundwater table from plant rooting zones that are rich in organic carbon. Despite this interaction, current riparian nitrogen models do not account for stream morphodynamics, stressing the need for inclusion of these processes for modeling riparian denitrification and nitrogen loading to streams. We developed statistical models to predict depth to groundwater and riparian denitrification based on a novel dataset collected at paired incised and unincised stream reaches in two small watersheds. We used the River Erosion Model (REM) to simulate potential channel morphodynamic change over 30 years and coupled REM results with our statistical models to predict nitrogen loading in these stream networks. We compared estimated nitrogen loading to an unincised base case for each site. Incision parameters such as the height of bank above the stream surface and width-depth ratio were important predictors of groundwater depth and riparian denitrification. Stratification of gaining and losing stream conditions improved denitrification model fit. Coupling these statistical models with REM simulations showed higher nitrogen loading at incised transects. Compared to an unincised base case, incision increased nitrogen loading from ~40-700% in the two small watersheds. These results indicate that channel incision can significantly increase nitrogen loading at the small network scale and, despite appreciable uncertainty in prediction accuracy, generally demonstrate the importance of coupled modeling of channel evolution and riparian nitrogen processes. To our knowledge, this is the first attempt to couple channel evolution and empirical riparian groundwater and denitrification models across a drainage network at decadal time

scales. Future research to fully couple these processes into a mechanistic model can allow for more robust quantification of the watershed-scale effects of channel incision on nitrogen loading.

Introduction

Addressing disturbances to the global nitrogen (N) cycle is an environmental management challenge of global significance. Anthropogenic activities have increased N loading to terrestrial and aquatic systems, which degrades their ecological integrity and limits provisioning of beneficial services (Mueller et al., 1995; Quinn, 1991; Vitousek et al., 1997). Riparian zones can be effective nitrogen sinks (Mulholland et al., 2008; Orr et al., 2007; Peterson et al., 2001), as they can permanently remove nitrogen via denitrification, an anoxic process in which microbes convert nitrate to inert dinitrogen gas using organic soil carbon (Hill, 1996). Therefore, locations where the riparian water table intersects the rhizosphere become hotspots for biogeochemical cycling, offering the greatest potential to reduce nitrate loading to streams. In addition to increased nutrient loading, anthropogenic activity can alter watershed hydrology and sediment supply, which contribute to erosive flows that trigger stream channel instability. Channel incision, or vertical downcutting via bed erosion, is widespread as a result of channel straightening and land development and conversion (e.g., Booth, 1990; Jacobson et al., 2001; Simon and Robbins, 1987). Small, low order streams, which make up the bulk of total stream length in watersheds, are especially susceptible to disturbance, making it likely that incision of these channels will significantly influence processes at the watershed scale.

The role of stream channel incision in riparian denitrification processes is often overlooked. Studies have observed lowered riparian water tables adjacent to incised streams (Groffman et al., 2002; Hardison et al., 2009; Schilling et al., 2006). These lower water tables create a larger unsaturated zone, disconnecting groundwater from carbon-rich surface soils,

limiting denitrification and potentially increasing nitrate loading to streams (Böhlke et al., 2007; Gift et al., 2010; Groffman et al., 2002; Mayer et al., 2010; Schilling et al., 2006). While these studies are valuable, they have largely been limited to a few urban watersheds in the mid-Atlantic (Böhlke et al., 2007; Groffman et al., 2002; Mayer et al., 2010) and a site in Iowa (Schilling et al., 2006; Schilling and Jacobson, 2014). Denitrification is notoriously difficult to measure (Groffman et al., 2006), and can occur sporadically in space and time when conditions are favorable (McClain et al., 2003). Thus, it is important to estimate the effect of channel incision on riparian denitrification and nitrate loading at longer and more continuous time scales and across wider spatial scales to enhance understanding of the coupled ecohydrological and nutrient cycling consequences of anthropogenic disturbances.

Several mechanistic models have been developed to simulate nitrogen transport and transformation in the riparian zone (Altier et al., 2001; Arnold et al., 1998; Bieger et al., 2017; Lowrance et al., 2000; Rassam et al., 2005). These models are useful but tend to be complex and data-intensive, and may not adequately represent relevant hydrologic, biogeochemical, and fluvial processes. A recent analysis found that existing models have little or no consideration of interactions between stream channel evolution and subsurface hydrology and, subsequently, biogeochemical processes such as denitrification (Buhr et al., 2022). In addition to these mechanistic models, empirical models based on field observations can be another viable method to quantify riparian nitrogen cycling. Numerous studies have used multiple linear regressions to predict denitrification rates in soil and groundwater. Soil properties, nitrogen concentrations, and carbon availability were the most prevalent predictor variables (Baker and Vervier, 2004; Barton et al., 1999b; de Klein and Van Logtestijn, 1994; Estavillo et al., 1994; Groffman and Tiedje, 1989; Hefting et al., 2003; Hunt et al., 2004; Jahangir et al., 2017, 2012; Jarvis et al., 1991;

Myrold, 1988; Parkin and Robinson, 1989; Parsons et al., 1991; Pinay et al., 1993; Robertson and Tiedje, 1984; Robertson and Klemedtsson, 1996; Schipper et al., 1993). The effect of the hydrologic connection between groundwater and streams on denitrification is underrepresented in these empirical models. Baker and Vervier (2004) were one of the only to explore this connection, finding higher denitrification in spring when hydrologic connections were most prominent. The prevalence of soil moisture as a predictor variable in other regressions alludes to the importance of hydrologic processes for denitrification. However, this does not account for fluvial processes like incision that can lower the groundwater table, thereby reducing moisture in surficial soil layers.

There are also a number of mechanistic models that simulate channel erosion processes (Langendoen and Alonso, 2008; Langendoen and Simon, 2008; Simon et al., 2011, 2000), though these are typically applied at the site scale. The River Erosion Model (REM) is a recent, open-source model of channel evolution that incorporates sufficient complexity of physical processes, but is applicable at the watershed scale. REM simulates bed and bank erosion processes throughout drainage networks, but with limited data requirements (Lammers and Bledsoe, 2018). Since research coupling channel morphodynamic models with riparian denitrification is limited, there is a need to incorporate site-specific riparian hydrologic and biogeochemical processes into a watershed-scale channel evolution model such as REM to explore linkages between channel erosion and riparian denitrification processes across decadal time scales.

It is important to advance modeling of the dynamics among stream geomorphological processes, groundwater-surface water exchange, and riparian nitrogen cycling to improve understanding of the effects of channel incision on nitrogen loading to streams. Coupled

modeling of channel incision and riparian denitrification processes at the small watershed scale can provide information about the relative importance of interactions between these processes. This underscores the need for effective hydromodification for water quality improvement and better inform future models that can be used to spatially prioritize watershed restoration.

Despite several available tools for simulating channel change and denitrification processes separately, there is a need to account for stream channel evolution in estimating riparian nitrogen cycling and long-term effects on diffuse pollution loading. To address this knowledge gap, we have: 1) developed statistical models for predicting riparian denitrification that accounts for groundwater-surface water interaction and stream morphology based on intensive field monitoring, and 2) coupled these models with simulations of network-scale morphodynamic change from the River Erosion Model (REM) to estimate long-term effects of channel incision on riparian nitrogen loading. To our knowledge, this is the first attempt to couple channel evolution modeling with site-specific empirical models for riparian groundwater and denitrification across a stream network at decadal time scales. Completing these objectives at two southeast US streams with contrasting physiographic context, soil type, land uses, and groundwater dynamics is useful for testing the applicability of the modeling approach beyond a single site. Estimating long-term changes in nitrogen loading in the context of channel evolution provides a relative assessment of the implications of channel change for diffuse nutrient pollution. This research can ultimately inform robust, watershed-scale modeling tools that more accurately simulate the influence of channel incision on riparian biogeochemistry and stream incision, yet remain parsimonious in terms of data requirements and complexity.

Methods

Field Data

The study sites, McQueen Branch and the UGA Teaching Dairy Farm, were described in Chapter 3. Physicochemical parameters from each monthly sampling event were used in this analysis, along with annual topographic surveys and initial characterizations of soil texture and organic carbon. Only measurements from the deep wells in each nest were included because denitrification was quantified in these wells. See Chapter 3 for detailed field data collection methods.

We developed several incision metrics based on our dataset: channel bankfull width-depth ratio (w:d); change in elevation from groundwater to stream surface (deltaElev), change in elevation from groundwater to stream bed (deltaBed), height of exposed bank above the stream surface (Ht_ExpBank), ratio of total bank height wetted by the stream (RatWetBank), and hydraulic gradient between the groundwater and stream (HydGrad). These variables differed at various scales. Width-depth ratio was constant across a transect and varied annually based on topographic survey results. Ht_ExpBank and RatWetBank were constant across a transect but varied monthly based on measured stream elevation. Finally, deltaElev, deltaBed, and HydGrad were different in each well and every month, based on observed stream and groundwater elevations. These metrics were inherently related, which we accounted for when exploring collinearity during statistical model development.

Regression Analyses

Best subsets multiple linear regression analysis was used to derive equations relating depth to groundwater and denitrification to physical and chemical characteristics. We analyzed the data for heteroscedasticity using the Breusch-Pagan test. When significant heteroscedasticity

was detected, data were perturbed to be greater than zero then log-transformed. The log-linear models had the following form:

$$Y = kX_1^{\beta_1}X_2^{\beta_2} \ldots X_n^{\beta_n}v \quad \text{[Eq. 4.1]}$$

Where Y is the output of interest (depth to groundwater or denitrification); X_i, 1,…, n are physical and chemical characteristics; k, β_i, 1,…, n are model parameters; and v are the lognormally distributed errors. When $\log_{10}$ of this model is taken, it becomes linear of the form:

$$log_{10}(Y) = \beta_0 + \beta_1 log_{10}(X_1) + \beta_2 log_{10}(X_2) + \cdots \beta_n log_{10}(X_n) + \varepsilon \quad \text{[Eq. 4.2]}$$

Where $\beta_0 = \log_{10}(k)$ and $\varepsilon = \log_{10}(v)$ are normally distributed residuals with mean zero and variance σ_ε^2.

Table 4.1. Variables used for statistical model development after removing variables due to physical understanding and collinearities.

Variable	Description	Units
Month	Month of year (1 to 12)	--
Nest	Set of wells relative to stream (1 to 3, with 1 nearest the stream)	--
DTW	Depth to groundwater	m
Temp	Groundwater temperature	C
DO	Dissolved oxygen	mg/L
pH	Groundwater pH	--
TN	Total nitrogen	ppm
DOC	Dissolved organic carbon	ppm
Denitrification	Denitrification end products (excess N_2 and N_2O)	mg/L
w:d	Channel bankfull width to depth ratio	--
Ht_ExpBank	Height of exposed bank above stream surface	m
HydGrad	Hydraulic gradient between groundwater and stream	--
Soil OC	Soil organic carbon	%
deltaBed	Difference in elevation from groundwater to stream bed	m
DistStr	Distance from the stream	m
% Sand	% sand in riparian soil	%

The pool of predictors was narrowed to around 25, using variables we collected monthly and incision metrics that we developed (Table C1). A Spearman correlation matrix was generated and collinearity was examined using the variance inflation factor (VIF). Variables were eliminated sequentially based on physical understanding and collinearity until all variables

had a VIF less than 10 (Hirsch et al., 1993). Eliminated variables due to high correlations were still largely represented by the retained variables, so minimal information was lost. The 16 variables considered for model selection are summarized in Table 4.1. It is generally desirable to have at least 10 observations per independent variable in the model (Hirsch et al., 1993), so the maximum number of independent variables was constrained based on the number of observations, with a maximum of 10. Models were cross-validated by training each model on 80% of the data then testing it with the remaining 20%. The best model was selected by balancing adjusted R^2 of the training data and the standard error of the cross-validation predictions, calculated with Equation 4.3 for $\log_{10}$-transformed data (adapted from natural log-transformed equation (Vogel et al., 1999)), where s_e^2 is the variance of the residuals of the estimated model and p is the number of independent variables in the model.

$$SE = \sqrt{10^{s_e^2(1+p)} - 1} \qquad \text{[Eq. 4.3]}$$

Physical understanding of the directionality of predictor variables was also used in model selection. For example, if a 6-variable model performed slightly better than a 5-variable model but included a variable acting opposite of its understood relationship (e.g., percent sand correlating negatively with depth to groundwater instead of correlating positively), then the 5-variable model was favored.

Several regressions were developed using these methods to explore trends in our dataset. We used the entire dataset to develop separate regressions to predict depth to groundwater and denitrification ("overall" models). We repeated this analysis after dividing the overall dataset by site (McQueen and dairy farm; "site-specific" models). When a dummy variable representing gaining and losing conditions was influential for the best denitrification models, we subset the

data into gaining and losing and generated denitrification regressions for each. We evaluated randomness in model error using Run's test on the residuals.

All statistical analyses were conducted in R (R Core Team, 2021) using the following packages: *caret* (Kuhn, 2022), *leaps* (Lumley, 2020), *car* (Fox and Weisberg, 2019), *corrplot* (Wei and Simko, 2021), *tidyverse* (Wickham et al., 2019), *randtests* (Caeiro and Mateus, 2022), and *lmtest* (Zeileis and Hothorn, 2002).

REM Simulation Setup

Watershed-scale channel evolution models were created in REM for each study site. Two scenarios were generated for each site: Scenario A to yield a moderate amount of incision and Scenario B to have worsened incision. REM required input data for the stream network, channel geometry, grain size, bank properties, discharge and sediment supply, and knickpoints. The dairy farm was simulated as two reaches: the unincised upstream reach and the incised downstream reach. McQueen Branch was simulated as three reaches: the incised mainstem, the unincised tributary, and their confluence. We did not include the reach with the confluence in our topographic surveys, so many physical variables were set similar to the upstream reach (incised), measured manually, or estimated based on LiDAR.

User-defined REM inputs for Scenario A are tabulated in Appendix C (Table C2). Measurements from our annual topographic surveys were used to specify initial channel and floodplain geometry – channel bottom width, bank height, bank angle, floodplain angle, and floodplain widths. Bed slope was also estimated based on a linear regression of our longitudinal survey stations and elevations. Reach lengths were approximated from the topographic surveys and extended at least 20 m upstream, as long as channel width observed using recent LiDAR appeared relatively constant. The downstream boundary of the modeled reach was set to the

confluence with the main channel at the dairy and to the culvert and road at McQueen. Cross-section spacing was set so each reach had at least five cross-sections. Channel and floodplain Manning's n values were estimated based on visual observations of sediment, wood, and sinuosity and comparisons to photographic evidence (Arcement and Schneider, 1989).

Grain sizes were estimated based on visual observations and adjusted such that each model was stable and produced results that resembled our observed channel changes over two years. Single grain sizes were used to simplify modeling. The depth to cohesive layer was estimated based on stratigraphy and incision (e.g., an incised channel could be closer to the cohesive layer) and field-tested with a tile probe. Bank and toe soil properties were chosen from distributions used for BSTEM geotechnical properties (Simon et al., 2011) based on riparian soil types and field observations. One knickpoint was specified at the dairy farm to simulate the headcut that we measured while surveying. No knickpoints were simulated at McQueen since incision had progressed through our entire modeled mainstem reaches.

Stream elevation was measured in stream gages at 5-minute intervals for approximately two years. This elevation was combined with surveyed stream channel geometry to calculate depth (h), area (A), and hydraulic radius (R) of flow at each time step. Assuming a hydraulically rough plane boundary, the relationship between depth average velocity (V_x; m/s) and shear velocity (u_*; m/s) was calculated using Equation 4.4 (Julien, 1995), where k_s' is grain roughness, calculated for sand-bed channels as $k_s' = 2\ D_{90}$ (Kamphuis, 1974) . D_{90}, the particle diameter (m) at which 90% of the particles are finer, was assumed for each stream reach based on visual observations.

$$\frac{V_x}{u_*} = 5.75 \log\left(\frac{12.2h}{k_s'}\right) \qquad \text{[Eq. 4.4]}$$

We converted this relationship to the Chezy coefficient (C) using gravitational acceleration (g; 9.8 m/s^2) and Manning's n using Equations 4.5 and 4.6, respectively.

$$\frac{V_x}{u_*} = \frac{C}{\sqrt{g}} \quad \text{[Eq. 4.5]}$$

$$C = \frac{R^{1/6}}{n} \quad \text{[Eq. 4.6]}$$

This Manning's n only accounted for grain roughness. We added form roughness that increased linearly and inversely with flow depth until the range and average Manning's n values were similar to our estimations based on field observations and photographic evidence. This total Manning's n was used to estimate flow velocity (v) with Manning's equation (Equation 4.7), where S is bed slope from our annual longitudinal surveys.

$$v = \frac{R^{2/3} S^{1/2}}{n} \quad \text{[Eq. 4.7]}$$

The continuity equation (Equation 4.8) was used to estimate discharge (Q) based on flow velocity and cross-sectional flow area (A).

$$Q = vA \quad \text{[Eq. 4.8]}$$

This process was repeated at each stream gage. Discharge for the confluence reach at McQueen, where there was no stream gage, was calculated as the sum of the discharges at the incised and unincised reaches. Our calculations slightly overestimated discharge relative to estimations from the USGS stream gage at the downstream end of this reach (active from 1990 to 2002). We attributed these differences to changes in watershed imperviousness and stormwater practices in the 20 years since the stream gage was inactivated, along with uncertainty in our estimation of Manning's n.

External Coupling

Each REM model was simulated at 5-minute time steps for 30 years, beginning with the onset of our monitoring, to better capture long-term channel evolution processes. The two years of calculated discharge were repeated. The total load equation for sediment transport was used and bank erosion from both fluvial processes and bank failure were simulated. We analyzed changes in channel width and depth over the simulation period to evaluate the predicted channel evolution.

REM station and elevation outputs were extracted to calculate channel geometry and stream elevation at daily time steps. These were used to calculate the physical measurements related to incision (e.g., width-depth ratio, bank height) that were important in our regression analyses. We aggregated our field dataset by calendar month and estimated mean and standard deviation for various physicochemical groundwater characteristics (e.g., temperature, pH, etc.) that were important in our regression analyses. We randomly selected a monthly value for each characteristic, assuming a log-normal distribution. We accounted for moderate correlations (Spearman correlation > 0.4) between these inputs by constraining a correlated variable to the upper or lower tail of its distribution, depending on the initial value of the other correlated variable and the direction of correlation. These characteristics were used to predict depth to groundwater with both the overall and site-specific regressions. We omitted the site-specific McQueen model due to consistent predicted hydraulic gradients beyond the range of observed. We compared the predicted depth to groundwater to the calculated stream elevation to determine if the stream was gaining or losing. The direction of groundwater-surface water interaction dictated which denitrification regression we used, when separate regressions were developed. We estimated total denitrification using both the overall and site-specific regressions daily and

computed a monthly average for each cross-section. We subtracted the estimated denitrification from a total nitrogen concentration assumed based on our field dataset (and constrained to be greater than total denitrification) to estimate the percent nitrogen removal and mass remaining. Groundwater discharge (Q) was estimated using Darcy's equation (Equation 4.9).

$$Q = KiA \quad \text{[Eq. 4.9]}$$

Where K is hydraulic conductivity estimated from the NRCS Web Soil Survey (Soil Survey Staff, 2022), i is the hydraulic gradient, and A is the cross-sectional area of groundwater discharge. If the stream was gaining at that time step, nitrogen in that groundwater discharge became a nitrogen load. Daily results were aggregated to estimate annual nitrogen loading and summed over the simulation to calculate a cumulative nitrogen load.

We compared nitrogen loading from the REM simulations to a base case in which the channel remained unincised over the 30-year simulation. Channel geometry, streamflow, and riparian parameters from the unincised reaches were applied to the entire drainage network. Our field observations showed that the unincised transect at McQueen switched to gaining from December through March with a peak in groundwater elevation in early January. To emulate the observed seasonal switching of gaining and losing conditions, we supplemented the hydrologic records produced by the statistical models which primarily trained on losing conditions to include gaining periods. Based on the maximum observed hydraulic gradient (0.02 m/m), we increased the groundwater table to this value on January 1 and then decreased it over three months with smoothing for ≤10 days at the transitions. Depth to groundwater was estimated with the statistical models during the remainder of each year, and subsequently used to estimate denitrification for the base cases.

Results

Coupled modeling of channel evolution and denitrification at both study sites showed that incision greatly reduced riparian denitrification, thereby increasing nitrogen loading. We found that incision parameters such as height of exposed streambank and channel width-depth ratio were important for building statistical models to predict both depth to groundwater and denitrification. Differentiating between gaining and losing conditions was useful for fitting our denitrification models. In this section, we present our statistical models, followed by results of coupled channel evolution and riparian denitrification modeling at both study sites, before comparing these results to our base case.

Statistical Modeling

Depth to groundwater was significantly correlated to many of the incision variables, particularly height of exposed bank (Figure C1). Denitrification was highly correlated with N_2O, an end product used in its calculation, along with temperature, dissolved oxygen, and groundwater nitrate concentration. The incision variables, which were largely calculated from similar channel geometry measurements, were highly correlated amongst themselves. Variables that were significantly correlated to many of the other parameters included specific conductance, pH, and the soil particle size classes. These correlations informed removal of highly collinear variables when developing regressions.

We did not detect significant heteroscedasticity in depth to groundwater across the entire dataset, and thus did not transform the data. All other datasets were log-transformed due to heteroscedasticity. The height of exposed streambank, soil organic carbon, temperature, and channel width-depth ratio were the most important variables (in that order, based on coefficient magnitude) for predicting depth to groundwater (Table 4.2). The overall regression and the site-

specific regression for McQueen explained over 80% of variance with three predictor variables. Month, temperature, pH, channel width-depth ratio, and distance from the stream were most important for predicting denitrification (Table 4.3). Distinguishing between gaining and losing conditions was important for the overall dataset and at the dairy farm, but not at McQueen. Adjusted R^2 values for the denitrification models ranged from 0.26 to 0.57. Prediction standard errors for denitrification were best at the dairy farm and lowest at McQueen and during gaining conditions with the overall model. Residuals were not produced in a random manner for all depth to groundwater regressions ($p < 0.001$; Figures C2, C3, and C4) and denitrification regressions for the overall dataset ($p < 0.001$ and $p = 0.02$ for gaining and losing models, respectively; Figures C5 and C6) and at McQueen ($p = 0.02$; Figure C9). Model errors were produced in a random manner for both denitrification models at the dairy farm ($p = 0.72$ and $p = 0.78$ for gaining and losing models, respectively; Figures C7 and C8).

Table 4.2. Summary of best subset regressions to predict depth to groundwater.

Dataset	n	Transform.	Adj. R^2	Var_1	Var_2	Var_3	k	β_1	β_2	β_3	MSE	SE
Overall	237	--	0.84	Temp	w:d	Ht_ExpBank	-0.678	0.044	0.035	0.855	0.08	0.28
Dairy	119	$Log_{10}(x)$	0.41	Temp	w:d	Ht_ExpBank	-2.22	1.24	0.451	1.78	0.03	0.56
MQ	118	$Log_{10}(x)$	0.87	Temp	Ht_ExpBank	SoilOC	-3.69	1.88	1.11	-1.96	0.02	0.48

Table 4.3. Summary of best subset regressions to predict denitrification.

Dataset	n	Direction	Transform.	Adj. R^2	Var_1	Var_2	Var_3	Var_4	Var_5	k	β_1	β_2	β_3	β_4	β_5	MSE	SE
Overall	76	Gaining	$Log_{10}(x)$	0.39	Month	DTW	pH	HydGrad		-1.861	-0.409	-0.234	3.14	2.08		0.14	2.05
	86	Losing	$Log_{10}(x)$	0.30	Month	w:d	DistStr			0.221	-0.291	0.304	-0.231			0.05	0.73
Dairy	32	Gaining	$Log_{10}(x)$	0.47	DTW	Temp	w:d	deltaBed		4.51	-1.92	-2.43	-5.14	-1.21		0.01	0.39
	51	Losing	$Log_{10}(x)$	0.57	Month	w:d	DistStr	% Sand		17.8	-0.406	0.366	-0.562	-9.83		0.01	0.31
MQ	79	--	$Log_{10}(x)$	0.26	Month	DO	pH	DOC	HydGrad	-4.62	-0.336	0.509	6.94	-0.164	5.79	0.12	1.97

Coupled Channel Evolution and Riparian Denitrification Modeling

Dairy Farm

Scenario A of the 30-year REM simulation generated maximum incision of less than 1 m (Figure 4.1a), which occurred near the junction of the unincised (upstream) and incised (downstream) reaches. This can mostly be attributed to knickpoint migration upstream through these cross-sections. Channel width increased by up to 0.3 m (Figure 4.1b), most of which occurred in the upstream end of the unincised reach. Scenario B resulted in nearly 2 m of maximum incision that occurred midway through the unincised reach due to accelerated knickpoint migration (Figure 4.1c). Width remained relatively constant, increasing by approximately 0.1 m (Figure 4.1d), mainly in the upstream reach.

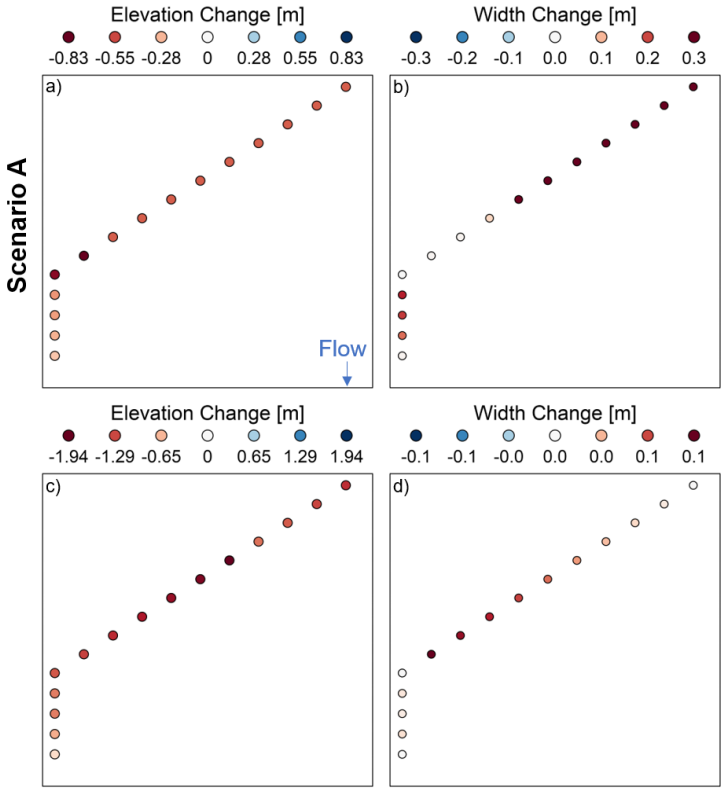

Figure 4.1. Changes in channel width and depth over the 30-year REM simulation at the dairy farm. Scenario A (panels a and b) portrays less incision than Scenario B (c and d). Each dot is a cross-section, spaced 10 m apart. Flow is moving from top (originally unincised reach) to bottom (incised reach).

The average depth to groundwater for Scenario A ranged from 0.6 m below the surface in the unincised reach to 1.61 m at the upstream end of the incised reach (Figure 4.2a). Denitrification followed a similar spatial pattern, with highest values at the upstream end of the incised reach (Figure 4.2b). Nearly all of the stream network nitrogen loading occurred in the incised reach, with 21.4% of the total load coinciding with the cross-section with the deepest groundwater (Figure 4.2d). Scenario B showed similar trends, with the downstream, incised reach, having deeper groundwater (Figure 4.2e) and greater nitrogen loading (Figure 4.2h). Denitrification was more spatially-variable, with the maximum occurring in the upstream portion of the modeled stream network (Figure 4.2f). In Scenario A, the unincised reach was losing more frequently than gaining, while the incised reach was predominantly gaining (Figure 4.2c). All cross-sections were predominantly gaining in Scenario B, with more gaining in the incised reach (Figure 4.2g). Results of the site-specific models are in Appendix C (Figure C10). The magnitude and spatial trend in depth to water were similar between the overall model and site-specific models, but the site-specific modeling predicted more losing conditions in both reaches than the overall modeling. The site-specific model predicted higher average denitrification than the overall denitrification model at locations in the unincised reach that were incised but not widened, but less denitrification in the incised reach. Contributions to total load were similar, except the site-specific model predicted little upstream nitrogen loading in Scenario B.

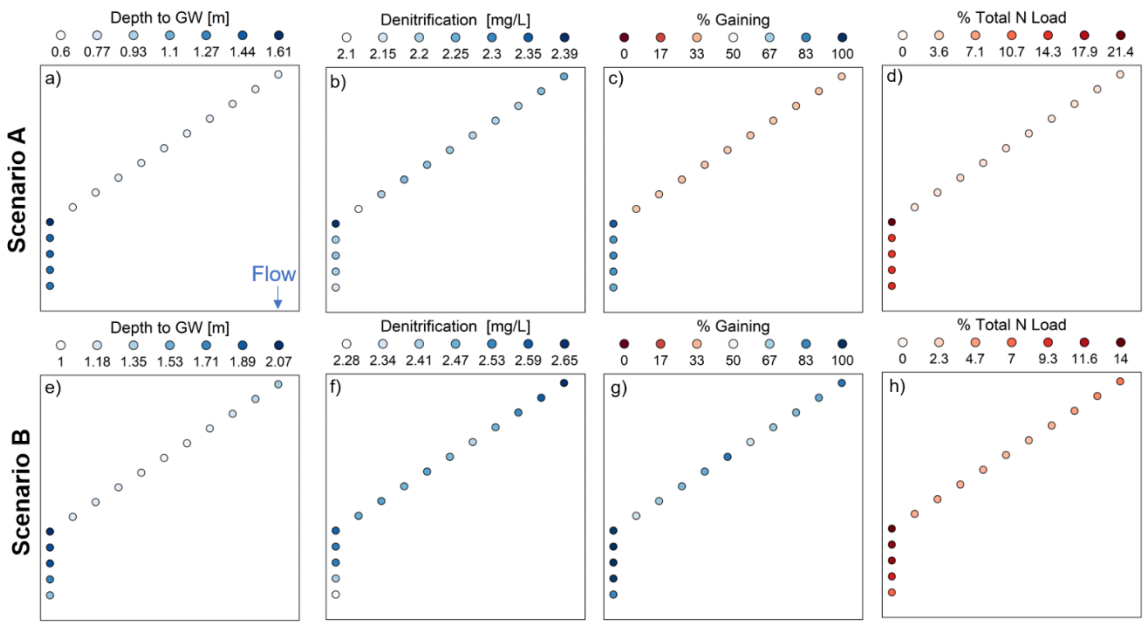

Figure 4.2. Average groundwater depth (panels a and e) and denitrification (b and f) across the 30-year REM simulation at the dairy farm, plus the percentage of gaining flows (c and g) and stream network nitrogen load from each cross-section (d and h), as predicted by the overall models. Scenario A (panels a-d) had less incision than Scenario B (e-h). Each dot is a cross-section, spaced 10 m apart. Flow is moving from top (unincised reach) to bottom (incised reach).

McQueen Branch

Scenario A of the REM simulations generated maximum incision of 0.26 m (Figure 4.3a) at the confluence of the unincised (top left) and incised (top right) reaches. The greatest increases in channel width occurred immediately upstream of the confluence (Figure 4.3b). Scenario B exhibited maximum channel incision of nearly 2 m throughout both upstream reaches and midway through the downstream reach (Figure 4.3c). Width also increased in the upstream reaches, with a maximum of 3.6 m widening near the upstream end of the incised reach (Figure 4.3d).

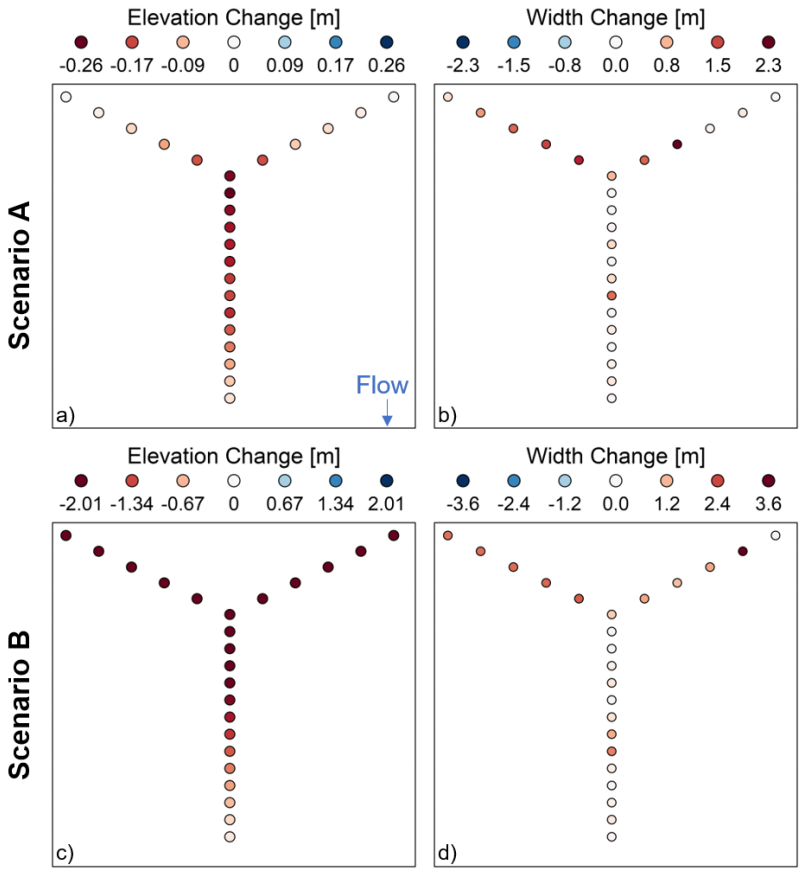

Figure 4.3. Changes in channel width and depth over the 30-year REM simulation at McQueen. Scenario A (panels a and b) portrays less incision than Scenario B (c and d). Each dot is a cross-section, spaced 20 m apart. Flow is moving top to bottom, from the originally unincised reach (top left) and incised reach (top right).

The average depth to groundwater for Scenario A ranged from 0.5 m below the surface in the unincised reach to 2.66 m in the incised reach (Figure 4.4a). Denitrification showed an inverse spatial trend, with highest values at the unincised reach (Figure 4.4b). Nearly all of the stream network nitrogen loading occurred in the incised and downstream reach, with over 10% of the total load coinciding with the cross-section with the deepest groundwater and least denitrification (Figure 4.4d). Scenario B was similar, with the originally unincised reach having more elevated groundwater (Figure 4.4e) and greater denitrification (Figure 4.4f). Total nitrogen loading was more spatially-variable, with the maximum occurring in the upstream cross-section

of the incised reach and near the confluence (Figure 4.4h). In Scenario A, the unincised reach was losing more frequently than gaining, a trend that diminished near the confluence (Figure 4.4c). The incised reach was mostly gaining and gaining increased nearer to the confluence. The downstream end of the confluence reach was mostly losing. All cross-sections except for the downstream end of the network were predominantly gaining in Scenario B, with more gaining in the incised reach (Figure 4.4g).

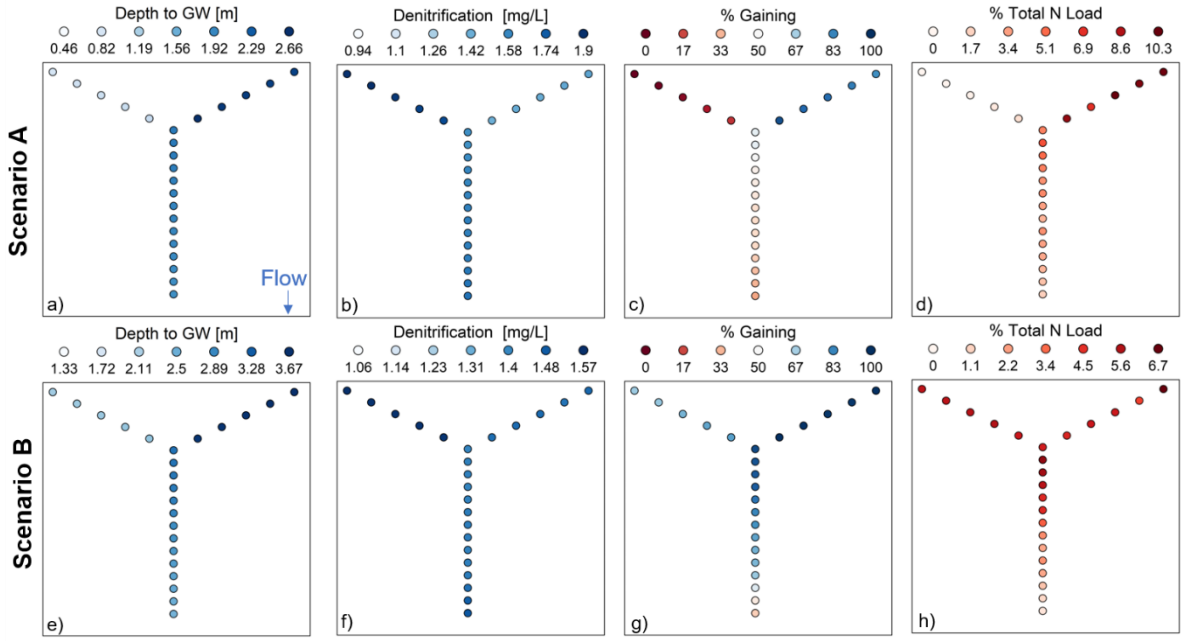

Figure 4.4. Average groundwater depth (panels a and e) and denitrification (b and f) across the 30-year REM simulation at McQueen, plus the percentage of gaining flows (c and g) and stream network nitrogen load from each cross-section (d and h), as predicted by the overall models. Scenario A (panels a-d) had less incision than Scenario B (e-h). Each dot is a cross-section, spaced 20 m apart. Flow is moving from top to bottom, from the originally unincised reach (top left) and incised reach (top right).

Comparison to the Base Case

Cumulative network nitrogen loading calculated using the overall models (based on data across both locations) was greater in each of our modeled scenarios than our base condition (Table 4.4). Our incised models had decreased denitrification and denitrification reaction progress (the proportion of available nitrogen that is removed by denitrification) compared to the

base. Scenario B (greater incision) at both sites yielded higher increases in nitrogen loading than Scenario A relative to the base condition, but lower reductions in denitrification and RP. Incised models also simulated an increased proportion of gaining flows, which increased with greater incision. Plots showing spatial variability in depth to groundwater, denitrification, and total N load contributions for the base case at each site are in Appendix C (Figure C11 for the overall models and Figure C12 for the dairy-specific models). Similar, yet generally reduced, differences in each output were predicted using the site-specific models at the dairy farm, except RP was 10% higher than the base case in Scenario B (Table C3).

Table 4.4. Comparison of estimated changes in total network nitrogen loading, riparian denitrification and reaction progress (RP), and proportion of gaining flows relative to the unincised base condition.

Model	Scenario	% Change in N Load	% Change in Denitrification	% Change in RP	% Change in Gaining
Dairy	Scenario A	45 %	-97 %	-17 %	84 %
	Scenario B	240 %	-93 %	-13 %	190 %
MQ	Scenario A	82 %	-89 %	-13 %	38 %
	Scenario B	740 %	-81 %	-17 %	150 %

The most substantial increases in nitrogen loading were observed in the incised reaches and during Scenario B, which had greater incision (Table 4.4). Scenario A showed a decrease in nitrogen loading relative to the base in the unincised reaches for both locations (Figure 4.5), likely caused by differences in the amount of gaining flows. Nitrogen loading at the dairy farm was most exacerbated in the upstream portion of the incised reach, which had the highest denitrification but was also where more incision relative to widening had occurred. Differences in nitrogen loading decrease moving downstream at McQueen, coinciding with decreased incision and increasing denitrification. Spatial patterns in differences using the site-specific dairy models were the same as for the overall models, but with higher percent differences (Figure C13).

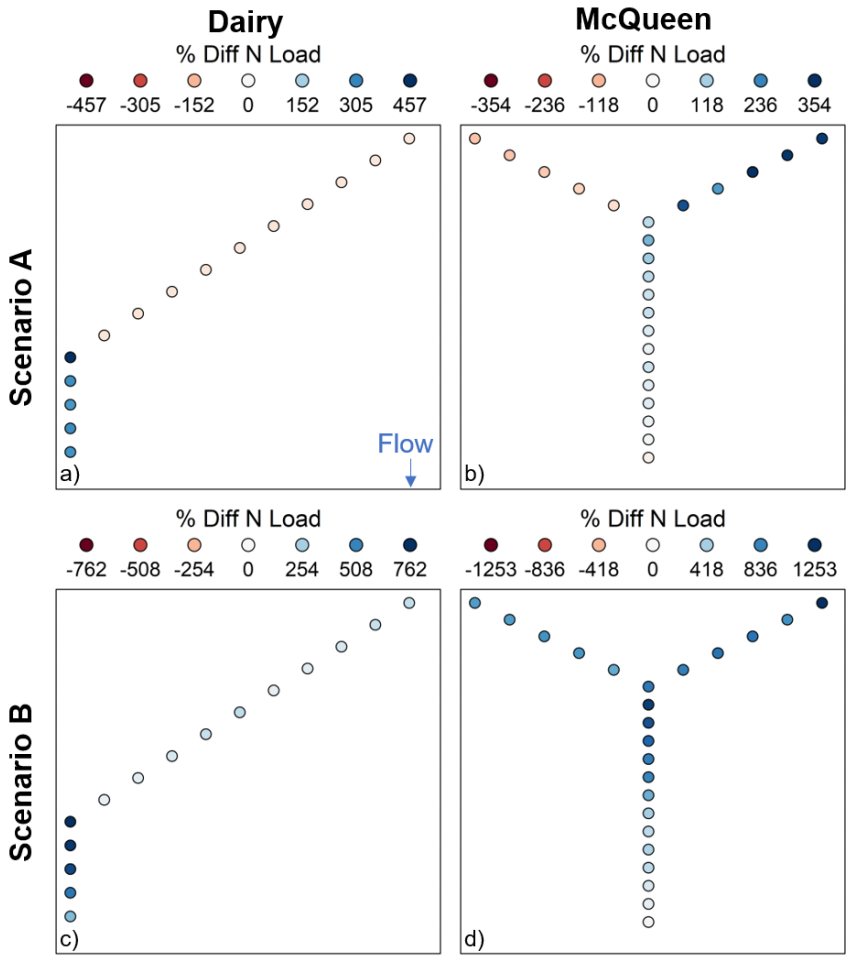

Figure 4.5. Spatial distribution of percent differences in nitrogen loading between each incision scenario and the base case and Dairy (panels a and c) and McQueen (b and d), as predicted by the overall models. Each dot is a cross-section, spaced 10 m and 20 m apart for Dairy and McQueen, respectively. Flow is moving from top to bottom.

Discussion

Groundwater and Denitrification Modeling

We found that variables representing channel incision were among the most important for predicting observed depths to groundwater and denitrification. The height of exposed bank captured fluctuations in stream elevation relative to the depth of incision, which both affect groundwater depth (Brunke and Gonser, 1997; Groffman et al., 2002; Hardison et al., 2009; Schilling et al., 2006). Width-depth ratio was an important predictor in both regressions, except

at McQueen, where we observed a narrower range of width-depth ratio than at the dairy farm (3.8-8 vs. 2-20). This also had the most important effect of all variables included in two denitrification models. Hydraulic gradient and deltaBed were likely important for denitrification because they related the groundwater elevation to the stream water and bed elevations, respectively. Stream and bed elevations are used to calculate degree of incision and stream stage, which were important indicators of adjacent depth to groundwater in a recent analysis (Pierce, 2020).

Distinguishing gaining and losing conditions was important for predicting denitrification with the dataset combined across both sites and the site-specific dataset at the dairy farm. This exemplifies that it is important to stratify data based on groundwater-surface water gradient direction when analyzing denitrification in incised stream networks. Denitrification models for losing conditions included parameters related to incision and groundwater depth, while gaining models also included common denitrification controls like temperature and pH (Heinen, 2006; Rivett et al., 2008). We did not find it useful to make the gaining and losing division at McQueen. However, the denitrification model at McQueen included hydraulic gradient, which inherently represents both gaining and losing, depending on the sign (positive or negative).

Past analyses found that soil properties such as moisture content, temperature, texture, and pH are common predictor variables for denitrification (Barton et al., 1999a; de Klein and Van Logtestijn, 1994; Estavillo et al., 1994; Groffman and Tiedje, 1989; Hefting et al., 2003; Jahangir et al., 2017; Jarvis et al., 1991; Myrold, 1988; Parsons et al., 1991; Pinay et al., 1993; Robertson and Tiedje, 1984; Robertson and Klemedtsson, 1996; Schipper et al., 1993). We observed at least one of these (assuming month is related to temperature) in each denitrification model, with pH being the strongest predictor in multiple models. We were surprised that organic

carbon only appeared in one of our denitrification models, given its prevalence in previous models (Baker and Vervier, 2004; Jahangir et al., 2012; Myrold, 1988; Parkin and Robinson, 1989; Parsons et al., 1991; Pinay et al., 1993; Robertson and Tiedje, 1984). Nitrate, ammonia, and total nitrogen have also been included in many denitrification models (de Klein and Van Logtestijn, 1994; Estavillo et al., 1994; Hefting et al., 2003; Hunt et al., 2004; Jahangir et al., 2017, 2012; Jarvis et al., 1991; Myrold, 1988; Parsons et al., 1991; Pinay et al., 1993; Robertson and Tiedje, 1984; Schipper et al., 1993). Total nitrogen was the only one included in our analysis, and it was not an important predictor. We excluded nitrate and ammonia from our pool of predictor variables because those analytical data were not current with denitrification measurements. We expect that a future iteration of the denitrification models will include a variable representing nitrogen concentration, particularly nitrate, since our correlation analysis found a significant positive relationship with denitrification.

Temperature has been used to predict groundwater depth in a recent model (Kumar et al., 2020), which is reasonable given that groundwater depth can vary seasonally (Harden and Spruill, 2008; Hardison et al., 2009). Soil organic carbon can be associated with soil type, with generally higher organic carbon in clays than sands (Magdoff and Van Es, 2021). We expected soil texture variables such as percent sand to be important predictors of depth to groundwater since clay soils generally have higher water-holding capacity than sandy soils (USDA Natural Resources Conservation Service, 2008). One reason we may not have found this to be important is because incision caused similar depths to groundwater across both sites, despite a difference of nearly 30% in sand content. It was surprising that depth to groundwater was an important predictor for denitrification only under gaining conditions, given that saturated conditions reduce dissolved oxygen (Pfeiffer et al., 2006), an important control on denitrification (Tiedje, 1998).

However, other parameters like width-depth ratio and hydraulic gradient were either already included in the depth to groundwater model or used groundwater elevation in their calculation.

Most predictor variables exhibited the expected directional relationship with the dependent variable, but some, such as width-depth ratio, acted opposite of our physical understanding. We expected that width-depth ratio, in which a decrease corresponds to greater incision, would be negatively correlated with depth to groundwater and positively correlated to denitrification. Our correlation analysis showed a negative correlation between depth to groundwater and width-depth ratio, yet our statistical models were the opposite. Width-depth ratio had the lowest influence on groundwater depth of the three predictors, so its inclusion in the models may indicate a marginal effect relative to the others. This relationship between width-depth ratio and denitrification was opposite of expected for the denitrification model when the dairy farm stream was gaining. Gaining only occurred at the incised reach at the dairy farm, which had different width-depth ratios each year based on annual surveys. Thus, inclusion of width-depth ratio in this model represents annual variation in denitrification more than effects of incision.

Several other parameters showed opposite influences on denitrification than expected. Temperature can be positively correlated with denitrification (Myrold, 1988; Rivett et al., 2008; Schipper et al., 1993), but our denitrification model for gaining at the dairy farm showed a negative relationship with temperature. This is likely due to outliers in denitrification measured during Jan-Feb 2022, driven by incomplete denitrification (N_2O). Higher dissolved oxygen generally decreases denitrification (Anderson et al., 2014; Tiedje, 1998; Trudell et al., 1986), but our denitrification model at McQueen predicted a positive relationship with DO. The McQueen denitrification model also showed a negative relationship with carbon, which should be a

positive relationship (Gift et al., 2010; Mayer et al., 2010; Pinay et al., 1993). Another reason for these opposing effects could be because we detected no difference between the amount of denitrification at incised and unincised transects (Chapter 3). These variations from our physical understanding in the McQueen denitrification model likely resulted from low adjusted R^2 and high standard error.

All of our statistical models except for the dairy-specific denitrification models had nonrandomly-generated residuals, indicating model fit could be improved. This finding may be due to variability or noise in water chemistry and water quality data, particularly at McQueen. Furthermore, there may be additional variables that were excluded from the models that drive the nonrandom distribution of residuals and should be included in subsequent analyses. This could include a nitrogen concentration variable for estimating denitrification, as described previously. Collecting additional data may facilitate the use of other statistical modeling approaches, such as tree-based models, that better represent nonlinearities and variable interactions.

Nitrogen Loading in Incised Stream Networks

Our results showed that channel incision can significantly increase network-scale nitrogen loading in certain contexts. The statistical models predicted a higher depth to groundwater at incised reaches, similar to observations in ours and other field studies (Groffman et al., 2002; Hardison et al., 2009; Schilling et al., 2006). This generally led to decreased denitrification and higher nitrogen loading at these cross-sections, also aligning with past research (Böhlke et al., 2007; Groffman et al., 2002). Channel incision lowered the stream bed and increased the prevalence of gaining conditions. Our denitrification models for gaining conditions were negatively correlated with depth to groundwater, meaning the deeper groundwater in these incised reaches decreased denitrification. Furthermore, nitrogen loads were

calculated only during gaining conditions, since water was flowing into the stream. Losing conditions, which occurred predominantly in the unincised reaches, did not contribute to the nitrogen load since flow exited the stream.

Compared to the base case, we found a substantial reduction in denitrification and corresponding increase in nitrogen loading in incised stream networks. The greatest differences occurred at locations where the channel primarily incised (with less widening), such as at the upstream end of each incised reach at McQueen. While these changes decreased width-depth ratio, the depth to water and denitrification were decreased by the increase in exposed bank height. The reason that originally unincised reaches showed lower nitrogen loading than the base case for Scenario A is because we imposed the generic hydrologic regime that forced gaining conditions in those reaches during winter. Before incising during the simulations, those reaches were predominantly losing and not contributing nitrogen load to the stream.

A prior study found that nutrient losses from riparian zones adjacent to incised streams did not greatly impact regional nitrogen loading (Schilling and Jacobson, 2014). That study compared nitrogen loading from perennial riparian buffers to total nitrogen loads for a region that included over 60% agricultural riparian cover. The spatial scale of our study was for small stream networks with only first- and second-order streams with a single adjacent land use. We also accounted for decadal-scale changes in channel incision that affected gaining and losing dynamics. It is possible that the exacerbated nitrogen loading we observed may become dampened across larger spatial scales, so applying our analyses to longer stream networks with variable land uses could better inform interpretation of our results for larger watersheds.

Similar predictions for groundwater depth and denitrification from the site-specific models at the dairy farm and the overall models illustrated that our models built on the combined

dataset may have broader applicability beyond our individual sites. The overlap in model variables, both in general and between the corresponding gaining and losing models for each dataset, indicated that the same controls are present at the dairy farm as across both sites. Upstream denitrification values predicted with the site-specific model may have been higher than prediction from the overall models due to the high intercept value in the losing, site-specific model and because our assumed distance to the stream (1 m), which was negatively correlated with denitrification, was slightly less than the values used to train the model. However, these estimates may have been more representative of actual denitrification given the much lower prediction errors and randomly-generated residuals for the site-specific models.

We recognize there is considerable uncertainty in our prediction accuracy and caution the interpretation of the magnitudes of our results. Our estimates of REM inputs such as grain size and bank properties that can be significant controls on channel incision and widening (Lammers and Bledsoe, 2018) introduce uncertainty in channel evolution predictions. Our statistical models propagate this uncertainty when predicting groundwater depth and denitrification. Future analysis with Monte Carlo simulations of REM to explore uncertainty would be useful for generating a range of plausible morphodynamic changes. Improving empirical model fit and input uncertainty would be helpful for enhancing our ability to quantify connections between channel incision and nitrogen loading. Despite this uncertainty, the relative comparisons of our results suggest that channel incision can appreciably increase nitrogen loading in certain contexts, an influence that warrants further research and attention in management.

We were surprised that portions of the incised reach at the dairy farm had higher modeled denitrification than the unincised reach, despite deeper groundwater tables. The likely cause of this is that incision lowered stream elevation sufficiently to generate higher gaining hydraulic

gradients, which counteracted the negative effects of groundwater depth in the overall denitrification model for gaining. When these hydraulic gradients were higher than the ones used for model development, denitrification estimates may have approached the expected maximum. This model also had the highest standard error of all our denitrification models, suggesting that prediction error could be partly responsible for these results.

Management Implications and Future Research

Our findings are useful for water resources management in response to extensive anthropogenic disturbance to stream networks. Incised streams are commonplace (Booth, 1990; Jacobson et al., 2001; Simon and Robbins, 1987), meaning that exacerbated nitrogen loading related to channel change may be more widespread than currently thought. While recent studies have summarized the current and potential prevalence of losing streams (Jasechko et al., 2021; Uhl et al., 2022), our findings suggest that incising stream networks may be primarily gaining, receiving nitrogen from the adjacent riparian zone that has undergone less denitrification than in a well-connected riparian zone. Estimating the potential magnitude of increased nitrogen loading in incised streams underscores the role of flow management in water quality improvement at the small watershed scale.

One limitation of this study is that our statistical models were built on limited temporal (fewer than two years) and spatial (four individual transects in first-order streams) data. Gaining and losing are spatially- and temporally-variable (Cardenas, 2009; Essaid and Caldwell, 2017; Gordon et al., 2004; Zimmer and McGlynn, 2017), and reaches can often be concurrently gaining and losing (Covino et al., 2011; Covino and McGlynn, 2007; Payn et al., 2009). The unincised transect at the dairy farm was always losing, which may have disproportionately influenced parameterization of our statistical models. Continued long-term monitoring at the existing

locations and expanded sampling longitudinally along the streams may better reveal spatial and temporal patterns in gaining and losing relevant to channel incision and allow us to refine our statistical models. Collecting similar field data in larger stream networks and across other regions and hydrogeomorphic settings to supplement our statistical models would increase their applicability to other watershed contexts.

To our knowledge, this is the first study to couple channel evolution modeling with site-based empirical riparian denitrification models to estimate the decadal effects of channel incision on network-scale nitrogen loading. Our findings demonstrate the necessity to improve understanding on this topic and develop models with more accurate numerical predictions of interactions between these processes. Future efforts to develop fully-coupled models are imperative to advance understanding and improve estimation of incision-related nitrogen loading. Using mechanistic groundwater and denitrification models instead of statistical models could greatly improve the applicability of findings across landscape settings. Such tools could assist water resources managers in identifying locations where channel incision causes a disproportionately large amount of nitrogen to enter streams, guiding spatial prioritization of ecological restoration practices for reducing channel erosion and nitrogen loads and, thus, eutrophication downstream.

Conclusions

We estimated the effects of channel incision on nitrogen loading to stream networks with coupled modeling of channel evolution and riparian denitrification. Using field data we collected at two sites with paired incised and unincised stream reaches, we developed statistical models to predict depth to groundwater and riparian denitrification. These data and empirical models enabled implementation of a novel coupled modeling approach to estimate changes in stream

network nitrogen loading in response to channel evolution based on 30-year simulations of the River Erosion Model (REM) at each site. We also compared these results to a base condition that represented an unincised stream network with a generic hydrologic regime with seasonal switching in gaining and losing.

Height of exposed streambank and stream width-depth ratio were the most common incision variables that were important for predicting observed depth to groundwater and riparian denitrification. Temperature, month, pH, and hydraulic gradient were other variables present in multiple statistical models. We expected that carbon and nitrogen concentrations would have been important in denitrification models, but effects of these variables were minimal. Our analyses indicated that stratifying denitrification models into gaining and losing conditions substantially improved model fit in accordance with our previous findings which highlighted the importance of differentiating between gaining and losing when analyzing near-stream effects of incision on groundwater and nitrogen dynamics.

In our coupled modeling results, channel incision substantially increased nitrogen loading in incised reaches by causing deeper groundwater tables and reduced denitrification. Incised reaches also contributed more nitrogen to the stream because they were gaining more often than unincised reaches, where groundwater nitrogen that was not denitrified could be retained in the riparian zone.

The results of this study show that channel incision can negatively affect water quality by reducing riparian denitrification and increasing nitrogen loading to stream networks. Our coupling of empirical models with REM portrays the importance of modeling long-term channel evolution and riparian processes at network scales. The limitations of this modeling approach stress the need for a fully-coupled model, with mechanistic riparian processes, to provide more

robust simulations of riparian dynamics and stream morphological changes. This enhanced modeling can ultimately inform scientists and water resources managers about the importance of addressing and mitigating channel incision through stream restoration and flow management for water quality protection.

CHAPTER 5

CONCLUSIONS

The goal of this research is to investigate the role of stream incision on groundwater-surface water exchange and nitrogen dynamics. This has been accomplished by analyzing existing models, collecting field data in small watersheds with contrasting soil types and land uses, and developing a novel coupling of channel morphodynamic and empirical denitrification models to estimate long-term changes in network-scale nitrogen loading. Specifically, this goal was met by achieving the following objectives:

1. Identify existing mechanistic riparian nitrogen models, recognizing the strengths and weaknesses of each, and use a time-varying, global sensitivity analysis to evaluate model structure and function in select models;
2. Collect a novel dataset describing groundwater-surface water interactions and riparian nitrogen cycling at paired incised and unincised streams in two watersheds in the southeast US, and explore variability and relationships within the dataset; and
3. Develop parsimonious statistical models to simulate groundwater depth and denitrification, and couple them with channel evolution modeling using the River Erosion Model (REM) to estimate long-term effects of stream incision on nitrogen loading across a drainage network.

Several models have been developed to simulate riparian nitrogen loading to streams at the scale of both individual sites and watersheds (Arnold et al., 1998; Bieger et al., 2017; Lowrance et al., 2000; Rassam et al., 2005; Wei et al., 2019); however, it is unclear how model

algorithms account for interactions with in-stream processes and what model parameters control riparian denitrification when concurrently varied across their plausible range. I addressed this gap by assessing the robustness of these existing riparian nitrogen models for simulating hydrology, nutrients, soils, vegetation, and stream connections. Global, time-varying sensitivity analyses for the Riparian Ecosystem Management Model (REMM) and the Soil and Water Assessment Tool+ (SWAT+) revealed which parameters were most influential for simulating riparian groundwater and nitrogen cycling dynamics.

Results indicated that existing models underrepresent the connection between riparian zones and stream morphodynamics. REMM and SWAT+ were most sensitive to soil and topographic parameters such as soil layer thickness and slope, but stream channel depth and incision showed little influence on water table depth and riparian denitrification. Parameter sensitivity fluctuated with scale (both spatial and temporal) and hydroclimatic conditions, indicating the importance of seasonal variability, precipitation, and streamflow in controlling riparian processes. These results demonstrated the need to incorporate linkages between channel incision processes, groundwater levels, and denitrification in riparian nitrogen models.

Past field studies have shown that channel incision can lower adjacent groundwater tables and reduce riparian denitrification, potentially increasing nitrogen loading to streams (Böhlke et al., 2007; Groffman et al., 2002; Mayer et al., 2010; Schilling et al., 2006). However, they have occurred at a few individual urban sites in the mid-Atlantic and one rural site in the Midwest. Therefore, there is a need to expand these studies to investigate network-scale effects of incision in small watersheds with various soil types, land uses, and hydrogeomorphic settings. I addressed this gap by collecting nearly two years of continuous groundwater and stream elevations, monthly water quality samples for dissolved nutrient and nitrogen gas analyses, and annual

topographic survey data at paired incised and unincised stream reaches at two field sites (the UGA Teaching Dairy Farm and McQueen Branch at the Savannah River Site) with contrasting soils, land uses, and physiography. I observed seasonal and event-based switching in gaining and losing stream conditions at both sites in response to changes in evapotranspiration. Riparian denitrification removed an estimated 40-95% of available nitrogen in deep wells across both sites. Channel incision had significant near-stream effects on riparian hydrology and nitrogen cycling, lowering the groundwater table, increasing gaining conditions, and, at the dairy farm, reducing the percentage of available nitrogen that was removed via denitrification.

To accomplish the third objective, I developed statistical models for predicting riparian depth to groundwater and denitrification from the field dataset and coupled these models with 30-year simulations of channel morphodynamics at each field site using REM. To my knowledge, this is the first analysis to couple channel morphodynamic modeling with empirical riparian groundwater and denitrification models across a drainage network at decadal time scales. Incision variables such as the height of exposed streambank and width-depth ratio were important for predicting depth to groundwater and denitrification. Temperature, month, pH, and hydraulic gradient were other common variables in the statistical models. Denitrification model fit was substantially improved by stratifying the dataset into gaining and losing conditions. Coupling these models with results from REM simulations showed that channel incision increased network-scale nitrogen loading from ~40-700% compared to an unincised base case. Channel incision decreased riparian denitrification by lowering the water table, disconnecting it from the carbon-rich rhizosphere. Incised reaches were also more often gaining than unincised reaches, meaning that groundwater nitrogen (which underwent less denitrification) was more frequently delivered to the stream. Despite considerable uncertainty in prediction accuracy, these

results demonstrate the importance of incorporating linkages between channel morphodynamic and riparian nitrogen processes into watershed models of diffuse nitrogen loading.

The results of these analyses underscore the effect of channel incision on groundwater-surface water interactions and riparian denitrification and demonstrate that channel incision can have a significant impact on long-term nitrogen loading at the small watershed scale. Neglecting this connection can result in underestimation of nitrogen loads and undervaluing the water quality benefits of flow management and stream restoration in incised stream networks. My modeling results illustrate the need for fully-coupled channel evolution and riparian nitrogen models to enhance understanding of the interplay between these processes and improve estimation of nitrogen loading in evolving stream networks. Intermediate complexity models that include channel-groundwater-nitrogen interactions can improve the accuracy of nonpoint source loading estimates, and help water resources managers identify locations where channel incision significantly increases nitrogen loading. This can guide spatial prioritization of ecological restoration for reducing channel erosion and nitrogen loading to downstream water bodies.

The fact that channel incision plays such a substantial role in nitrogen loading to streams emphasizes the need for enhanced study and modeling of incised stream networks. This research can help address that need by serving as a template for collecting and analyzing field datasets in different regional and hydrogeomorphic settings to investigate these relationships under different controls, and improving models for identifying locations to target management interventions to reduce nitrogen pollution and eutrophication risk.

REFERENCES

Adler, D., Kelley, S.T., Elliott, T., Adamson, J., 2022. vioplot: violin plot. R package version 0.4.0. URL. https://github.com/TomKellyGenetics/vioplot.

Alexander, M., 1977. Introduction to soil microbiology, 2nd ed. John Wiley & Sons.

Allen, P.M., Arnold, J.G., Jakubowski, E., 1999. Prediction of stream channel erosion potential. Environ. Eng. Geosci. 5, 339–351.

Altier, L.S., Lowrance, R., Williams, R.G., Inamdar, S.P., Bosch, D.D., Sheridan, J.M., Hubbard, R.K., Thomas, D.L., 2002. Riparian Ecosystem Management Model: Simulator for ecological processes in riparian zones.

Altier, L.S., Lowrance, R., Williams, R.G., Inamdar, S.P., Bosch, D.D., Sheridan, J.M., Thomas, D.L., Hubbard, R.K., 2001. Riparian Ecosystem Management Model (REMM): Documentation. USDA Conservation Research Report.

Altman, S.J., Parizek, R.R., 1995. Dilution of nonpoint-source nitrate in groundwater. J. Environ. Qual. 24, 707–718. https://doi.org/10.2134/jeq1995.00472425002400040023x

Amatya, D.M., Skaggs, R.W., Gregory, J.D., Herrmann, R.B., 1997. Hydrology of a drained forested pocosin watershed. J. Am. Water Resour. Assoc. 33, 535–546. https://doi.org/10.1111/j.1752-1688.1997.tb03530.x

Anderson, T.R., Groffman, P.M., Kaushal, S.S., Walter, M.T., 2014. Shallow groundwater denitrification in riparian zones of a headwater agricultural landscape. J. Environ. Qual. 43, 732–744. https://doi.org/10.2134/jeq2013.07.0303

Aoki, T., Uemura, S., Munemori, M., 1983. Continuous flow fluorometric determination of

ammonia in water. Anal. Chem. 55, 1620–1622. https://doi.org/10.1021/ac00260a044

Arcement, G.J., Schneider, V.R., 1989. Guide for selecting Manning's roughness coefficients for natural channels and flood plains, United States Geological Survey Water-Supply Paper 2339.

Arnold, J.G., Srinivasan, R., Muttiah, R.S., Williams, J.R., 1998. Large area hydrologic modeling and assessment. Part I: Model development. J. Am. Water Resour. Assoc. 34, 73–89.

Bailey, R.T., Park, S., Bieger, K., Arnold, J.G., Allen, P.M., 2020. Enhancing SWAT+ simulation of groundwater flow and groundwater-surface water interactions using MODFLOW routines. Environ. Model. Softw. 126, 104660. https://doi.org/10.1016/j.envsoft.2020.104660

Baker, M.A., Vervier, P., 2004. Hydrological variability, organic matter supply and denitrification in the Garonne River ecosystem. Freshw. Biol. 49, 181–190. https://doi.org/10.1046/j.1365-2426.2003.01175.x

Balestrini, R., Sacchi, E., Tidili, D., Delconte, C.A., Buffagni, A., 2016. Factors affecting agricultural nitrogen removal in riparian strips: Examples from groundwater-dependent ecosystems of the Po Valley (Northern Italy). Agric. Ecosyst. Environ. 221, 132–144. https://doi.org/10.1016/j.agee.2016.01.034

Baroni, G., Francke, T., 2020. An effective strategy for combining variance- and distribution-based global sensitivity analysis. Environ. Model. Softw. 134. https://doi.org/10.1016/j.envsoft.2020.104851

Barrie, C.J., Rasmussen, T.C., Tollner, E.W., Golladay, S.W., Brantley, S.T., 2022. Steady vs dynamic stream-aquifer interactions: Lower Flint River Basin, Southwest Georgia, USA. J.

Hydrol. Reg. Stud. 40. https://doi.org/10.1016/j.ejrh.2022.101046

Barton, L., McLay, C.D.A., Schipper, L.A., Smith, C.T., 1999a. Denitrification rates in a wastewater-irrigated forest soil in New Zealand. J. Environ. Qual. 28, 2008–2014. https://doi.org/10.2134/jeq1999.00472425002800060042x

Barton, L., McLay, C.D.A., Schipper, L.A., Smith, C.T., 1999b. Annual denitrification rates in agricultural and forest soils: A review. Aust. J. Soil Res. 37, 1073–1093. https://doi.org/10.1071/SR99009

Bates, D., Maechler, M., 2021. Matrix: Sparse and Dense Matrix Classes and Methods. R package version 1.3-4. URL. https://cran.r-project.org/web/packages/Matrix/Matrix.pdf.

Batlle-Aguilar, J., Brovelli, A., Luster, J., Shrestha, J., Niklaus, P.A., Barry, D.A., 2012. Analysis of carbon and nitrogen dynamics in riparian soils: Model validation and sensitivity to environmental controls. Sci. Total Environ. 429, 246–256. https://doi.org/10.1016/j.scitotenv.2012.04.026

Bieger, K., Arnold, J.G., Rathjens, H., White, M.J., Bosch, D.D., Allen, P.M., Volk, M., Srinivasan, R., 2017. Introduction to SWAT+, a completely restructured version of the Soil and Water Assessment Tool. J. Am. Water Resour. Assoc. 53, 115–130. https://doi.org/10.1111/1752-1688.12482

Blanco-Canqui, H., Lal, R., Post, W.M., Izaurralde, R.C., Shipitalo, M.J., 2006. Organic carbon influences on soil particle density and rheological properties. Soil Sci. Soc. Am. J. 70, 1407–1414. https://doi.org/10.2136/sssaj2005.0355

Blasone, R.S., Madsen, H., Rosbjerg, D., 2007. Parameter estimation in distributed hydrological modelling: Comparison of global and local optimisation techniques. Nord. Hydrol. 38, 451–476. https://doi.org/10.2166/nh.2007.024

Blazejewski, G.A., Stolt, M.H., Gold, A.J., Gurwick, N., Groffman, P.M., 2009. Spatial distribution of carbon in the subsurface of riparian zones. Soil Sci. Soc. Am. J. 73, 1733–1740. https://doi.org/10.2136/sssaj2007.0386

Blicher-Mathiesen, G., Hoffmann, C.C., 1999. Denitrification as a sink for dissolved nitrous oxide in a freshwater riparian fen. J. Environ. Qual. 28, 257–262. https://doi.org/10.2134/jeq1999.00472425002800010031x

Böhlke, J.K., Denver, J.M., 1995. Combined use of groundwater dating, chemical, and isotopic analyses to resolve the history and fate of nitrate contamination in two agricultural watersheds, Atlantic coastal plain, Maryland. Water Resour. Res. 31, 2319–2339. https://doi.org/10.1029/95WR01584

Böhlke, J.K., O'Connell, M.E., Prestegaard, K.L., 2007. Ground water stratification and delivery of nitrate to an incised stream under varying flow conditions. J. Environ. Qual. 36, 664–680. https://doi.org/10.2134/jeq2006.0084

Booth, D.B., 1990. Stream-channel incision following drainage-basin urbanization. Water Resour. Bull. 26, 407–417. https://doi.org/10.1111/j.1752-1688.1990.tb01380.x

Booth, D.B., Fischenich, C.J., 2015. A channel evolution model to guide sustainable urban stream restoration. Area 47, 408–421. https://doi.org/10.1111/area.12180

Borgonovo, E., Lu, X., Plischke, E., Rakovec, O., Hill, M.C., 2017. Making the most out of a hydrological model data set: Sensitivity analyses to open the model black-box. Water Resour. Res. 53, 7933–7950. https://doi.org/10.1002/2017WR020767

Bouwman, A.F., Beusen, A.H.W., Griffioen, J., Van Groenigen, J.W., Hefting, M.M., Oenema, O., Van Puijenbroek, P.J.T.M., Seitzinger, S., Slomp, C.P., Stehfest, E., 2013. Global trends and uncertainties in terrestrial denitrification and N_2O emissions. Philos. Trans. R. Soc. B

368, 20130112. https://doi.org/10.1098/rstb.2013.0112

Brady, N.C., Weil, R.R., 1996. The Nature and Properties of Soil. Prentice Hall, Inc.

Brunke, M., Gonser, T., 1997. The ecological significance of exchange processes between rivers and groundwater. Freshw. Biol. 37, 1–33. https://doi.org/10.1046/j.1365-2427.1997.00143.x

Buhr, D.X., Lammers, R.W., Bledsoe, B.P., 2022. Global sensitivity analyses of key riparian nitrogen models. Environ. Model. Softw. 158, 105542. https://doi.org/10.1016/j.envsoft.2022.105542

Burgin, A.J., Groffman, P.M., 2012. Soil O_2 controls denitrification rates and N_2O yield in a riparian wetland. J. Geophys. Res. Biogeosciences 117. https://doi.org/10.1029/2011JG001799

Burgin, A.J., Hamilton, S.K., 2007. Have we overemphasized the role of denitrification in aquatic ecosystems? A review of nitrate removal pathways. Front. Ecol. Environ. 5, 89–96. https://doi.org/10.1890/1540-9295(2007)5[89:HWOTRO]2.0.CO;2

Burt, T., Pinay, G., Sabater, S., 2010. What do we still need to know about the ecohydrology of riparian zones? Ecohydrology 3, 373–377. https://doi.org/10.1002/eco.140

Burt, T.P., Matchett, L.S., Goulding, K.W.T., Webster, C.P., Haycock, N.E., 1999. Denitrification in riparian buffer zones: The role of floodplain hydrology. Hydrol. Process. 13, 1451–1463. https://doi.org/10.1002/(SICI)1099-1085(199907)13:10<1451::AID-HYP822>3.0.CO;2-W

Burt, T.P., Pinay, G., Matheson, F.E., Haycock, N.E., Butturini, A., Clement, J.C., Danielescu, S., Dowrick, D.J., Hefting, M.M., Hillbricht-Ilkowska, A., Maitre, V., 2002. Water table fluctuations in the riparian zone: Comparative results from a pan-European experiment. J. Hydrol. 265, 129–148. https://doi.org/10.1016/S0022-1694(02)00102-6

Byrd, J.L., Melching, C.S., 2005. Uncertainty evaluation in the design of instream structures for stream restoration, in: Proceedings of XXXI Congress of the International Association for Hydraulic Engineering and Research. Seoul, Korea, pp. 2172–2182.

Caeiro, F., Mateus, A., 2022. randtests: Testing Randomness in R. R packages version 1.0.1. URL. https://CRAN.R-project.org/package=randtests.

Canadell, J., Jackson, R.B., Ehleringer, J.R., Mooney, H.A., Sala, O.E., Schulze, E.-D., 1996. Maximum rooting depth of vegetation types at the global scale. Oecologia 108, 583–595. https://doi.org/10.1007/bf00329030

Cardenas, M.B., 2009. Stream-aquifer interactions and hyporheic exchange in gaining and losing sinuous streams. Water Resour. Res. 45, 1–13. https://doi.org/10.1029/2008WR007651

Castro, J.M., Thorne, C.R., 2019. The stream evolution triangle: Integrating geology, hydrology, and biology. River Res. Appl. 35, 315–326. https://doi.org/10.1002/rra.3421

Chasar, L.S., Chanton, J.P., Glaser, P.H., Siegel, D.I., Rivers, J.S., 2000. Radiocarbon and stable carbon isotopic evidence for transport and transformation of dissolved organic carbon, dissolved inorganic carbon, and CH_4 in a northern Minnesota Peatland. Global Biogeochem. Cycles 14, 1095–1108. https://doi.org/10.1029/1999GB001221

Chow, V.T., 1959. Open Channel Hydraulics. McGraw-Hill Book Company, New York.

Clesceri, L.S., Greenberg, A.E., Eaton, A.., 1998. Standard Methods for the Examination of Water and Wastewater, 20th ed.

Climate Watch, 2022. Climate Watch Historical GHG Emissions. Washington, D.C. World Resour. Institute. Available online www.climatewatchdata.org.

Cluer, B., Thorne, C., 2014. A stream evolution model integrating habitat and ecosystem benefits. River Res. Appl. 30, 135–154. https://doi.org/10.1002/rra.2631

Conway, T.M., 2007. Impervious surface as an indicator of pH and specific conductance in the urbanizing coastal zone of New Jersey, USA. J. Environ. Manage. 85, 308–316. https://doi.org/10.1016/j.jenvman.2006.09.023

Cooper, J.R., Gilliam, J.W., Daniels, R.B., Robarge, W.P., 1987. Riparian areas as filters for agricultural sediment. Soil Sci. Soc. Am. J. 51, 416–420. https://doi.org/10.2136/sssaj1987.03615995005100020029x

Covino, T., McGlynn, B., Mallard, J., 2011. Stream-groundwater exchange and hydrologic turnover at the network scale. Water Resour. Res. 47, 1–11. https://doi.org/10.1029/2011WR010942

Covino, T.P., McGlynn, B.L., 2007. Stream gains and losses across a mountain-to-valley transition: Impacts on watershed hydrology and stream water chemistry. Water Resour. Res. 43, 1–14. https://doi.org/10.1029/2006WR005544

Craig, L.S., Palmer, M.A., Richardson, D.C., Filoso, S., Bernhardt, E.S., Bledsoe, B.P., Doyle, M.W., Groffman, P.M., Hassett, B.A., Kaushal, S.S., Mayer, P.M., Smith, S.M., Wilcock, P.R., 2008. Stream restoration strategies for reducing river nitrogen loads. Front. Ecol. Environ. 6, 529–538. https://doi.org/10.1890/070080

Davis, J.H., Griffith, S.M., Horwath, W.R., Steiner, J.J., Myrold, D.D., 2008. Denitrification and nitrate consumption in an herbaceous riparian area and perennial ryegrass seed cropping system. Soil Sci. Soc. Am. J. 72, 1299–1310. https://doi.org/10.2136/sssaj2007.0279

Dayanthi, W.K.C.N., Shigematsu, T., Tanaka, H., Yamashita, N., Odencrantz, J.E., 2008. Modeling nitrogen dynamics in a soil column with reclaimed water: Okinawa, Japan application. Adv. Asian Environ. Eng. 7.

de Graaf, I.E.M., Gleeson, T., van Beek, L.P.H. (Rens), Sutanudjaja, E.H., Bierkens, M.F.P.,

2019. Environmental flow limits to global groundwater pumping. Nature 574, 90–94. https://doi.org/10.1038/s41586-019-1594-4

de Klein, C.A.M., Van Logtestijn, R.S.P., 1994. Denitrification in the top soil of managed grasslands in The Netherlands in relation to soil type and fertilizer level. Plant Soil 163, 33–44. https://doi.org/10.1007/BF00033938

Dean, W.E., 1974. Determination of carbonate and organic matter in calcareous sediments and sedimentary rocks by loss on ignition: comparison with other methods. J. Sediment. Petrol. 44, 242–248.

Dingman, S.L., 2002. Physical Hydrology, 2nd ed. Prentice Hall, Inc.

Dosskey, M.G., Bertsch, P.M., 2016. Forest sources and pathways of organic matter transport to a blackwater stream: A hydrologic approach. Biogeochemistry 24, 1–19.

Duff, J.H., Jackman, A.P., Triska, F.J., Sheibley, R.W., Avanzino, R.J., 2007. Nitrate retention in riparian ground water at natural and elevated nitrate levels in north central Minnesota. J. Environ. Qual. 36, 343–353. https://doi.org/10.2134/jeq2006.0019

Dukes, M.D., Evans, R.O., 2003. Riparian Ecosystem Management Model: Hydrology performance and sensitivity in the North Carolina middle coastal plain. Trans. ASAE 46, 1567–1579. https://doi.org/10.13031/2013.15645

Duncan, J.M., Band, L.E., Groffman, P.M., Bernhardt, E.S., 2015. Mechanisms driving the seasonality of catchment scale nitrate export: Evidence for riparian ecohydrologic controls. Water Resour. Res. 51, 3982–3997. https://doi.org/10.1002/2015WR016937

Duong, T., 2021. ks: Kernel Smoothing. R package version 1.13.2. URL. https://cran.r-project.org/web/packages/ks/ks.pdf.

Dutang, C., Savicky, P., 2021. randtoolbox: Generating and Testing Random Numbers. R

package version 1.31.1. URL. https://cran.r-project.org/web/packages/randtoolbox/randtoolbox.pdf.

Eddelbuettel, D., 2013. Seamless R and C++ Integration with Rcpp. R package version 1.0.9. URL. https://cran.r-project.org/web/packages/Rcpp/Rcpp.pdf.

Eddelbuettel, D., Balamuta, J.J., 2018. Extending R with C++: A Brief Introduction to Rcpp. Am. Stat. 72, 28–36.

Eddelbuettel, D., Francois, R., 2011. Rcpp: Seamless R and C++ Integration. J. Stat. Softw. 40.

Essaid, H.I., Caldwell, R.R., 2017. Evaluating the impact of irrigation on surface water–groundwater interaction and stream temperature in an agricultural watershed. Sci. Total Environ. 599–600, 581–596. https://doi.org/10.1016/j.scitotenv.2017.04.205

Estavillo, J.M., Rodriguez, M., Domingo, M., 1994. Denitrification losses from a natural grassland in the Basque Country under organic and inorganic fertilization. Plant Soil 162, 19–29.

Feaster, T.D., Gotvald, A.J., Weaver, J.C., 2014. Methods for estimating the magnitude and frequency of floods for urban and small, rural streams in Georgia, South Carolina, and North Carolina, 2011.

Fennessy, M.S., Cronk, J.K., 1997. The effectiveness and restoration potential of riparian ecotones for the management of nonpoint source pollution, particularly nitrate. Crit. Rev. Environ. Sci. Technol. 27, 285–317. https://doi.org/10.1080/10643389709388502

Ferguson, M.C., Badhwar, G.D., Chhikara, R.S., Pitts, D.E., 1986. Field size distributions for selected agricultural crops in the United States and Canada. Remote Sens. Environ. 19, 25–45. https://doi.org/10.1016/0034-4257(86)90039-8

Ferretti, F., Saltelli, A., Tarantola, S., 2016. Trends in sensitivity analysis practice in the last

decade. Sci. Total Environ. 568, 666–670. https://doi.org/10.1016/j.scitotenv.2016.02.133

Fox, J., Weisberg, S., 2019. An R Companion to Applied Regressions, Third Edition, Thousand Oaks, CA: Sage. URL. https://cran.r-project.org/web/packages/car/car.pdf.

Galloway, J.N., Dentener, F.J., Capone, D.G., Boyer, E.W., Howarth, R.W., Seitzinger, S.P., Asner, G.P., Cleveland, C.C., Green, P.A., Holland, E.A., Karl, D.M., Michaels, A.F., Porter, J.H., Townsend, A.R., Vorosmarty, C.J., 2004. Nitrogen cycles: Past, present, and future. Biogeochemistry 70, 153–226.

Gee, C.S., Pfeffer, J.T., Suidan, M.T., 1990. *Nitrosomonas* and *Nitrobacter* interactions in biological nitrification. J. Environ. Eng. 116, 4–17.

Gee, G.W., Bauder, J.W., 1979. Particle size analysis by hydrometer: A simplified method for routine textural analysis and a sensitivity test of measurement parameters. Soil Sci. Soc. Am. J. 43, 1004–1007. https://doi.org/10.2136/sssaj1979.03615995004300050038x

Georgia Soil and Water Conservation Commission, 2016. Manual for erosion and sediment control in Georgia. Athens, GA.

Ghasemizade, M., Baroni, G., Abbaspour, K., Schirmer, M., 2017. Combined analysis of time-varying sensitivity and identifiability indices to diagnose the response of a complex environmental model. Environ. Model. Softw. 88, 22–34. https://doi.org/10.1016/j.envsoft.2016.10.011

Ghoreishi, M., Sheikholeslami, R., Elshorbagy, A., Razavi, S., Belcher, K., 2021. Peering into agricultural rebound phenomenon using a global sensitivity analysis approach. J. Hydrol. 602, 126739. https://doi.org/10.1016/j.jhydrol.2021.126739

Gift, D.M., Groffman, P.M., Kaushal, S.S., Mayer, P.M., 2010. Denitrification potential, root biomass, and organic matter in degraded and restored urban riparian zones. Restor. Ecol. 18,

113–120. https://doi.org/10.1111/j.1526-100X.2008.00438.x

Goni, M.A., Gardner, L.R., 2003. Seasonal dynamics in dissolved organic carbon concentrations in a coastal water-table aquifer at the forest-marsh interface. Aquat. Geochemistry 9, 209–232. https://doi.org/10.1023/B:AQUA.0000022955.82700.ed

Gordon, N.D., McMahon, T.A., Finlayson, B.L., Gippel, C.J., Nathan, R.J., 2004. Stream Hydrology, 2nd ed, An Introduction for Ecologists. Wiley. https://doi.org/10.1080/03632415.2016.1172482

Graff, C.D., Sadeghi, A.M., Lowrance, R.R., Williams, R.G., 2005. Quantifying the sensitivity of the Riparian Ecosystem Management Model (REMM) to changes in climate and buffer characteristics common to conservation practices. Trans. ASAE 48, 1377–1387. https://doi.org/10.13031/2013.19195

Green, W.H., Ampt, G.A., 1911. Studies on soil physics. J. Agric. Sci. 4, 1–24.

Groffman, P.M., Altabet, M. a., Bohlke, J.K., Butterbach-Bahl, K., David, M.B., Firestone, M.K., Giblin, A.E., Kana, T.M., Nielsen, L.P., Voyteck, M. a., 2006. Methods for measuring denitrification: Diverse approaches to a difficult problem. Ecol. Appl. 16, 2091–2122. https://doi.org/10.1890/1051-0761(2006)016[2091:mfmdda]2.0.co;2

Groffman, P.M., Bain, D.J., Band, L.E., Belt, K.T., Brush, G.S., Grove, J.M., Pouyat, R. V., Yesilonis, I.C., Zipperer, W.C., 2003. Down by the riverside: Urban riparian ecology. Front. Ecol. Environ. 1, 315–321. https://doi.org/10.1890/1540-9295(2003)001[0315:dbtrur]2.0.co;2

Groffman, P.M., Boulware, N.J., Zipperer, W.C., Pouyat, R. V, Band, L.E., Colosimo, M.F., 2002. Soil nitrogen cycle processes in urban riparian zones. Environ. Sci. Technol. 36, 4547–4552. https://doi.org/10.1021/es020649z

Groffman, P.M., Gold, A.J., Jacinthe, P.A., 1998. Nitrous oxide production in riparian zones and groundwater. Nutr. Cycl. Agroecosystems 52, 179–186. https://doi.org/10.1023/a:1009719923861

Groffman, P.M., Tiedje, J.M., 1989. Denitrification in north temperate forest soils: Spatial and temporal patterns at the landscape and seasonal scales. Soil Biol. Biochem. 21, 613–620. https://doi.org/10.1016/0038-0717(89)90053-9

Große, F., Fennel, K., Laurent, A., 2019. Quantifying the relative importance of riverine and open-ocean nitrogen sources for hypoxia formation in the northern Gulf of Mexico. J. Geophys. Res. Ocean. 124, 5451–5467. https://doi.org/10.1029/2019JC015230

Guillaume, J.H.A., Jakeman, J.D., Marsili-Libelli, S., Asher, M., Brunner, P., Croke, B., Hill, M.C., Jakeman, A.J., Keesman, K.J., Razavi, S., Stigter, J.D., 2019. Introductory overview of identifiability analysis: A guide to evaluating whether you have the right type of data for your modeling purpose. Environ. Model. Softw. 119, 418–432. https://doi.org/10.1016/j.envsoft.2019.07.007

Hamilton, R.L., Trimmer, M., Bradley, C., Pinay, G., 2016. Deforestation for oil palm alters the fundamental balance of the soil N cycle. Soil Biol. Biochem. 95, 223–232. https://doi.org/10.1016/j.soilbio.2016.01.001

Hanson, G.C., Groffman, P.M., Gold, A.J., 1994. Symptoms of nitrogen saturation in a riparian wetland. Ecol. Appl. 4, 750–756. https://doi.org/10.2307/1942005

Harden, S.L., Spruill, T.B., 2008. Factors affecting nitrate delivery to streams from shallow ground water in the North Carolina coastal plain. USGS Scientific Investigations Report 2008 – 5021.

Hardison, E.C., O'Driscoll, M.A., Deloatch, J.P., Howard, R.J., Brinson, M.M., 2009. Urban

land use, channel incision, and water table decline along coastal plain streams, North Carolina. J. Am. Water Resour. Assoc. 45, 1032–1046. https://doi.org/10.1111/j.1752-1688.2009.00345.x

Hawkins, R.H., 1980. Infiltration and curve numbers: Some pragmatic and theoretical relationships, in: Symposium on Water Management 1980. American Society of Civil Engineers, pp. 925–937.

Hawley, R.J., Bledsoe, B.P., Stein, E.D., Haines, B.E., 2012. Channel evolution model of semiarid stream response to urban-induced hydromodification. J. Am. Water Resour. Assoc. 48, 722–744. https://doi.org/10.1111/j.1752-1688.2012.00645.x

Heaton, T.H.E., Vogel, J.C., 1981. "Excess air" in groundwater. J. Hydrol. 50, 201–216. https://doi.org/10.1016/0022-1694(81)90070-6

Hefting, M., Beltman, B., Karssenberg, D., Rebel, K., Van Riessen, M., Spijker, M., 2006. Water quality dynamics and hydrology in nitrate loaded riparian zones in the Netherlands. Environ. Pollut. 139, 143–156. https://doi.org/10.1016/j.envpol.2005.04.023

Hefting, M.M., Bobbink, R., de Caluwe, H., 2003. Nitrous oxide emission and denitrification in chronically nitrate-loaded riparian buffer zones. J. Environ. Qual. 32, 1194. https://doi.org/10.2134/jeq2003.1194

Heinen, M., 2006. Simplified denitrification models: Overview and properties. Geoderma 133, 444–463. https://doi.org/10.1016/j.geoderma.2005.06.010

Herman, J.D., Kollat, J.B., Reed, P.M., Wagener, T., 2013a. From maps to movies: High-resolution time-varying sensitivity analysis for spatially distributed watershed models. Hydrol. Earth Syst. Sci. 17, 5109–5125. https://doi.org/10.5194/hess-17-5109-2013

Herman, J.D., Reed, P.M., Wagener, T., 2013b. Time-varying sensitivity analysis clarifies the

effects of watershed model formulation on model behavior. Water Resour. Res. 49, 1400–1414. https://doi.org/10.1002/wrcr.20124

Herman, J.D., Reed, P.M., Zeff, H.B., Characklis, G.W., 2015. How should robustness be defined for water systems planning under change? J. Water Resour. Plan. Manag. 141, 1–14. https://doi.org/10.1061/(ASCE)WR.1943-5452.0000509

Hester, E.T., Guth, C.R., Scott, D.T., Jones, C.N., 2016. Vertical surface water–groundwater exchange processes within a headwater floodplain induced by experimental floods. Hydrol. Process. 30, 3770–3787. https://doi.org/10.1002/hyp.10884

Hill, A.R., 2019. Groundwater nitrate removal in riparian buffer zones: A review of research progress in the past 20 years. Biogeochemistry 143, 347–369. https://doi.org/10.1007/s10533-019-00566-5

Hill, A.R., 1996. Nitrate removal in stream riparian zones. J. Environ. Qual. 25, 743–755. https://doi.org/10.2134/jeq1996.00472425002500040014x

Hill, A.R., 1979. Denitrification in the nitrogen budget of a river ecosystem. Nature 291–292. https://doi.org/10.1038/281291a0

Hill, A.R., Devito, K.J., Campagnolo, S., Sanmugadas, K., 2000. Subsurface denitrification in a forest riparian zone: Interactions between hydrology and supplies of nitrate and organic carbon. Biogeochemistry 51, 193–223. https://doi.org/10.1023/A:1006476514038

Hill, A.R., Devito, K.J., Vidon, P.G., 2014. Long-term nitrate removal in a stream riparian zone. Biogeochemistry 121, 425–439. https://doi.org/10.1007/s10533-014-0010-2

Hill, A.R., Vidon, P.G.F., Langat, J., 2004. Denitrification potential in relation to lithology in five headwater riparian zones. J. Environ. Qual. 33, 911–919. https://doi.org/10.2134/jeq2004.0911

Hinkle, S.R., Duff, J.H., Triska, F.J., Laenen, A., Gates, E.B., Bencala, K.E., Wentz, D.A., Silva, S.R., 2001. Linking hyporheic flow and nitrogen cycling near the Willamette River - a large river in Oregon, USA. J. Hydrol. 244, 157–180. https://doi.org/10.1016/S0022-1694(01)00335-3

Hinton, M.J., Schiff, S.L., English, M.C., 1993. Physical properties governing groundwater flow in a glacial till catchment. J. Hydrol. 142, 229–249. https://doi.org/10.1016/0022-1694(93)90012-X

Hirsch, R.M., Helsel, D.R., Cohn, T.A., Gilroy, E.J., 1993. Statistical analysis of hydrologic data, in: Maidment, D.R. (Ed.), Handbook of Hydrology. McGraw-Hill, New York.

Hoang, L., van Griensven, A., Mynett, A., 2017. Enhancing the SWAT model for simulating denitrification in riparian zones at the river basin scale. Environ. Model. Softw. 93, 163–179. https://doi.org/10.1016/j.envsoft.2017.03.017

Holmes, R.M., 2000. The importance of ground water to stream ecosystem function, in: Streams and Ground Waters. pp. 137–148.

Howarth, R., Chan, F., Conley, D.J., Garnier, J., Doney, S.C., Marino, R., Billen, G., 2011. Coupled biogeochemical cycles: Eutrophication and hypoxia in temperate estuaries and coastal marine ecosystems. Front. Ecol. Environ. 9, 18–26. https://doi.org/10.1890/100008

Howarth, R.W., 2008. Coastal nitrogen pollution: A review of sources and trends globally and regionally. Harmful Algae 8, 14–20. https://doi.org/10.1016/j.hal.2008.08.015

Howarth, R.W., Sharpley, A., Walker, D., 2002. Sources of nutrient pollution to coastal waters in the United States: Implications for achieving coastal water quality goals. Estuaries 25, 656–676.

Hozo, S.P., Djulbegovic, B., Hozo, I., 2005. Estimating the mean and variance from the median,

range, and the size of a sample. BMC Med. Res. Methodol. 5, 1–10. https://doi.org/10.1186/1471-2288-5-13

Hunt, P.G., Matheny, T.A., Stone, K.C., 2004. Denitrification in a coastal plain riparian zone contiguous to a heavily loaded swine wastewater spray field. J. Environ. Qual. 33, 2367–2374. https://doi.org/10.2134/jeq2004.2367

International Energy Agency, 2022. Global Energy Review: CO_2 Emissions in 2021. Global emissions rebound sharply to highest ever level.

Israel, D.W., Showers, W.J., Fountain, M., Fountain, J., 2005. Nitrate movement in shallow ground water from swine-lagoon-effluent spray fields managed under current application regulations. J. Environ. Qual. 34, 1828–1842. https://doi.org/10.2134/jeq2004.0338

Jacobson, R.B., Femmer, S.R., McKenney, R.A., 2001. Land-use changes and the physical habitat of streams - A review with emphasis on studies within the U.S. Geological Survey Federal-State Cooperative Program, CIrcular 1175.

Jahangir, M.M.R., Fenton, O., Müller, C., Harrington, R., Johnston, P., Richards, K.G., 2017. *In situ* denitrification and DNRA rates in groundwater beneath an integrated constructed wetland. Water Res. 111, 254–264. https://doi.org/10.1016/j.watres.2017.01.015

Jahangir, M.M.R., Johnston, P., Barrett, M., Khalil, M.I., Groffman, P.M., Boeckx, P., Fenton, O., Murphy, J., Richards, K.G., 2013. Denitrification and indirect N_2O emissions in groundwater: Hydrologic and biogeochemical influences. J. Contam. Hydrol. 152, 70–81. https://doi.org/10.1016/j.jconhyd.2013.06.007

Jahangir, M.M.R., Khalil, M.I., Johnston, P., Cardenas, L.M., Hatch, D.J., Butler, M., Barrett, M., O'flaherty, V., Richards, K.G., 2012. Denitrification potential in subsoils: A mechanism to reduce nitrate leaching to groundwater. Agric. Ecosyst. Environ. 147, 13–23.

https://doi.org/10.1016/j.agee.2011.04.015

Jarvis, S.C., Barraclough, D., Williams, J., Rook, A.J., 1991. Patterns of denitrification loss from grazed grassland: Effects of N fertilizer inputs at different sites. Plant Soil 131, 77–88.

Jasechko, S., Seybold, H., Perrone, D., Fan, Y., Kirchner, J.W., 2021. Widespread potential loss of streamflow into underlying aquifers across the USA. Nature 591, 391–395. https://doi.org/10.1038/s41586-021-03311-x

Jeffers, J.B., 2018. In situ measurement of riparian groundwater denitrification in a short-rotation pine dominated watershed. Master's Thesis. University of Georgia.

Jencso, K.G., McGlynn, B.L., Gooseff, M.N., Bencala, K.E., Wondzell, S.M., 2010. Hillslope hydrologic connectivity controls riparian groundwater turnover: Implications of catchment structure for riparian buffering and stream water sources. Water Resour. Res. 46, 1–18. https://doi.org/10.1029/2009WR008818

Jencso, K.G., McGlynn, B.L., Gooseff, M.N., Wondzell, S.M., Bencala, K.E., Marshall, L.A., 2009. Hydrologic connectivity between landscapes and streams: Transferring reach- and plot-scale understanding to the catchment scale. Water Resour. Res. 45, 1–16. https://doi.org/10.1029/2008WR007225

Jimenez-Fernandez, O., Schwientek, M., Osenbrück, K., Glaser, C., Schmidt, C., Fleckenstein, J.H., 2022. Groundwater-surface water exchange as key control for instream and groundwater nitrate concentrations along a first-order agricultural stream. Hydrol. Process. 36, 1–16. https://doi.org/10.1002/hyp.14507

Julien, P.Y., 1995. Erosion and Sedimentation. Cambridge University Press, Cambridge. https://doi.org/http://dx.doi.org/10.1017/CBO9781139174107

Jung, M., Burt, T.P., Bates, P.D., 2004. Toward a conceptual model of floodplain water table

response. Water Resour. Res. 40, 1–13. https://doi.org/10.1029/2003WR002619

Jurado, A., Borges, A. V., Brouyère, S., 2017. Dynamics and emissions of N_2O in groundwater: A review. Sci. Total Environ. 584–585, 207–218. https://doi.org/10.1016/j.scitotenv.2017.01.127

Kamphuis, J.W., 1974. Determination of sand roughness for fixed beds. J. Hydraul. Res. 12, 193–203.

Kana, T.M., Darkangelo, C., Hunt, M.D., Oldham, J.B., Bennett, G.E., Cornwell, J.C., 1994. Membrane inlet mass spectrometer for rapid high-precision determination of N_2, O_2, and Ar in environmental water samples. Anal. Chem. 66, 4166–4170. https://doi.org/10.1021/ac00095a009

Karr, J.D., Showers, W.J., Gilliam, J.W., Andres, A.S., 2001. Tracing nitrate transport and environmental impact from intensive swine farming using delta nitrogen-15. J. Environ. Qual. 1163–1175.

Karr, J.D., Showers, W.J., Jennings, G.D., 2003. Low-level nitrate export from confined dairy farming detected in North Carolina streams using δ15N. Agric. Ecosyst. Environ. 95, 103–110. https://doi.org/10.1016/S0167-8809(02)00103-2

Kassambara, A., 2023. rstatix: Pipe-Friendly Framework for Basic Statistical Tests. R package version 0.7.2. URL. https://CRAN.R-project.org/package=rstatix.

Kayabalı, K., Çelik, M., Karatosun, H., Arıgün, Z., Koçbay, A., 1999. The influence of a heavily polluted urban river on the adjacent aquifer systems. Environ. Geol. 38, 233–243. https://doi.org/10.1007/s002540050420

Kim, D.-G., Isenhart, T.M., Parkin, T.B., Schultz, R.C., Loynachan, T.E., 2009. Nitrate and dissolved nitrous oxide in groundwater within cropped fields and riparian buffers.

Biogeosciences Discuss. 6, 651–685.

Kim, I.J., Hutchinson, S.L., Hutchinson, J.M.S., Young, C.B., 2007. Riparian Ecosystem Management Model: Sensitivity to soil, vegetation, and weather input parameters. J. Am. Water Resour. Assoc. 43, 1171–1182. https://doi.org/10.1111/j.1752-1688.2007.00096.x

Knisel, W.G., Davis, F.M., 2000. Groundwater Loading Effects of Agricultural Management Systems: User manual.

Korol, A.R., Noe, G.B., Ahn, C., 2019. Controls of the spatial variability of denitrification potential in nontidal floodplains of the Chesapeake Bay watershed, USA. Geoderma 338, 14–29. https://doi.org/10.1016/j.geoderma.2018.11.015

Kozak, J.A., Ahuja, L.R., Green, T.R., Ma, L., 2007. Modelling crop canopy and residue rainfall interception effects on soil hydrological components for semi-arid agriculture. Hydrol. Process. 229–241. https://doi.org/10.1002/hyp.6235

Krause, S., Bronstert, A., Zehe, E., 2007. Groundwater-surface water interactions in a North German lowland floodplain - Implications for the river discharge dynamics and riparian water balance. J. Hydrol. 347, 404–417. https://doi.org/10.1016/j.jhydrol.2007.09.028

Kuhn, M., 2022. caret: Classification and Regression Training. R package version 6.0-93. URL. https://CRAN.R-project.org/package=caret.

Kumar, D., Roshni, T., Singh, A., Jha, M.K., Samui, P., 2020. Predicting groundwater depth fluctuations using deep learning, extreme learning machine and Gaussian process: a comparative study. Earth Sci. Informatics 13, 1237–1250. https://doi.org/10.1007/s12145-020-00508-y

Lammers, R.W., 2015. Uncertainty and sensitivity in a bank stability model: Implications for estimating phosphorus loading. Master's Thesis. Colorado State University.

Lammers, R.W., Bledsoe, B.P., 2018. A network scale, intermediate complexity model for simulating channel evolution over years to decades. J. Hydrol. 566, 886–900. https://doi.org/10.1016/j.jhydrol.2018.09.036

Lammers, R.W., Bledsoe, B.P., 2017. What role does stream restoration play in nutrient management? Crit. Rev. Environ. Sci. Technol. 47, 335–371. https://doi.org/10.1080/10643389.2017.1318618

Lammers, R.W., Bledsoe, B.P., Langendoen, E.J., 2017. Uncertainty and sensitivity in a bank stability model: Implications for estimating phosphorus loading. Earth Surf. Process. Landforms 42, 612–623. https://doi.org/10.1002/esp.4004

Langendoen, E.J., Alonso, C. V., 2008. Modeling the evolution of incised streams: I. Model formulation and validation of flow and streambed evolution components. J. Hydraul. Eng. 134, 749–762. https://doi.org/10.1061/(ASCE)0733-9429(2008)134:6(749)

Langendoen, E.J., Lowrance, R.R., Simon, A., 2009. Assessing the impact of riparian processes on streambank stability. Ecohydrology 2, 360–369. https://doi.org/10.1002/eco.78

Langendoen, E.J., Lowrance, R.R., Williams, R.G., Simon, A., 2005. Modeling the impact of riparian buffer systems on bank stability of an incised stream. Impacts Glob. Clim. Chang. 1–12.

Langendoen, E.J., Simon, A., 2008. Modeling the evolution of incised streams: II. Streambank erosion. J. Hydraul. Eng. 134, 905–915.

Larkin, R.G., Sharp, J.M., 1992. On the relationship between river-basin geomorphology, aquifer hydraulics, and ground-water flow direction in alluvial aquifers. Geol. Soc. Am. Bull. 104, 1608–1620. https://doi.org/10.1130/0016-7606(1992)104<1608:OTRBRB>2.3.CO;2

Lasagna, M., De Luca, D.A., Franchino, E., 2016. Nitrate contamination of groundwater in the

western Po Plain (Italy): The effects of groundwater and surface water interactions. Environ. Earth Sci. 75, 1–16. https://doi.org/10.1007/s12665-015-5039-6

Leopold, L.B., 1953. Downstream changes in velocity in rivers. Am. J. Sci. 251, 606–624. https://doi.org/10.2475/ajs.251.8.606

Leuthold, S.J., Ewing, S.A., Payn, R.A., Miller, F.R., Custer, S.G., 2021. Seasonal connections between meteoric water and streamflow generation along a mountain headwater stream. Hydrol. Process. 35, 1–17. https://doi.org/10.1002/hyp.14029

Lowrance, R., 1992. Groundwater nitrate and denitrification in a coastal plain riparian forest. J. Environ. Qual. 21, 401–405. https://doi.org/10.2134/jeq1992.00472425002100030017x

Lowrance, R., Altier, L.S., Williams, R.G., Inamdar, S.P., Sheridan, J.M., Bosch, D.D., Hubbard, R.K., Thomas, D.L., 2000. REMM: The Riparian Ecosystem Management Model. J. Soil Water Conserv. 55, 27–34.

Lumley, T., 2020. leaps: Regression Subset Selection. R package version 3.1. URL. https://cran.r-project.org/web/packages/leaps/leaps.pdf.

Magdoff, F., Van Es, H., 2021. Building soils for better crops: Ecological management for healthy soils.

Magilligan, F.J., Stamp, M.L., 1997. Historical land-cover changes and hydrogeomorphic adjustment in a small Georgia watershed. Ann. Assoc. Am. Geogr. 87, 614–635.

Mason, D.D., Lutz, J.F., Petersen, R.G., 1957. Hydraulic conductivity as related to certain soil properties in a number of great soil groups-Sampling errors involved. Soil Sci. Soc. Am. J. 21, 554–560. https://doi.org/10.2136/sssaj1957.03615995002100050025x

Mayer, P.M., Groffman, P.M., Striz, E.A., Kaushal, S.S., 2010. Nitrogen dynamics at the groundwater-surface water interface of a degraded urban stream. J. Environ. Qual. 39, 810–

823. https://doi.org/10.2134/jeq2009.0012

McAleer, E.B., Coxon, C.E., Richards, K.G., Jahangir, M.M.R., Grant, J., Mellander, P.E., 2017. Groundwater nitrate reduction versus dissolved gas production: A tale of two catchments. Sci. Total Environ. 586, 372–389. https://doi.org/10.1016/j.scitotenv.2016.11.083

McCallum, A.M., Andersen, M.S., Kelly, B.F.J., Giambastiani, B., Acworth, R.I., 2009. Hydrological investigations of surface water-groundwater interactions in a sub-catchment in the Namoi Valley, NSW, Australia, in: Trends and Sustainability of Groundwater in Highly Stressed Aquifers. Proceedings of Symposium JS.2. at the Joint IAHS & IAH Convention, Hyderabad, India, September 2009. pp. 157–166.

McClain, M.E., Boyer, E.W., Dent, C.L., Gergel, S.E., Grimm, N.B., Groffman, P.M., Hart, S.C., Harvey, J.W., Johnston, C.A., Mayorga, E., McDowell, W.H., Pinay, G., 2003. Biogeochemical hot spots and hot moments at the interface of terrestrial and aquatic ecosystems. Ecosystems 6, 301–312. https://doi.org/10.1007/s10021-003-0161-9

McGlynn, B.L., McDonnell, J.J., 2003. Role of discrete landscape units in controlling catchment dissolved organic carbon dynamics. Water Resour. Res. 39. https://doi.org/10.1029/2002WR001525

McIntyre, N., Jackson, B., Wade, A.J., Butterfield, D., Wheater, H.S., 2005. Sensitivity analysis of a catchment-scale nitrogen model. J. Hydrol. 315, 71–92. https://doi.org/10.1016/j.jhydrol.2005.04.010

McManamay, R.A., DeRolph, C.R., 2019. A stream classification system for the conterminous United States. Sci. Data 6, 1–18. https://doi.org/10.1038/sdata.2019.17

McPhillips, L.E., Groffman, P.M., Goodale, C.L., Walter, M.T., 2015. Hydrologic and biogeochemical drivers of riparian denitrification in an agricultural watershed. Water. Air.

Soil Pollut. 226. https://doi.org/10.1007/s11270-015-2434-2

Melching, C.S., Bauwens, W., 2001. Uncertainty in coupled nonpoint source and stream water-quality models. J. Water Resour. Plan. Manag. 127, 403–413. https://doi.org/10.1061/(asce)0733-9496(2001)127:6(403)

Millard, S., 2013. EnvStats: An R Package for Environmental Statistics. R package version 2.7.0. URL. https://cran.r-project.org/web/packages/EnvStats/EnvStats.pdf.

Minamikawa, K., Nishimura, S., Sawamoto, T., Nakajima, Y., Yagi, K., 2010. Annual emissions of dissolved CO_2, CH_4, and N_2O in the subsurface drainage from three cropping systems 796–809. https://doi.org/10.1111/j.1365-2486.2009.01931.x

Miralles, D.G., Gash, J.H., Holmes, T.R.H., De Jeu, R.A.M., Dolman, A.J., 2010. Global canopy interception from satellite observations. J. Geophys. Res. Atmos. 115, 1–8. https://doi.org/10.1029/2009JD013530

Mosier, A.R., Doran, J.W., Freney, J.R., 2002. Managing soil denitrification. J. Soil Water Conserv. 57, 505–513.

Mueller, D.K., Hamilton, P.A., Helsel, D.R., Hitt, K.J., Ruddy, B.C., 1995. Nutrients in ground water and surface water of the United States: An analysis of data through 1992. Water-Resources Investigations Report 95-4031, USGS Report 95-4031.

Mukundan, R., Radcliffe, D.E., Ritchie, J.C., 2011. Channel stability and sediment source assessment in streams draining a Piedmont watershed in Georgia, USA. Hydrol. Process. 25, 1243–1253. https://doi.org/10.1002/hyp.7890

Mulholland, P.J., 1992. Regulation of nutrient concentrations in a temperate forest stream: Roles of upland, riparian, and instream processes. Limnol. Oceanogr. 37, 1512–1526. https://doi.org/10.4319/lo.1992.37.7.1512

Mulholland, P.J., Helton, A.M., Poole, G.C., Hall, R.O., Hamilton, S.K., Peterson, B.J., Tank, J.L., Ashkenas, L.R., Cooper, L.W., Dahm, C.N., Dodds, W.K., Findlay, S.G., Gregory, S. V, Grimm, N.B., Johnson, S.L., McDowell, W.H., Meyer, J.L., Valett, H.M., Webster, J.R., Arango, C.P., Beaulieu, J.J., Bernot, M.J., Burgin, A.J., Crenshaw, C.L., Johnson, L.T., Niederlehner, B.R., O'Brien, J.M., Potter, J.D., Sheibley, R.W., Sobota, D.J., Thomas, S.M., 2008. Stream denitrification across biomes and its response to anthropogenic nitrate loading. Nature 452, 202–5. https://doi.org/10.1038/nature06686

Mulholland, P.J., Valett, H.M., Webster, J.R., Thomas, S.A., Cooper, L.W., Hamilton, S.K., Peterson, B.J., 2004. Stream denitrification and total nitrate uptake rates measured using a field ^{15}N tracer addition approach. Limnol. Oceanogr. 49, 809–820. https://doi.org/10.4319/lo.2004.49.3.0809

Myrold, D.D., 1988. Denitrification in ryegrass and winter wheat cropping systems of western Oregon. Soil Sci. Soc. Am. J. 52, 412–416. https://doi.org/10.2136/sssaj1988.03615995005200020019x

Nägele, W., Conrad, R., 1990. Influence of soil pH on the nitrate-reducing microbial populations and their potential to reduce nitrate to NO and N_2O. FEMS Microbiol. Lett. 74, 49–57. https://doi.org/10.1111/j.1574-6968.1990.tb04051.x

Naiman, R.J., Decamps, H., McClain, M.E., 2010. Riparia: ecology, conservation, and management of streamside communities. Elsevier.

Neitsch, S.., Arnold, J.., Kiniry, J.., Williams, J.., 2011. Soil & Water Assessment Tool, Theoretical Documentation, Version 2009, Texas Water Resources Institute Technical Report No. 406.

Neuwirth, E., 2014. RColorBrewer: ColorBrewer Palettes. R package version 1.1-2. URL.

https://cran.r-project.org/web/packages/RColorBrewer/RColorBrewer.pdf.

Newbold, J.D., Herbert, S., Sweeney, B.W., Kiry, P., Alberts, S.J., 2010. Water quality functions of a 15-year-old riparian forest buffer system. J. Am. Water Resour. Assoc. 46, 299–310. https://doi.org/10.1111/j.1752-1688.2010.00421.x

Nippgen, F., McGlynn, B.L., Emanuel, R.E., 2009. The spatial and temporal evolution of contributing areas. Water Resour. Res. 4550–4573. https://doi.org/10.1002/2014WR016719

Nogueira, G.E.H., Schmidt, C., Trauth, N., Fleckenstein, J.H., 2021. Seasonal and short-term controls of riparian oxygen dynamics and the implications for redox processes. Hydrol. Process. 35, 1–16. https://doi.org/10.1002/hyp.14055

NRCS, 2007. Stream Restoration Design. National Engineering Handbook, Part 654 210-VI-NEH.

Ogle, D., Doll, J., Wheeler, A., Dinno, A., 2023. FSA: Simple Fisheries Stock Assessment Methods. R package version 0.9.4. URL. https://CRAN.R-project.org/package=FSA.

Omar, M.Y., Le Roux, P.A.L., Van Tol, J.J., 2014. Interactions between stream channel incision, soil water levels and soil morphology in a wetland in the Hogsback area, South Africa. South African J. Plant Soil 31, 187–194. https://doi.org/10.1080/02571862.2014.944593

Omonode, R.A., Vyn, T.J., 2006. Vertical distribution of soil organic carbon and nitrogen under warm-season native grasses relative to croplands in west-central Indiana, USA. Agric. Ecosyst. Environ. 117, 159–170. https://doi.org/10.1016/j.agee.2006.03.031

Orr, C.H., Stanley, E.H., Wilson, K.A., Finlay, J.C., 2007. Effects of restoration and reflooding on soil denitrification in a leveed midwestern floodplain. Ecol. Appl. 17, 2365–2376. https://doi.org/10.1890/06-2113.1

Pappenberger, F., Beven, K.J., 2006. Ignorance is bliss: Or seven reasons not to use uncertainty

analysis. Water Resour. Res. 42, 1–8. https://doi.org/10.1029/2005WR004820

Parkin, T.B., Robinson, J.A., 1989. Stochastic models of soil denitrification. Appl. Environ. Microbiol. 55, 72–77. https://doi.org/10.1128/aem.55.1.72-77.1989

Parsons, L.L., Smith, M.S., Murray, R.E., 1991. Soil denitrification dynamics: Spatial and temporal variations of enzyme activity, populations, and nitrogen gas loss. Soil Sci. Soc. Am. J. 55, 90–95. https://doi.org/10.2136/sssaj1991.03615995005500010016x

Parton, W.J., Schimel, D.S., Cole, C. V., Ojima, D.S., 1987. Analysis of factors controlling soil organic matter levels in Great Plains grasslands. Soil Sci. Soc. Am. J. 51, 1173–1179. https://doi.org/10.2136/sssaj1987.03615995005100050015x

Payn, R.A., Gooseff, M.N., McGlynn, B.L., Bencala, K.E., Wondzell, S.M., 2009. Channel water balance and exchange with subsurface flow along a mountain headwater stream in Montana, United States. Water Resour. Res. 45. https://doi.org/10.1029/2008WR007644

Peterjohn, W., Correll, D.L., 1984. Nutrient dynamics in an agricultural watershed: Observations on the role of a riparian forest. Ecology 65, 1466–1475. https://doi.org/10.2307/1939127

Peterson, B.J., Wollheim, W.M., Mulholland, P.J., Webster, J.R., Meyer, J.L., Tank, J.L., Marti, E., Bowden, W.B., Valett, H.M., Hershey, A.E., McDowell, W.H., Dodds, W.K., Hamilton, S.K., Gregory, S., Morrall, D.D., 2001. Control of nitrogen export from watersheds by headwater streams. Science (80-.). 292, 86–90. https://doi.org/10.1126/science.1056874

Petralia, J., 2022. The effects of channel incision and land use on surface-water / groundwater interactions in the Teanaway River Basin, Washington, USA. Master's Thesis. Central Washington University.

Pfeiffer, S.M., Bahr, J.M., Beilfuss, R.D., 2006. Identification of groundwater flowpaths and denitrification zones in a dynamic floodpain aquifier. J. Hydrol. 325, 262–272.

https://doi.org/10.1016/j.jhydrol.2005.10.019

Pianosi, F., Wagener, T., 2016. Understanding the time-varying importance of different uncertainty sources in hydrological modelling using global sensitivity analysis. Hydrol. Process. 30, 3991–4003. https://doi.org/10.1002/hyp.10968

Pierce, H., 2020. Effect of stream channel incision on the depth to groundwater in riparian corridors across southwestern Minnesota. Master's Thesis. University of Minnesota.

Pinardi, M., Soana, E., Severini, E., Racchetti, E., Celico, F., Bartoli, M., 2022. Agricultural practices regulate the seasonality of groundwater-river nitrogen exchanges. Agric. Water Manag. 273. https://doi.org/10.1016/j.agwat.2022.107904

Pinay, G., Bernal, S., Abbott, B.W., Lupon, A., Marti, E., Sabater, F., Krause, S., 2018. Riparian corridors: A new conceptual framework for assessing nitrogen buffering across biomes. Front. Environ. Sci. 6, 1–11. https://doi.org/10.3389/fenvs.2018.00047

Pinay, G., Roques, L., Fabre, A., 1993. Spatial and temporal patterns of denitrification in a riparian forest. J. Appl. Ecol. 30, 581–591.

Pitts, D.E., Badhwar, G., 1980. Field size, length, and width distributions based on LACIE ground truth data. Remote Sens. Environ. 10, 201–213. https://doi.org/10.1016/0034-4257(80)90024-3

Plischke, E., Borgonovo, E., Smith, C.L., 2013. Global sensitivity measures from given data. Eur. J. Oper. Res. 226, 536–550. https://doi.org/10.1016/j.ejor.2012.11.047

Poff, N.L., Bledsoe, B.P., Cuhaciyan, C.O., 2006. Hydrologic variation with land use across the contiguous United States: Geomorphic and ecological consequences for stream ecosystems. Geomorphology 79, 264–285. https://doi.org/10.1016/j.geomorph.2006.06.032

Qiong, W., Kang-fei, F., Zhi-ping, F., Fa-yun, L., Jun, W., Shan-xiang, W., Ya-ni, T., 2020.

Nitrogen pollutant removal by riparian buffer zone: A review. Chinese J. Ecol. 39, 665–677.

Quinn, J.M., 1991. Guidelines for the control of undesirable biological growths in water (Consultancy Report No. 6213/2). Water Quality Centre, Hamilton, New Zealand.

R Core Team, 2021. R: A language and environment for statistical computing. R Foundation for Statistical Computing, Vienna, Austria. URL. https://www.r-project.org/.

Ranalli, A.J., Macalady, D.L., 2010. The importance of the riparian zone and in-stream processes in nitrate attenuation in undisturbed and agricultural watersheds - A review of the scientific literature. J. Hydrol. 389, 406–415. https://doi.org/10.1016/j.jhydrol.2010.05.045

Rankinen, K., Granlund, K., Futter, M.N., Butterfield, D., Wade, A.J., Skeffington, R., Arvola, L., Veijalainen, N., Huttunen, I., Lepistö, A., 2013. Controls on inorganic nitrogen leaching from Finnish catchments assessed using a sensitivity and uncertainty analysis of the INCA-N model. Boreal Environ. Res. 18, 373–386.

Rassam, D., Pagendam, D., Hunter, H., 2005. The riparian nitrogen model (RNM)- Basic theory and conceptualisation. Technical Report 05/9.

Reusser, D.E., Buytaert, W., Zehe, E., 2011. Temporal dynamics of model parameter sensitivity for computationally expensive models with the Fourier amplitude sensitivity test. Water Resour. Res. 47. https://doi.org/10.1029/2010WR009947

Reusser, D.E., Zehe, E., 2011. Inferring model structural deficits by analyzing temporal dynamics of model performance and parameter sensitivity. Water Resour. Res. 47, 1–15. https://doi.org/10.1029/2010WR009946

Rheinhardt, R.D., McKenney-Easterling, M., Brinson, M.M., Masina-Rubbo, J., Brooks, R.P., Whigham, D.F., O'Brien, D., Hite, J.T., Armstrong, B.K., 2009. Canopy composition and forest structure provide restoration targets for low-order riparian ecosystems. Restor. Ecol.

17, 51–59. https://doi.org/10.1111/j.1526-100X.2007.00333.x

Rivett, M.O., Buss, S.R., Morgan, P., Smith, J.W.N., Bemment, C.D., 2008. Nitrate attenuation in groundwater: A review of biogeochemical controlling processes. Water Res. 42, 4215–4232. https://doi.org/10.1016/j.watres.2008.07.020

Robertson, G.P., Tiedje, J.M., 1984. Denitrification and nitrous oxide production in successional and old-growth Michigan forests. Soil Sci. Soc. Am. J. 48, 383–389. https://doi.org/10.2136/sssaj1984.03615995004800020032x

Robertson, K., Klemedtsson, L., 1996. Assessment of denitrification in organogenic forest soil by regulating factors. Plant Soil 178, 49–57.

Rodhe, A., Seibert, J., 2011. Groundwater dynamics in a till hillslope: Flow directions, gradients and delay. Hydrol. Process. 25, 1899–1909. https://doi.org/10.1002/hyp.7946

Roy, A.H., Rosemond, A.D., Paul, M.J., Leigh, D.S., Wallace, J.B., 2003. Stream macroinvertebrate response to catchment urbanisation (Georgia, U.S.A.). Freshw. Biol. 48, 329–346. https://doi.org/10.1046/j.1365-2427.2003.00979.x

Ruehl, C.R., Fisher, A.T., Los Huertos, M., Wankel, S.D., Wheat, C.G., Kendall, C., Hatch, C.E., Shennan, C., 2007. Nitrate dynamics within the Pajaro River, a nutrient-rich, losing stream. J. North Am. Benthol. Soc. 26, 191–206. https://doi.org/10.1899/0887-3593(2007)26[191:NDWTPR]2.0.CO;2

Rutlidge, H., McDonough, L.K., Oudone, P., Andersen, M.S., Meredith, K., Chinu, K., Peterson, M., Baker, A., 2021. Characterisation of groundwater dissolved organic matter using LC-OCD: Implications for water treatment. Water Res. 188, 116422. https://doi.org/10.1016/j.watres.2020.116422

Rütting, T., Boeckx, P., Müller, C., Klemedtsson, L., 2011. Assessment of the importance of

dissimilatory nitrate reduction to ammonium for the terrestrial nitrogen cycle. Biogeosciences 8, 1779–1791. https://doi.org/10.5194/bg-8-1779-2011

Ryu, J., Cho, J., Kim, I.J., Mun, Y., Moon, J.P., Kim, N.W., Kim, S.J., Kong, D.S., Lim, K.J., 2011. Enhancement of SWAT-REMM to simulate reduction of total nitrogen with riparian buffer. Trans. ASABE 54, 1791–1798. https://doi.org/10.13031/2013.39845

Saltelli, A., Aleksankina, K., Becker, W., Fennell, P., Ferretti, F., Holst, N., Li, S., Wu, Q., 2019. Why so many published sensitivity analyses are false: A systematic review of sensitivity analysis practices. Environ. Model. Softw. 114, 29–39. https://doi.org/10.1016/j.envsoft.2019.01.012

Saltelli, A., Annoni, P., Azzini, I., Campolongo, F., Ratto, M., Tarantola, S., 2010. Variance based sensitivity analysis of model output. Design and estimator for the total sensitivity index. Comput. Phys. Commun. 181, 259–270. https://doi.org/10.1016/j.cpc.2009.09.018

Saltelli, A., Tarantola, S., Campolongo, F., Ratto, M., 2004. Sensitivity Analysis in Practice. John Wiley & Sons, LTD, Chichester.

Saltelli, A., Tarantola, S., Chan, K.P.S., 1999. A quantitative model-independen method for global sensitivity analysis of model output. Technometrics 41, 39–56.

Sarkar, D., 2008. Lattice: Multivariate Data Visualization with R. R package version 0.20-45. URL. https://cran.r-project.org/web/packages/lattice/lattice.pdf.

Schilling, K.E., Jacobson, P., 2014. Effectiveness of natural riparian buffers to reduce subsurface nutrient losses to incised streams. Catena 114, 140–148. https://doi.org/10.1016/j.catena.2013.11.005

Schilling, K.E., Jacobson, P., 2008. Groundwater nutrient concentrations near an incised midwestern stream: Effects of floodplain lithology and land management. Biogeochemistry

87, 199–216. https://doi.org/10.1007/s10533-008-9177-8

Schilling, K.E., Jacobson, P.J., Wolter, C.F., 2018. Using riparian zone scaling to optimize buffer placement and effectiveness. Landsc. Ecol. 33, 141–156. https://doi.org/10.1007/s10980-017-0589-5

Schilling, K.E., Li, Z., Zhang, Y.K., 2006. Groundwater-surface water interaction in the riparian zone of an incised channel, Walnut Creek, Iowa. J. Hydrol. 327, 140–150. https://doi.org/10.1016/j.jhydrol.2005.11.014

Schilling, K.E., Zhang, Y.K., Drobney, P., 2004. Water table fluctuations near an incised stream, Walnut Creek, Iowa. J. Hydrol. 286, 236–248. https://doi.org/10.1016/j.jhydrol.2003.09.017

Schipper, L.A., Cooper, A.B., Harfoot, C.G., Dyck, W.J., 1993. Regulators of denitrification in an organic riparian soil. Soil Biol. Biochem. 25, 925–933. https://doi.org/10.1016/0038-0717(93)90095-S

Schoeneberger, P.J., Wysocki, D.A., Benham, E.C., Soil Survey Staff, 2012. Field book for describing and sampling soils, Version 3.0.

Schoonover, J.E., 2005. Hydrology, water quality, and channel morphology across an urban-rural land use gradient in the Georgia piedmont, USA. Auburn University.

Schumm, S.A., Harvey, M.D., Watson, C.C., 1984. Incised Channels: Morphology, Dynamics and Control. Water Resources Publications, Littleton, CO.

Schürz, C., 2019. SWATplusR: Running SWAT2012 and SWAT+ Projects in R. https://doi.org/10.5281/zenodo.3373859

Shangguan, W., Hengl, T., Mendes de Jesus, J., Yuan, H., Dai, Y., 2017. Mapping the global depth to bedrock for land surface modeling. J. Adv. Model. Earth Syst. 65–88. https://doi.org/10.1002/2016MS000686

Sherman, M., Hripto, J., Peck, E.K., Gold, A.J., Peipoch, M., Imhoff, P., Inamdar, S., 2022. Backed-up, saturated, and stagnant: Effect of milldams on upstream riparian groundwater hydrologic and mixing regimes. Water Resour. Res. 58, 1–20. https://doi.org/10.1029/2022wr033038

Shields, F.D., Lizotte, R.E., Knight, S.S., Cooper, C.M., Wilcox, D., 2010. The stream channel incision syndrome and water quality. Ecol. Eng. 36, 78–90. https://doi.org/10.1016/j.ecoleng.2009.09.014

Showers, W.J., Genna, B., Mcdade, T., Bolich, R., Fountain, J.C., 2008. Nitrate contamination in groundwater on an urbanized dairy farm. Environ. Sci. Technol. 42, 4683–4688. https://doi.org/10.1021/es071551t

Shuai, P., Cardenas, M.B., Knappett, P.S.K., Bennett, P.C., Neilson, B.T., 2017. Denitrification in the banks of fluctuating rivers: The effects of river stage amplitude, sediment hydraulic conductivity and dispersivity, and ambient groundwater flow. Water Resour. Res. 53, 7951–7967. https://doi.org/10.1002/2017WR020610

Šimek, M., Cooper, J.E., 2002. The influence of soil pH on denitrification: Progress towards the understanding of this interaction over the last 50 years. Eur. J. Soil Sci. 53, 345–354. https://doi.org/10.1046/j.1365-2389.2002.00461.x

Simon, A., 1989. A model of channel response in disturbed alluvial channels. Earth Surf. Process. Landforms 14, 11–26.

Simon, A., Curini, A., Darby, S.E., Langendoen, E.J., 2000. Bank and near-bank processes in an incised channel. Geomorphology 35, 193–217. https://doi.org/10.1016/S0169-555X(00)00036-2

Simon, A., Darby, S.E., 2002. Effectiveness of grade-control structures in reducing erosion along

incised river channels: The case of Hotophia Creek, Mississippi. Geomorphology 42, 229–254. https://doi.org/10.1016/S0169-555X(01)00088-5

Simon, A., Pollen-Bankhead, N., Thomas, R.E., 2011. Development and application of a deterministic bank stability and toe erosion model for stream restoration, in: Simon, A., Bennett, S., Castro, J. (Eds.), Stream Restoration in Dynamic Fluvial Systems: Scientific Approaches, Analyses, and Tools. American Geophysical Union, Washington, D.C., pp. 453–474.

Simon, A., Robbins, C.H., 1987. Man-induced gradient adjustment of the South Fork Forked Deer River, West Tennessee. Environ. Geol. Water Sci. 9, 109–118. https://doi.org/10.1007/bf02449942

Siple, G.E., 1967. Geology and ground water of the Savannah River Plant and vicinity South Carolina. Geological Survey Water-Supply Paper 1841. US Atomic Energy Commission, US Department of the Interior, Washington, DC.

Smil, V., 2001. Enriching the earth: Fritz Haber, Carl Bosch, and the transformation of world food production. MIT Press.

Soil Science Division Staff, 2017. Soil Survey Manual, USDA Handbook 18.

Soil Survey Staff, 2022. Web Soil Survey [WWW Document]. URL http://websoilsurvey.sc.egov.usda.gov/

Song, X., Zhang, J., Zhan, C., Xuan, Y., Ye, M., Xu, C., 2015. Global sensitivity analysis in hydrological modeling: Review of concepts, methods, theoretical framework, and applications. J. Hydrol. 523, 739–757. https://doi.org/10.1016/j.jhydrol.2015.02.013

Sophocleous, M., 2002. Interactions between groundwater and surface water: The state of the science. Hydrogeol. J. 10, 52–67. https://doi.org/10.1007/s10040-001-0170-8

Spruill, T.B., 2000. Statistical evaluation of effects of riparian buffers on nitrate and ground water quality. J. Environ. Qual. 29, 1523–1538. https://doi.org/10.2134/jeq2000.00472425002900050020x

Stein, L.Y., Klotz, M.G., 2016. The nitrogen cycle. Curr. Biol. 26, R94–R98. https://doi.org/10.1016/j.cub.2015.12.021

Sterte, E.J., Lidman, F., Sjöberg, Y., Ploum, S.W., Laudon, H., 2022. Groundwater travel times predict DOC in streams and riparian soils across a heterogeneous boreal landscape. Sci. Total Environ. 849. https://doi.org/10.1016/j.scitotenv.2022.157398

Sun, X., Bernard-Jannin, L., Garneau, C., Volk, M., Arnold, J.G., Srinivasan, R., Sauvage, S., Sánchez-Pérez, J.M., 2016. Improved simulation of river water and groundwater exchange in an alluvial plain using the SWAT model. Hydrol. Process. 30, 187–202. https://doi.org/10.1002/hyp.10575

Sun, X., Bernard-Jannin, L., Grusson, Y., Sauvage, S., Arnold, J., Srinivasan, R., Sanchez Pérez, J.M., 2018. Using SWAT-LUD model to estimate the influence of water exchange and shallow aquifer denitrification on water and nitrate flux. Water (Switzerland) 10, 1–19. https://doi.org/10.3390/w10040528

Tague, C., 2009. Modeling hydrologic controls on denitrification: Sensitivity to parameter uncertainty and landscape representation. Biogeochemistry 93, 79–90. https://doi.org/10.1007/s10533-008-9276-6

Tamanna, M., 2021. Optimization of riparian zone nitrogen management through the development of riparian model. Dissertation. University of Rhode Island.

Tamanna, M., Pradhanang, S.M., Gold, A.J., Addy, K., Vidon, P.G., 2021. Riparian zone nitrogen management through the development of the Riparian Ecosystem Management

Model (REMM) in a formerly glaciated watershed of the US Northeast. Agriculture 11. https://doi.org/10.3390/agriculture11080743

Texas A&M University, 2022. SWAT+ IO Documentation [WWW Document]. SWAT+ Doc. URL https://swatplus.gitbook.io/docs/user/io

The Center for Agroecology and Sustainable Food Systems, 2015. Teaching organic farming & gardening, Third. ed.

Tian, W., 2013. A review of sensitivity analysis methods in building energy analysis. Renew. Sustain. Energy Rev. 20, 411–419. https://doi.org/10.1016/j.rser.2012.12.014

Tiedje, J.M., 1998. Ecology of denitrification and dissimilatory nitrate reduction to ammonium. Biol. Anaerob. Microorg. 179–244.

Tilak, A.S., 2012. Modeling groundwater hydrology and nitrate-nitrogen (NO_3-N) dynamics of two riparian buffers located in the upper eastern coastal plain of North Carolina using Riparian Ecosystem Management Model (REMM). Dissertation. North Carolina State University.

Trauth, N., Musolff, A., Knöller, K., Kaden, U.S., Keller, T., Werban, U., Fleckenstein, J.H., 2018. River water infiltration enhances denitrification efficiency in riparian groundwater. Water Res. 130, 185–199. https://doi.org/10.1016/j.watres.2017.11.058

Trudell, M.R., Gillham, R.W., Cherry, J.A., 1986. An in-situ study of the occurrence and rate of denitrification in a shallow unconfined sand aquifer. J. Hydrol. 83, 251–268. https://doi.org/10.1016/0022-1694(86)90155-1

U.S. EPA, 2016. National Rivers and Streams Assessment 2008-2009: A collaborative survey. Washington, DC.

Uhl, A., Hahn, H.J., Jäger, A., Luftensteiner, T., Siemensmeyer, T., Döll, P., Noack, M.,

Schwenk, K., Berkhoff, S., Weiler, M., Karwautz, C., Griebler, C., 2022. Making waves: Pulling the plug—Climate change effects will turn gaining into losing streams with detrimental effects on groundwater quality. Water Res. 220. https://doi.org/10.1016/j.watres.2022.118649

USDA Natural Resources Conservation Service, 2014. Soil quality indicators: Soil nitrate, Soil Quality Information Sheet.

USDA Natural Resources Conservation Service, 2008. Soil quality indicators: Available water capacity, Soil Quality Information Sheet. https://doi.org/10.1007/978-90-481-3585-1_528

USDA Natural Resources Conservation Service, 1998. Soil quality indicators: pH, Soil Quality Information Sheet.

Van Den Heuvel, R.N., Bakker, S.E., Jetten, M.S.M., Hefting, M.M., 2011. Decreased N_2O reduction by low soil pH causes high N_2O emissions in a riparian ecosystem. Geobiology 9, 294–300. https://doi.org/10.1111/j.1472-4669.2011.00276.x

van Meerveld, H.J., Seibert, J., Peters, N.E., 2015. Hillslope-riparian-stream connectivity and flow directions at the Panola Mountain Research Watershed. Hydrol. Process. 29, 3556–3574. https://doi.org/10.1002/hyp.10508

Verry, E.S., 2003. Estimating ground water yield in small research basins. GroundWater 41, 1001–1004. https://doi.org/10.1111/j.1745-6584.2003.tb02441.x

Vidon, P., Allan, C., Burns, D., Duval, T.P., Gurwick, N., Inamdar, S., Lowrance, R., Okay, J., Scott, D., Sebestyen, S., 2010. Hot spots and hot moments in riparian zones: Potential for improved water quality management. J. Am. Water Resour. Assoc. 46, 278–298. https://doi.org/10.1111/j.1752-1688.2010.00420.x

Vidon, P.G., Hill, A.R., 2006. A landscape-based approach to estimate riparian hydrological and

nitrate removal functions. J. Am. Water Resour. Assoc. 42, 1099–1112. https://doi.org/10.1111/j.1752-1688.2006.tb04516.x

Vidon, P.G.F., Hill, A.R., 2004. Landscape controls on the hydrology of stream riparian zones. J. Hydrol. 292, 210–228. https://doi.org/10.1016/j.jhydrol.2004.01.005

Vilain, G., Garnier, J., Tallec, G., Tournebize, J., 2012. Indirect N_2O emissions from shallow groundwater in an agricultural catchment (Seine Basin, France). Biogeochemistry 111, 253–271. https://doi.org/10.1007/s10533-011-9642-7

Vitousek, P.M., Aber, J.D., Howarth, R.W., Likens, G.E., Matson, P.A., Schindler, D.W., Schlesinger, W.H., Tilman, D.G., 1997. Human alteration of the global nitrogen cycle: Sources and consequences. Ecol. Appl. 7, 737–750. https://doi.org/10.1890/1051-0761(1997)007[0737:HAOTGN]2.0.CO;2

Vogel, R.M., Wilson, I., Daly, C., 1999. Regional regression models of annual streamflow for the United States. J. Irrig. Drain. Eng. 125, 148–157.

Voltz, T., Gooseff, M., Ward, A.S., Singha, K., Fitzgerald, M., Wagener, T., 2013. Riparian hydraulic gradient and stream-groundwater exchange dynamics in steep headwater valleys. J. Geophys. Res. Earth Surf. 118, 953–969. https://doi.org/10.1002/jgrf.20074

Wagener, T., McIntyre, N., Lees, M.J., Wheater, H.S., Gupta, H. V., 2003. Towards reduced uncertainty in conceptual rainfall-runoff modelling: Dynamic identifiability analysis. Hydrol. Process. 17, 455–476. https://doi.org/10.1002/hyp.1135

Wallace, C.D., Soltanian, M.R., 2021. Surface water-groundwater exchange dynamics in buried-valley aquifer systems. Hydrol. Process. 35. https://doi.org/10.1002/hyp.14066

Wand, M., 2021. KernSmooth: Functions for Kernel Smoothing Supporting Wand & Jones (1995). R package version 2.23-20. URL. https://cran.r-

project.org/web/packages/KernSmooth/KernSmooth.pdf.

Waters, E.R., Morse, J.L., Bettez, N.D., Groffman, P.M., 2014. Differential carbon and nitrogen controls of denitrification in riparian zones and streams along an urban to exurban gradient. J. Environ. Qual. 43, 955. https://doi.org/10.2134/jeq2013.12.0504

Webster, J.R., Mulholland, P.J., Tank, J.L., Valett, H.M., Dodds, W.K., Peterson, B.J., Bowden, W.B., Dahm, C.N., Findlay, S., Gregory, S., Grimm, N.B., Hamilton, S.K., Johnson, S.L., Marti, E., McDowell, W.H., Meyer, J.L., Morrall, D.D., Thomas, S.A., Wollheim, W.M., 2003. Factors affecting ammonium uptake in streams – an inter-biome perspective. Freshw. Biol. 48, 1329–1352.

Wei, T., Simko, V., 2021. R package "corrplot": Visualization of a Correlation Matrix. Version 0.92. URL. https://cran.r-project.org/web/packages/corrplot/corrplot.pdf.

Wei, X., Bailey, R.T., Records, R.M., Wible, T.C., Arabi, M., 2019. Comprehensive simulation of nitrate transport in coupled surface-subsurface hydrologic systems using the linked SWAT-MODFLOW-RT3D model. Environ. Model. Softw. 122. https://doi.org/10.1016/j.envsoft.2018.06.012

Weiss, R.F., 1970. The solubility of nitrogen, oxygen and argon in water and seawater. Deep. Res. Oceanogr. Abstr. 17, 721–735. https://doi.org/10.1016/0011-7471(70)90037-9

Well, R., Flessa, H., Jaradat, F., Toyoda, S., Yoshida, N., 2005. Measurement of isotopomer signatures of N_2O in groundwater. J. Geophys. Res. Biogeosciences 110, 1–13. https://doi.org/10.1029/2005JG000044

Wenger, S., 1999. A review of the scientific literature on riparian buffer width, extent and vegetation.

Weymann, D., Well, R., Flessa, H., Von Der Heide, C., Deurer, M., Meyer, K., Konrad, C.,

Walther, W., 2008. Groundwater N_2O emission factors of nitrate-contaminated aquifers as derived from denitrification progress and N_2O accumulation. Biogeosciences 5, 1215–1226. https://doi.org/10.5194/bg-5-1215-2008

Wickham, H., 2011. The Split-Apply-Combine Stategy for Data Analysis. J. Stat. Softw. 40, 1–29.

Wickham, H., Averick, M., Bryan, J., Chang, W., McGowan, L., François, R., Grolemund, G., Hayes, A., Henry, L., Hester, J., Kuhn, M., Pedersen, T., Miller, E., Bache, S., Müller, K., Ooms, J., Robinson, D., Seidel, D., Spinu, V., Takahashi, K., Vaughan, D., Wilke, C., Woo, K., Yutani, H., 2019. Welcome to the Tidyverse. J. Open Source Softw. 4, 1686. https://doi.org/10.21105/joss.01686

Wickham, H., Francois, R., Henry, L., Muller, K., 2020. dplyr: A Grammar of Data Manipulation. R package version 1.0.2. URL. https://cran.r-project.org/web/packages/dplyr/dplyr.pdf.

Williams, M.R., Buda, A.R., Elliott, H.A., Hamlett, J., Boyer, E.W., Schmidt, J.P., 2014. Groundwater flow path dynamics and nitrogen transport potential in the riparian zone of an agricultural headwater catchment. J. Hydrol. 511, 870–879. https://doi.org/10.1016/j.jhydrol.2014.02.033

Winter, T.C., 1999. Relation of streams, lakes, and wetlands to groundwater flow systems. Hydrogeol. J. 7, 28–45. https://doi.org/10.1007/s100400050178

Winter, T.C., Harvey, J.W., Franke, O.L., Alley, W.M., 1999. Ground Water and Surface Water: A Single Resource. Denver, Colorado.

Wiseman, J.D., Burchell, M.R., Grabow, G.L., Osmond, D.L., Messer, T.L., 2014. Groundwater nitrate concentration reductions in a riparian buffer enrolled in the NC Conservation

Reserve Enhancement Program. J. Am. Water Resour. Assoc. 50, 653–664. https://doi.org/10.1111/jawr.12209

Wolman, G., 1955. The natural channel of Brandywine Creek Pennsylvania, Geological Survey Professional Paper 271.

Wroblicky, G.J., Campana, M.E., Dahm, N., 1998. Seasonal variation in surface-subsurface water exchange and lateral hyporheic area of two stream-aquifer systems. Water Resour. Res. 34, 317–328.

Wu, S., Tetzlaff, D., Yang, X., Soulsby, C., Ecology, F., Fisheries, I., Analysis, A.E., Centre, H., 2022. Identifying dominant processes in time and space: Time-varying spatial sensitivity analysis for a grid-based nitrate model. Water Resour. Res. 58. https://doi.org/https://doi.org/10.1029/2021WR031149

Xie, H., Shen, Z., Chen, L., Qiu, J., Dong, J., 2017. Time-varying sensitivity analysis of hydrologic and sediment parameters at multiple timescales: Implications for conservation practices. Sci. Total Environ. 598, 353–364. https://doi.org/10.1016/j.scitotenv.2017.04.074

Zeileis, A., Hothorn, T., 2002. Diagnostic Checking in Regression Relationship. R News 2, 7–10.

Zhang, C., Li, S., Jamieson, R.C., Meng, F.R., 2017a. Segment-based assessment of riparian buffers on stream water quality improvement by applying an integrated model. Ecol. Modell. 345, 1–9. https://doi.org/10.1016/j.ecolmodel.2016.12.005

Zhang, C., Li, S., Qi, J., Xing, Z., Meng, F., 2017b. Assessing impacts of riparian buffer zones on sediment and nutrient loadings into streams at watershed scale using an integrated REMM-SWAT model. Hydrol. Process. 31, 916–924. https://doi.org/10.1002/hyp.11073

Zhang, Z.Y., Schmidt, C., Nixdorf, E., Kuang, X., Fleckenstein, J.H., 2021. Effects of

heterogeneous stream-groundwater exchange on the source composition of stream discharge and solute load. Water Resour. Res. 57, 1–19. https://doi.org/10.1029/2020WR029079

Zimmer, M.A., McGlynn, B.L., 2017. Bidirectional stream–groundwater flow in response to ephemeral and intermittent streamflow and groundwater seasonality. Hydrol. Process. 31, 3871–3880. https://doi.org/10.1002/hyp.11301

APPENDIX A

SUPPLEMENTARY MATERIAL FOR GLOBAL SENSITIVITY ANALYSES OF KEY RIPARIAN NITROGEN MODELS

Parameter Distributions and Statistics

Table A1. Ranges and distributions defined for selecting values of REMM buffer parameters in the Monte Carlo analysis. All means and standard deviations for parameters with a log-normal distribution are listed as natural logarithms.

Parameter	Distribution	Mean	StDev	Min	Max	Source (s) /Notes
Surface drainage area (ha)	Log-normal	0.397	1.407	0.04	40	Ferguson et al. (1986); Pitts and Badhwar (1980)
Stream depth (m)	Log-normal	-1.624	1.802	0.1	20	Assumed
Soil temperature (°C)	Normal	18.8	6.25	5	30	Assumed
Zone width (m)	Log-normal	2.103	0.631	2.5	30.5	Georgia Soil and Water Conservation Commission (2016); Wenger (1999); assumed
Surface slope (%)	Log-normal	-0.293	1.404	0.1	20	Cooper et al. (1987)
Deep seepage (mm/d)	Log-normal	-1.722	0.902	0.02	1.19	Verry (2003)
Overland Manning's n	Log-normal	-1.956	0.833	0.1	0.9	Chow (1959); Lammers (2015)

Table A2. Ranges and distributions defined for selecting values of REMM soil parameters in the Monte Carlo analysis. All means and standard deviations for parameters with a log-normal distribution are listed as natural logarithms.

Parameter	Distribution	Mean	StDev	Min	Max	Source (s) /Notes
Ammonium (kg/ha)	Log-normal	2.896	0.289	7.74	30	Assumed
Nitrate (kg/ha)	Log-normal	4.539	0.363	0.1	150	Brady and Weil (1996); USDA Natural Resources Conservation Service (2014)
Depth to bedrock (m)	Log-normal	2.451	0.707	0	3125	Shangguan et al. (2017)
Pore Size Distribution	Uniform	0.422	0.136	0.15	0.694	REMM
Layer thickness (cm)	Log-normal	3.977	0.668	1	200	Assumed
Wilting point (cm/cm)	Uniform	--	--	0.03	0.3	REMM
Field capacity (cm/cm)	Uniform	--	--	0.11	0.4	REMM
Porosity	Uniform	--	--	0.3	0.5	Knisel and Davis (2000); assumed
Volumetric water (cm^3/cm^3)	Uniform	--	--	0.01	0.5	Assumed
Permeability (cm/hr)	Uniform	--	--	3.60E-03	54	(Schoeneberger et al., 2012)
% clay	Uniform	--	--	5	90	REMM
Bulk density (g/cm^3)	Normal	1.45	0.275	0.9	2	REMM
pH	Normal	6	1	4	8	USDA Natural Resources Conservation Service (1998); assumed
Structural carbon (kg/ha)	Normal	5800	1450	2900	8700	REMM; assumed
Metabolic carbon (kg/ha)	Normal	120	30	60	180	REMM; assumed
Active humus carbon (kg/ha)	Normal	400	100	200	600	REMM; assumed
Slow humus carbon (kg/ha)	Normal	12000	3000	6000	18000	REMM; assumed
Passive humus carbon (kg/ha)	Normal	7600	1900	3800	11400	REMM; assumed
Lignin carbon (kg/ha)	Normal	3360	840	1680	5040	REMM; assumed

Table A3. Ranges and distributions defined for selecting values of REMM vegetation parameters in the Monte Carlo analysis. All means and standard deviations for parameters with a log-normal distribution are listed as natural logarithms.

Parameter	Distribution	Mean	StDev	Min	Max	Source/Notes
Rainfall interception canopy	Uniform	--	--	0.05	0.5	Kozak et al. (2007); Miralles et al. (2010)
N max, buds (g/kg)	Normal	20	5	10	30	Assumed
N max, leaves (g/kg)	Normal	20	5	10	30	Assumed
N max, stems (g/kg)	Normal	5	1.25	2.5	7.5	Assumed
N max, branches (g/kg)	Normal	10	2.5	5	15	Assumed
N max, coarse roots (g/kg)	Normal	5	1.25	2.5	7.5	Assumed
N max, fine roots (g/kg)	Normal	5	1.25	2.5	7.5	Assumed
N min, buds (g/kg)	Normal	8	2	4	12	Assumed
N min, leaves (g/kg)	Normal	8	2	4	12	Assumed
N min, stems (g/kg)	Normal	1.5	0.375	0.75	2.25	Assumed
N min, branches (g/kg)	Normal	5	1.25	2.5	7.5	Assumed
N min, coarse roots (g/kg)	Normal	1.5	0.375	0.75	2.25	Assumed
N min, fine roots (g/kg)	Normal	1.5	0.375	0.75	2.25	Assumed
Max rooting depth (cm)	Normal	500	251.25	15	1020	Canadell et al. (1996)
Rooting depth (cm)	Normal	100	50	15	250	Lammers (2015); assumed

Table A4. Ranges and distributions defined for selecting values of REMM rate parameters in the Monte Carlo analysis. All means and standard deviations for parameters with a log-normal distribution are listed as natural logarithms.

Parameter	Distribution	Mean	StDev	Min	Max	Source/Notes
Residue metabolic decay (day^{-1})	Normal	0.05	0.018263	0.00195	0.075	Parton et al. (1987)
Residue structural decay (day^{-1})	Normal	0.013429	0.004928	0.00043	0.0201429	Parton et al. (1987)
Humus active decay (day^{-1})	Normal	0.02	0.007013	0.00195	0.03	Parton et al. (1987)
Humus slow decay (day^{-1})	Normal	0.000543	0.000195	3.45E-05	0.0008144	Parton et al. (1987)
Humus passive decay (day^{-1})	Normal	1.86E-05	6.73E-06	0.000001	0.0000279	Parton et al. (1987)
Denitrification K (kg/cm/ha)	Log-normal	-5.587	1.401	0.001	0.1	Dayanthi et al. (2008); assumed

Table A5. Ranges and distributions defined for selecting values of SWAT+ parameters in the Monte Carlo analysis. All means and standard deviations for parameters with a log-normal distribution are listed as natural logarithms.

	Change	Distribution	Mean	StDev	Min	Max	Source/Notes
Basin Characteristics							
Nitrate percolation	Percent	Uniform	--	--	-99	400	Assumed
Denitrification rate	Percent	Uniform	--	--	-99	100	SWAT+ recommendation
Denitrification saturation threshold	Percent	Uniform	--	--	-99	100	Assumed
Soil Properties							
Soil layer thickness	Percent	Log-normal	-33	50	-99	100	Assumed
Bulk density	Percent	Normal	30	35	-40	100	Assumed
Available water capacity	Percent	Normal	200	150	-99	500	SWAT+ rec.
Hydraulic conductivity	Percent	Normal	50	75	-99	200	Assumed
Soil carbon	Percent	Uniform	--	--	-86	500	SWAT+ rec.
Clay content	Percent	Uniform	--	--	-99	100	Assumed
pH	Percent	Normal	30	35	-40	100	SWAT+ rec.
Aquifer and Routing Parameters							
Stream depth	Percent	Log-normal	100	500	-60	2000	Assumed
Aquifer bottom depth	Absolute value	Normal	6.5	1.75	3	10	SWAT+ rec.
Maximum baseflow	Absolute value	Normal	1	0.5	0	2	SWAT+ rec.
WTD return flow	Absolute value	Normal	5	2.475	0.1	10	SWAT+ rec.
HRU Characteristics							
Slope	Percent	Log-normal	-25	49	-96	100	Assumed
Slope length	Absolute value	Log-normal	100	247.5	10	1000	Assumed
Lateral length	Percent	Log-normal	10	50	-90	100	Assumed
Field width	Absolute value	Log-normal	100	112.5	50	500	Assumed
Field length	Absolute value	Log-normal	500	225	100	1000	Assumed

Correlations

We accounted for several simple correlations among parameters in REMM to ensure that the parameter sets represented realistic conditions. Drainage area was used as an input to USGS flood regressions, assuming 17.4% imperviousness and a 24-hour, 50-year rainfall depth of 22.1 cm for a 1 ha drainage area, in the southern coastal plain (Region 4) to specify a range of median annual floods (50% exceedance discharges) (Feaster et al., 2014). We then used downstream hydraulic geometry equations to approximate slope based on a discharge randomly selected from that range (Leopold, 1953; Wolman, 1955). Additionally, clay percentage was randomly selected from a uniform distribution and used to specify a general soil texture or group of possible textures (e.g., coarse, medium, fine) (Soil Science Division Staff, 2017). We used these textures to choose bulk densities for each of the three soil layers from distributions parameterized by means and standard deviations from Mason et al. (1957). Soil permeability was also determined from distributions associated with each soil texture group (The Center for Agroecology and Sustainable Food Systems, 2015). Other correlations were deemed less important and were ignored, so as to test randomly across that entire parameter range. Ratios for litter layer bulk density and structural carbon relative to the top soil layer remained unchanged in all simulations.

Furthermore, we checked logical relationships between parameters and adjusted them based on literature or knowledge of the system. For example, if the randomly selected value for field capacity equaled or exceeded the selected porosity value, field capacity was reduced to 7/9 that of porosity (Dingman, 2002). We applied the same multiplier for situations where the randomly selected wilting point exceeded field capacity. Depth to bedrock had to be at least three times the selected layer thickness to accommodate all three soil layers. Volumetric water content was constrained to less than soil porosity. When initial rooting depth equaled or exceed

maximum rooting depth, the initial value was restricted to 90% of the maximum. When minimum nitrogen concentrations by plant part were at least as large as the corresponding maximum, the minimum was reassigned to 75% of the maximum. Finally, we applied several amendments to parameter values to address model errors and restrictions. While REMM operates on fixed starting C:N ratios, this analysis was expanded to test across a range of C:N values by altering soil nitrogen pools (structural, active humus, passive humus, and slow humus) in conjunction with the randomly selected soil carbon pool sizes. Errors occurred when the riparian zone would flush all the water in less than a day, so we capped permeability at 90% its maximum value based on zone width.

For SWAT+, we used correlations similar to those in REMM, this time by accounting for directional and relative magnitude relationships among several parameters. Clay content constrained values for bulk density and hydraulic conductivity. Since both parameters were inversely related to clay content, if clay content was increased by some percentage, bulk density and hydraulic conductivity were decreased by a similar percentage. The correlations between slope length and slope (inverse) and lateral length (direct) were incorporated in an analogous way.

Additional Results

Figure A1 shows complete results for the REMM sensitivity analysis of the full simulation. Total sensitivity (summed across all parameters) in REMM stabilized around 400 simulations, indicating that our 1000 simulations adequately estimated sensitivity (Figure A2). Figures A3 and A4 depict the time-varying results for denitrification and total nitrogen, respectively, in REMM and were discussed in Chapter 2.

SWAT+ additional results are shown in Figures A5 and A6. Total sensitivity (summed across all parameters) in SWAT+ stabilized around 300 simulations, indicating that our 500 simulations were sufficient to estimate sensitivity (Figure A5). Figure A6 depicts the time-varying results for denitrification, which were discussed in the Chapter 2.

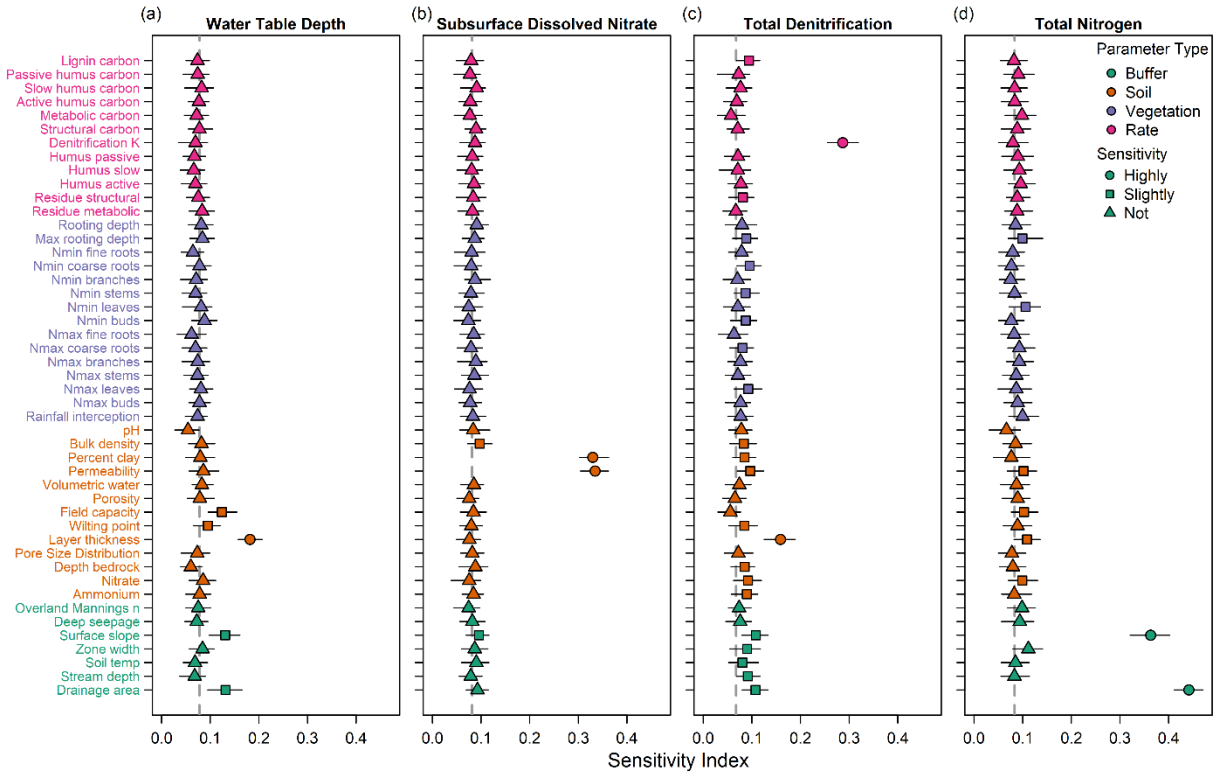

Figure A1. Sensitivity of the four chosen REMM outputs to each of the selected 47 input parameters. The dashed vertical line is the sensitivity of that output to a dummy variable. Error bars represent the minimum and maximum sensitivity across all simulations with bootstrapping.

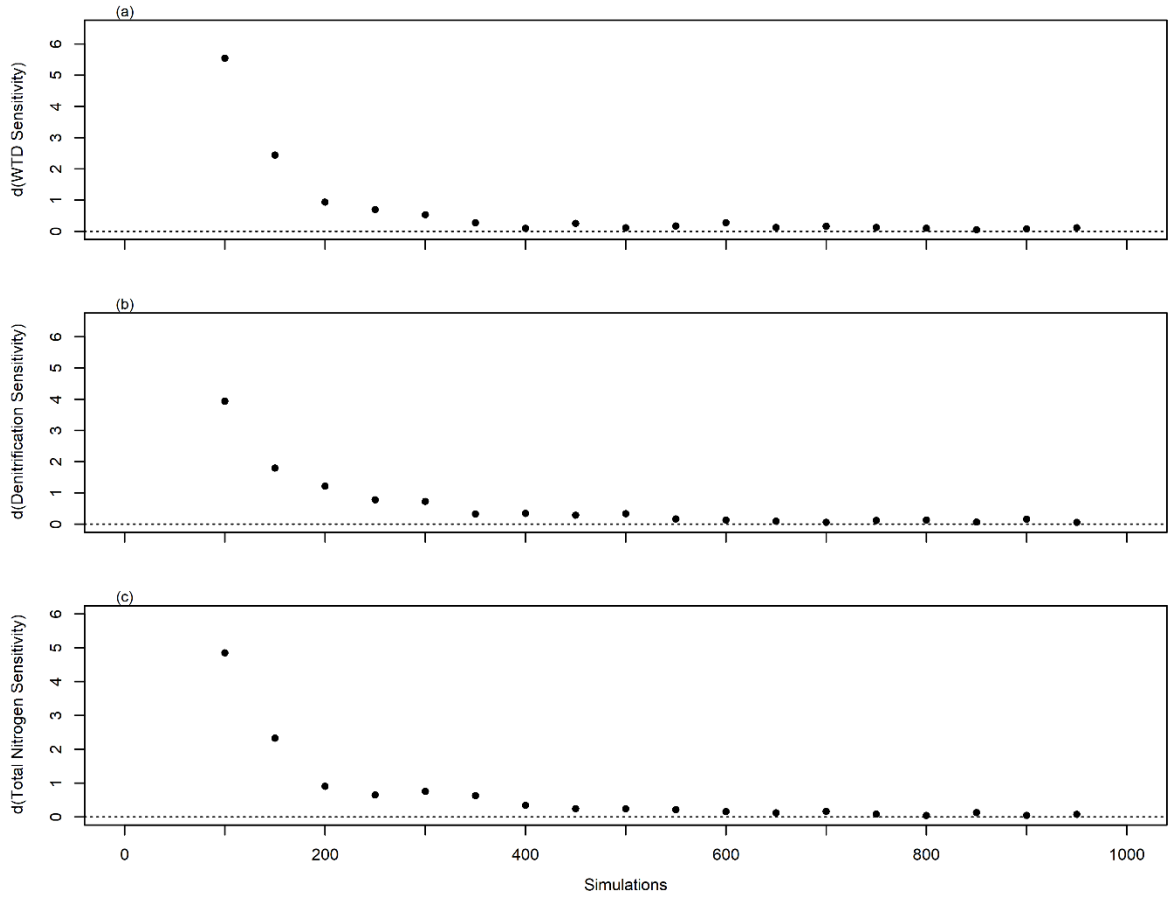

Figure A2. Change in total REMM output sensitivity (sum of all parameters of interest) as the number of simulations increased, relative to the next interval of 50.

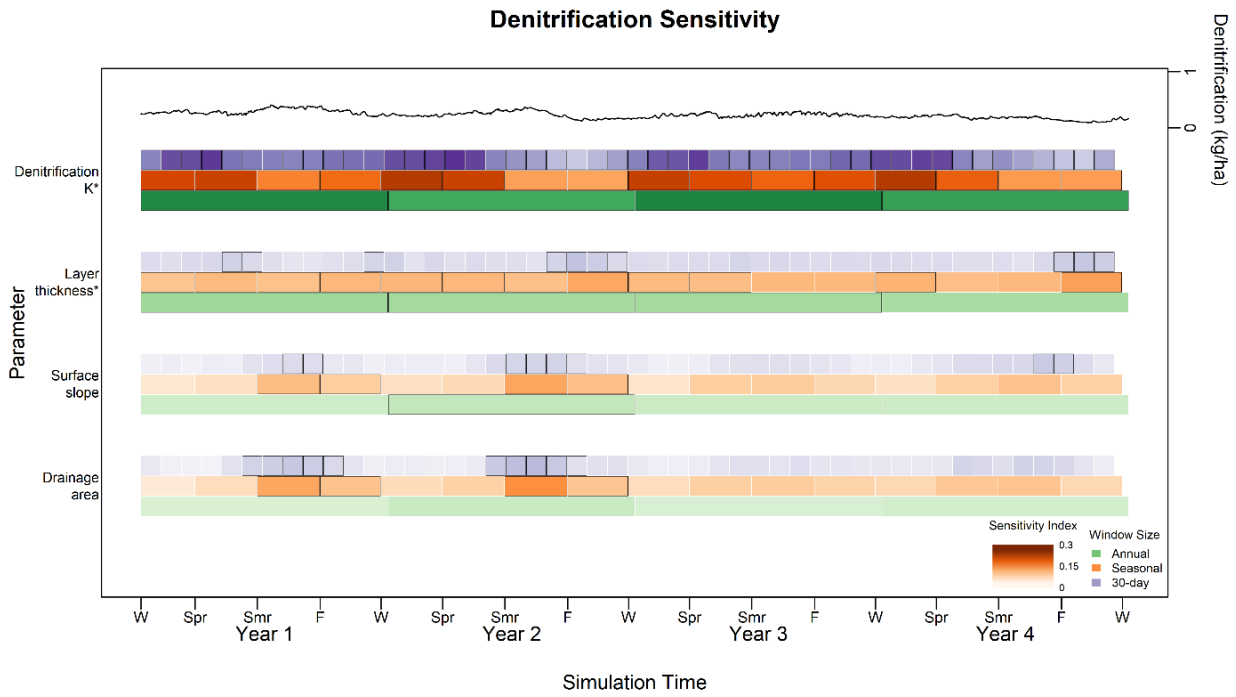

Figure A3. Sensitivity of the denitrification output in REMM to the most influential parameters at varying time windows. Time windows are shaded according to the value of the sensitivity index. Times when parameters were highly sensitive (no overlap with the dummy variable sensitivity) are outlined. Parameters that were sensitive across the entire simulation length are denoted with an *. The average daily denitrification across all model runs is shown at the top.

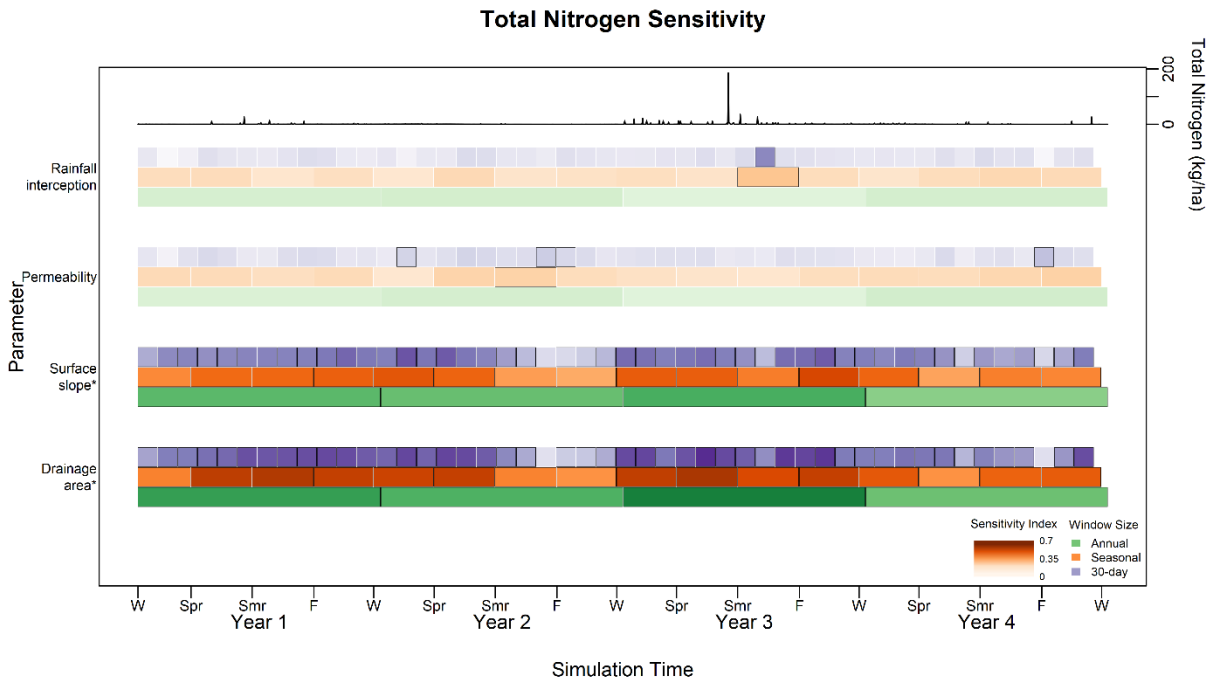

Figure A4. Sensitivity of the total nitrogen output in REMM to the most influential parameters at varying time windows. Time windows are shaded according to the value of the sensitivity index. Times when parameters were highly sensitive (no overlap with the dummy variable sensitivity) are outlined. Parameters that were sensitive across the entire simulation length are denoted with an *. The average daily total nitrogen across all model runs is shown at the top.

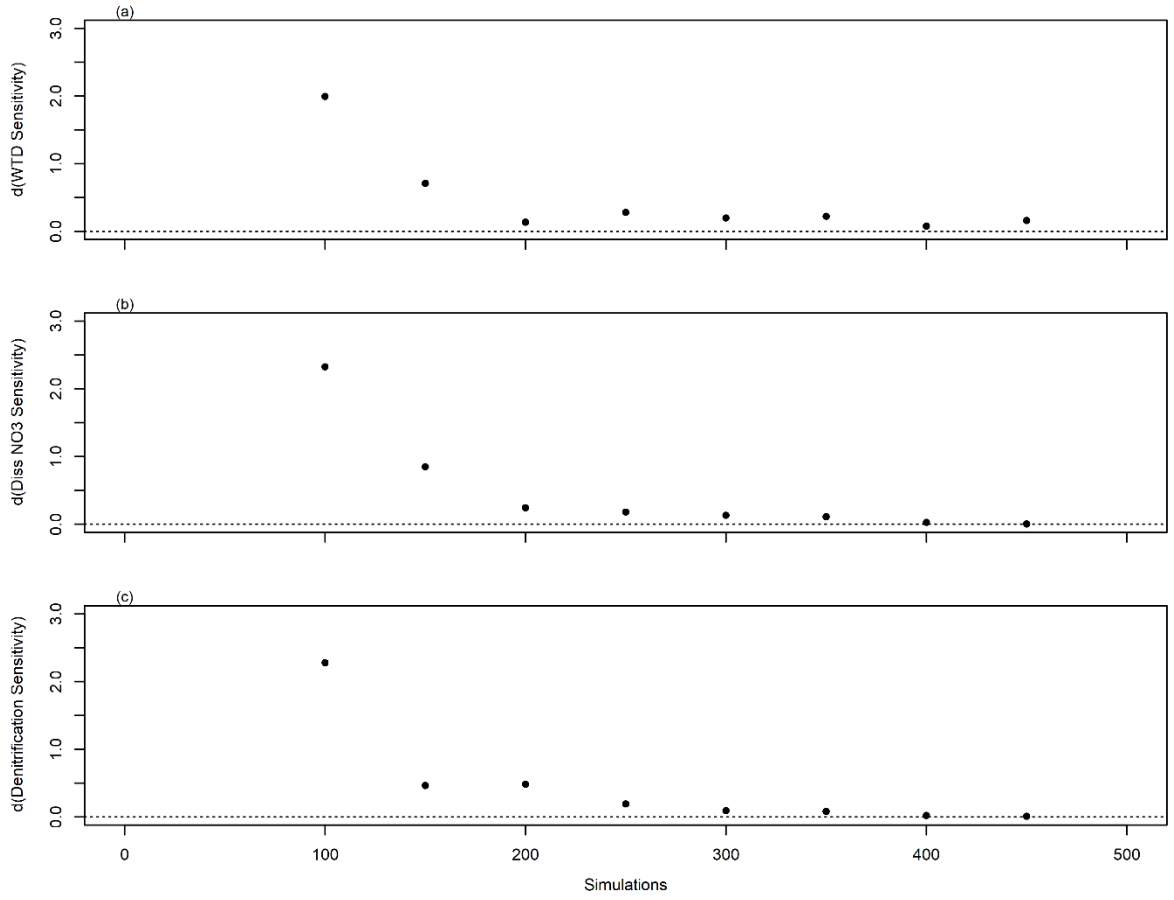

Figure A5. Change in the total SWAT+ output sensitivity (sum of all parameters of interest) as the number of simulations increased, relative to the next interval of 50.

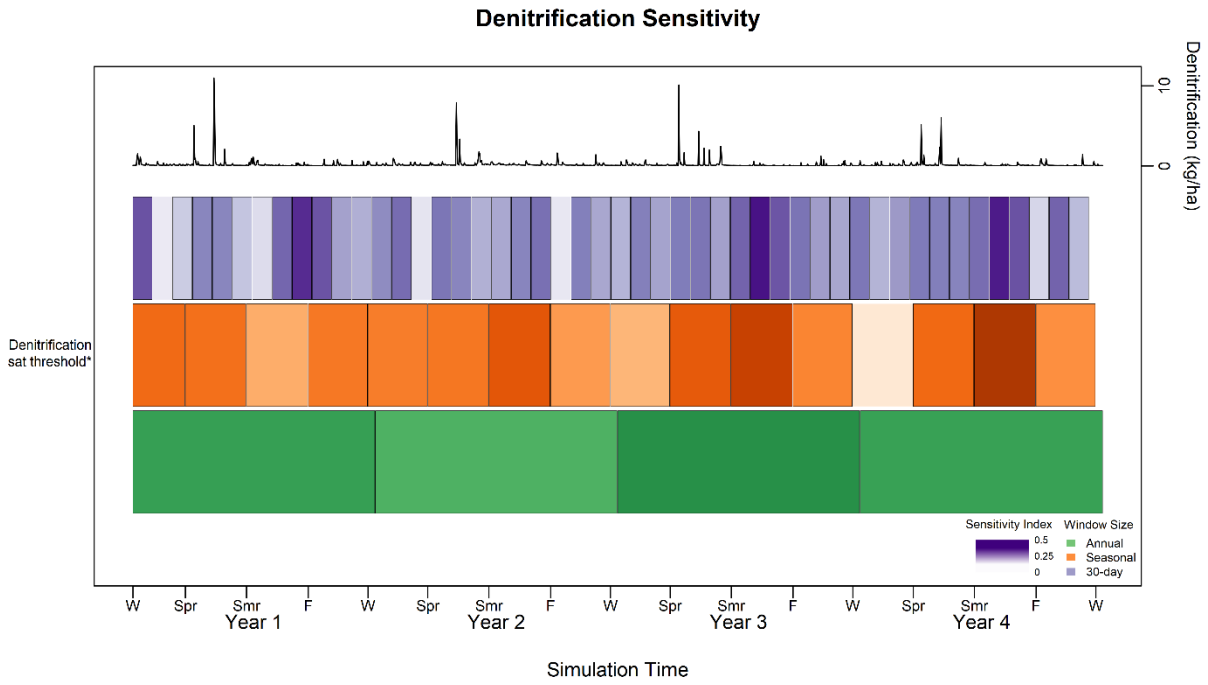

Figure A6. Sensitivity of the denitrification output in SWAT+ to the only influential parameter, denitrification saturation threshold, at varying time windows. Time windows are shaded according to the value of the sensitivity index. Times when parameters were highly sensitive (no overlap with the dummy variable sensitivity) are outlined. An * denotes the parameters was sensitive across the entire simulation length. Times when parameters were highly sensitive (no overlap with dummy variable sensitivity) are outlined. The average daily denitrification across all model runs is shown at the top.

APPENDIX B

SUPPLEMENTARY MATERIAL FOR EFFECTS OF STREAM INCISION ON GROUNDWATER-SURFACE WATER INTERACTIONS AND RIPARIAN DENITRIFICATION

Nitrogen Calculations

Membrane-inlet mass spectrometry yielded mass signals for N_2, Ar, and O_2, which were compared to determine gas ratios of N_2:Ar and O_2:Ar. Expected concentrations of N_2, Ar, and N_2:Ar were calculated with gas solubility coefficients and standard temperatures, then corrected for instrument drift using linear regression (Weiss, 1970). Dissolved dinitrogen gas in excess of the expected concentration at that sampling temperature was assumed to be from denitrification in the groundwater. Excess N_2 was calculated using Equation B1, sourced from previous *in situ* denitrification studies (Jahangir et al., 2013; McAleer et al., 2017; Weymann et al., 2008).

$$X_{Excess\ N_2} = X_{Total\ N_2} - X_{EA\ N_2} - X_{EQ\ N_2} \quad \text{[Eq. B1]}$$

Where X is the molar concentration of dissolved N_2 components. $X_{Total\ N_2}$ is the total N_2 in the sample, $X_{EA\ N_2}$ is the amount of N_2 dissolved in water from entrapment or dissolution of gas bubbles in the unsaturated zone (Heaton and Vogel, 1981), and $X_{EQ\ N_2}$ is the equilibrium concentration of N_2 with the atmosphere. $X_{EA\ N_2}$ can be estimated using Equation B2.

$$X_{EA\ N_2} = \left(X_{Total\ Ar} - X_{EQ\ Ar}\right) * \left(\frac{X_{Atm\ N_2}}{X_{Atm\ Ar}}\right) \quad \text{[Eq. B2]}$$

Where $X_{Total\ Ar}$ is the concentration of argon in the sample, $X_{EQ\ Ar}$ is the concentration of argon equilibrated with the atmosphere at the sampling temperature, and $\frac{X_{Atm\ N_2}}{X_{Atm\ Ar}}$ is the ratio of N_2 to argon in the atmosphere.

Total denitrification was calculated as the sum of excess N_2-N and N_2O-N. These were used to estimate the total initial nitrogen concentration ($N_{initial}$) in the groundwater with total nitrogen (TN; Eq. B3).

$$N_{initial} = TN + (Excess\ N_2 - N) + (N_2O - N) \quad \text{[Eq. B3]}$$

This calculation was used to estimate the progress of the denitrification reaction (RP; Eq. B4), which compares the byproducts of denitrification to the initial nitrogen concentration (Jahangir et al., 2013; McAleer et al., 2017; Weymann et al., 2008).

$$RP = \frac{(Excess\ N_2 - N) + (N_2O - N)}{N_{initial}} \quad \text{[Eq. B4]}$$

Incomplete denitrification was calculated using the fraction of N_2O-N to the sum of the denitrification gases (Eq. B5).

$$Frac\ N_2O = \frac{N_2O-N}{(Excess\ N_2-N)+(N_2O-N)} \quad \text{[Eq. B5]}$$

Additional Results

Both incised reaches were deeper and steeper than unincised reaches (Table B1), and the dairy incised reach was the steepest due to step-like headcuts upstream of our transect. The channels at the dairy farm were similar in bankfull width. The incised McQueen mainstem channel is approximately five times wider than its unincised tributary. Minor changes in top width and slope were measured at each transect, although the effect of channel evolution processes was not noticeable over one year. The dairy channels widened by more than 0.5 m between the first and second surveys, which we attributed to human-induced bank erosion from accessing the stream and scour around the stream gages. We also observed a bank failure at the incised transect after a storm event in early 2022. A slight deepening of these channels could have resulted from scour around the stream gages, although the change in depth is within our measurement uncertainty. Bank erosion from human and animal traffic appeared to have caused the observed widening at McQueen incised. The incised transect at McQueen also showed a mobile sand bed, meaning our measurements of bankfull depth and bed slope may have depended on the timing and magnitude of previous storm events that moved plugs of sand throughout the channel. McQueen unincised became narrower and shallower between surveys – opposite trends from the other channels. These changes were reasonable, as we observed sediment aggradation around vegetation and roots in this low-gradient stream.

Table B1. Summary of annual survey measurements at the four study transects. Top width and depth are estimated for bankfull conditions, while slope represents bed slope.

		2021			2022		
Stream	**Incision**	**Top width (m)**	**Depth (m)**	**Slope**	**Top width (m)**	**Depth (m)**	**Slope**
Dairy	Incised	2.6	1.3	0.033	3.3	1.4	0.029
	Unincised	2.0	0.1	0.019	2.6	0.2	0.014
McQueen	Incised	9.5	2.5	0.0125	9.9	2.6	0.0107
	Unincised	1.8	0.3	0.0044	1.6	0.2	0.0036

Figure B1 shows the temporal trends in total nitrogen and dissolved organic carbon at the dairy farm. TN did not significantly vary with month ($\chi^2 = 16.6$, $p = 0.12$). These trends at McQueen are shown in Figure B2. A more detailed explanation is in Chapter 3.

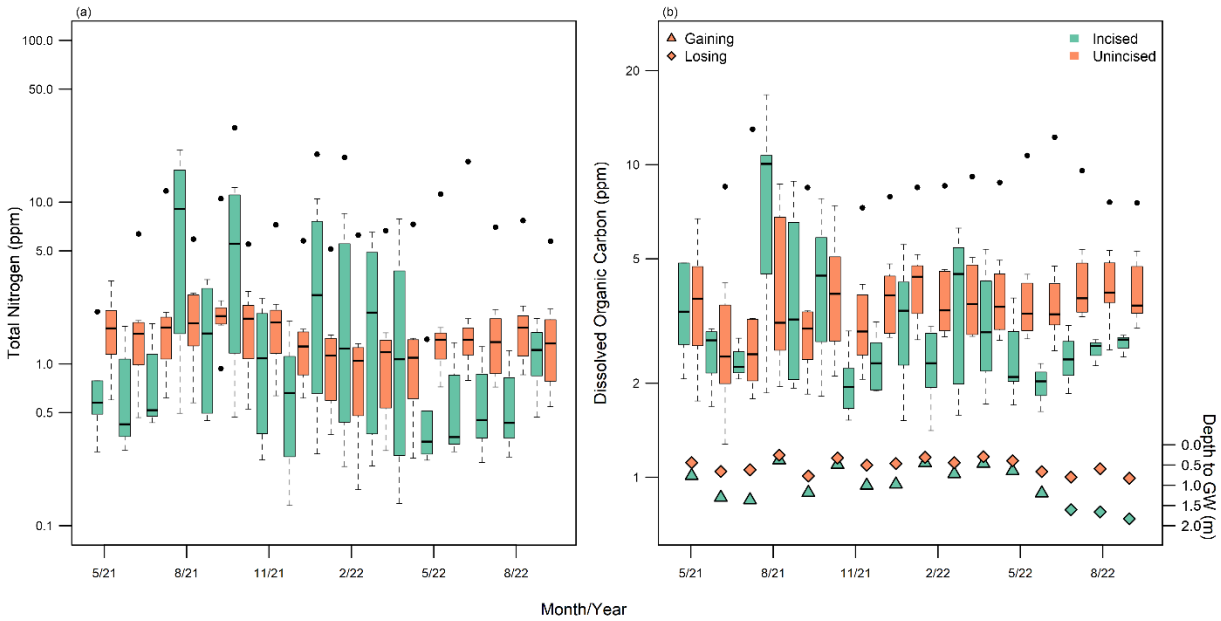

Figure B1. Distribution of monthly groundwater total nitrogen (a) and dissolved organic carbon (b) for the incised and unincised transects at the dairy farm. Vertical axes are logarithmic to aid visualization of distributions. Transect-averaged groundwater depths are noted with triangles for gaining conditions and diamonds for losing conditions (b). Boxes represent the quartiles and median, and whiskers show the non-outlier maximum and minimum.

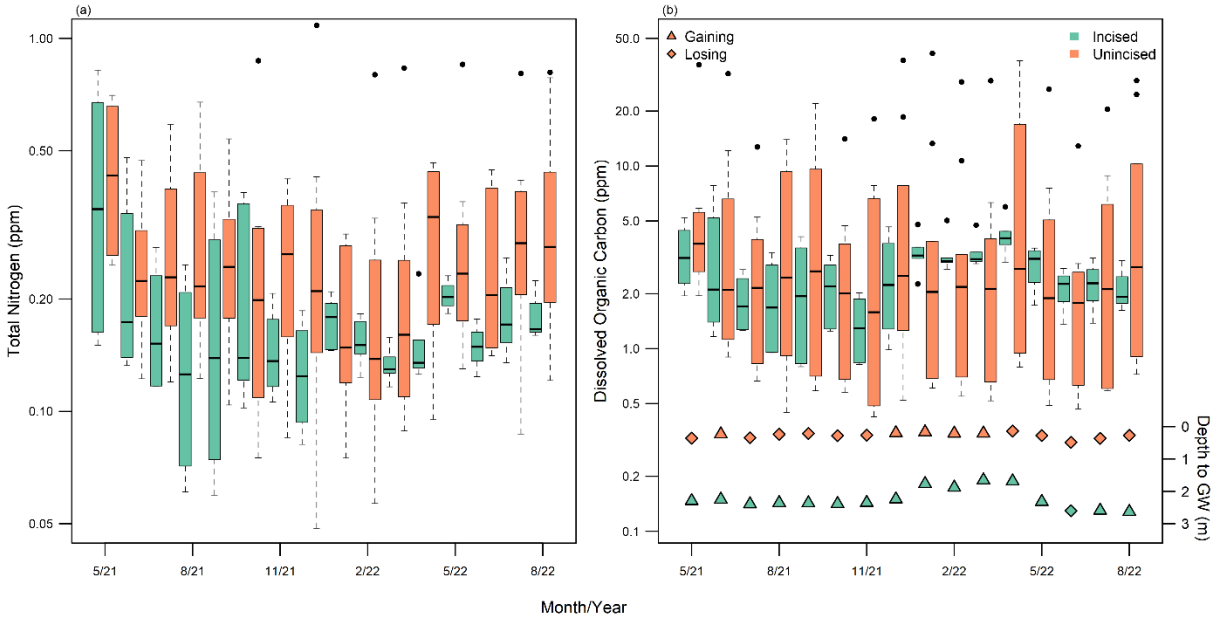

Figure B2. Distribution of monthly total nitrogen (a) and dissolved organic carbon (b) for the incised and unincised transects at McQueen Branch. Vertical axes are logarithmic to aid visualization of distributions. Transect-averaged groundwater depths are noted with triangles for gaining conditions and diamonds for losing conditions (b). Boxes represent the quartiles and median, and whiskers show the non-outlier maximum and minimum.

APPENDIX C

SUPPLEMENTARY MATERIAL FOR COUPLED MODELING OF THE EFFECTS OF STREAM INCISION AND GROUNDWATER-SURFACE WATER INTERACTIONS ON NETWORK-SCALE NITROGEN LOADING

Model Inputs

Table C1. Table of all variables considered for statistical model development.

Variable	Description	Units
Month	Month of year (1 to 12)	--
Nest	Set of wells relative to stream (1 to 3, with 1 nearest the stream)	--
DTW	Depth to groundwater	m
Temp	Groundwater temperature	C
DO	Dissolved oxygen	mg/L
SpC	Specific conductance	µS/cm
pH	Groundwater pH	--
NO3-N	Groundwater dissolved nitrate (as nitrogen)	ppb
NH3-N	Groundwater dissolved ammonia (as nitrogen)	ppb
DOC	Dissolved organic carbon	ppm
TN	Total dissolved nitrogen	ppm
Cl	Dissolved chloride	ppm
N2O	Dissolved nitrous oxide gas	ppm
ExcessN2	Excess nitrogen gas	ppm
Denitrification	Denitrification end products (excess N_2 and N_2O)	mg/L
RP	Denitrification reaction progress	--
w:d	Channel bankfull width to depth ratio	--
deltaElev	Difference in elevation from groundwater to stream surface	m
Ht_ExpBank	Height of exposed bank above stream surface	m
RatWetBank	Ratio of total bank height wetted by stream	
HydGrad	Hydraulic gradient between groundwater and stream	--
SoilOC	Soil organic carbon	%
deltaBed	Difference in elevation from groundwater to stream bed	m
DistStr	Distance from the stream	m
% sand	% sand in riparian soil	%
% silt	% silt in riparian soil	%
% clay	% clay in riparian soil	%

Table C2. Major input parameters for REM models under Scenario A. Bank properties and the cohesive layer depth were adjusted to generate greater incision for Scenario B.

Stream	**Dairy**		**McQueen**			
Reach	**Unincised**	**Incised**	**Unincised**	**Incised**	**Main stem**	**Sources**
XS Spacing (m)	10	10	20	20	20	Assumed
Channel slope	0.014	0.029	0.004	0.0116	0.0107	Measured
Reach length (m)	100	50	100	100	280	Assumed
Depth to cohesive layer (m)	0.5	0.25	2	2	2	Field-estimated
Cohesive layer τ_c (Pa)	99	99	99	99	99	Assumed
Channel bottom width (m)	1.4	1.43	0.94	3.65	3.15	Measured
Bank height (m)	0.18	1.28	0.19	2.57	1.6	Measured
Toe height (m)	0.1	0.1	0.01	0.01	0.01	Assumed
Bank angle (deg)	16.4	38.6	52.7	24.6	24.6	Measured
Toe angle (deg)	16.4	38.6	52.7	24.6	24.6	Assumed
Floodplain angle (deg)	0.18	1.01	3.45	1.22	1.22	Measured
Left floodplain width (m)	20	20	15	20	20	Measured, rounded
Right floodplain width (m)	20	20	15	20	20	Measured, rounded
Channel n	0.035	0.04	0.035	0.03	0.03	Field-estimated
Floodplain n	0.08	0.08	0.07	0.07	0.07	Field-estimated
Grain size (mm)	0.75	0.75	0.5	1.0	1.0	Field-estimated
Bank τ_c (Pa)	10	30	2	60	60	Calibrated
Bank cohesion (kPa)	8.2	12.6	3	2.35	2.35	Simon et al. (2011), calibrated
Toe cohesion (kPa)	8.2	12.6	3	2.35	2.35	Simon et al. (2011), calibrated
Bank ϕ	21.1	11.4	27	28.45	28.45	Simon et al. (2011), calibrated
Toe ϕ	21.1	11.4	27	28.45	28.45	Simon et al. (2011), calibrated
Bank saturated weight (kN/m^3)	17.7	16.9	18.1	18.25	18.25	Simon et al. (2011), calibrated
Toe saturated weight (kN/m^3)	17.7	16.9	18.1	18.25	18.25	Simon et al. (2011), calibrated
Bedload bank (proportion)	0.5	0.5	0.5	0	0	Calibrated
Bedload bed (proportion)	0.5	0.5	0.5	0.7	0.7	Calibrated
Sediment supply (proportion; -1 = transport capacity)	-0.02	-0.03	-1	-1	0	Calibrated

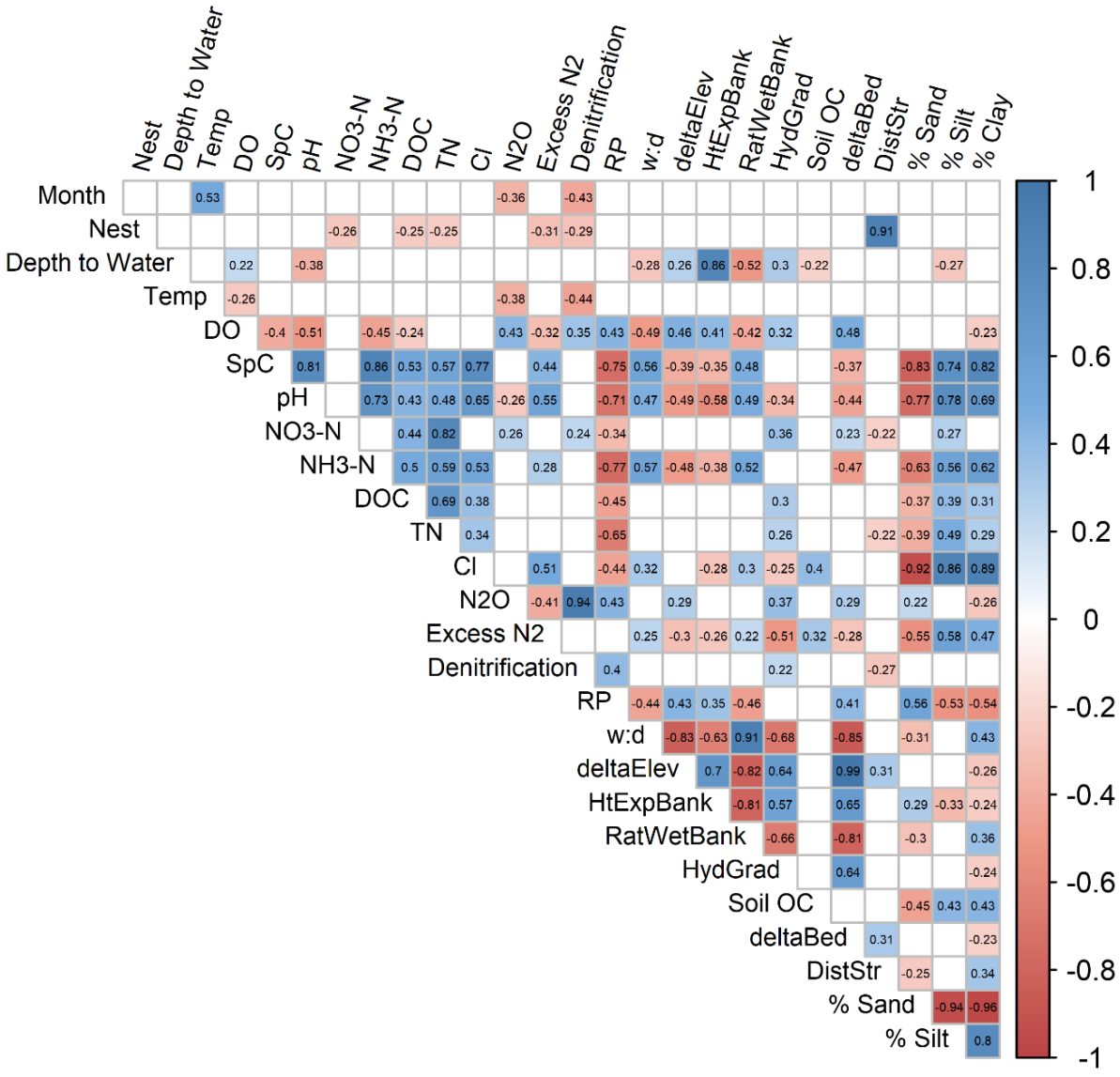

Figure C1. Spearman correlation matrix between all variables considered in statistical model development. Statistically-significant correlations are colored based on direction of correlation and labeled with correlation strength. Parameter names are described in Table C1.

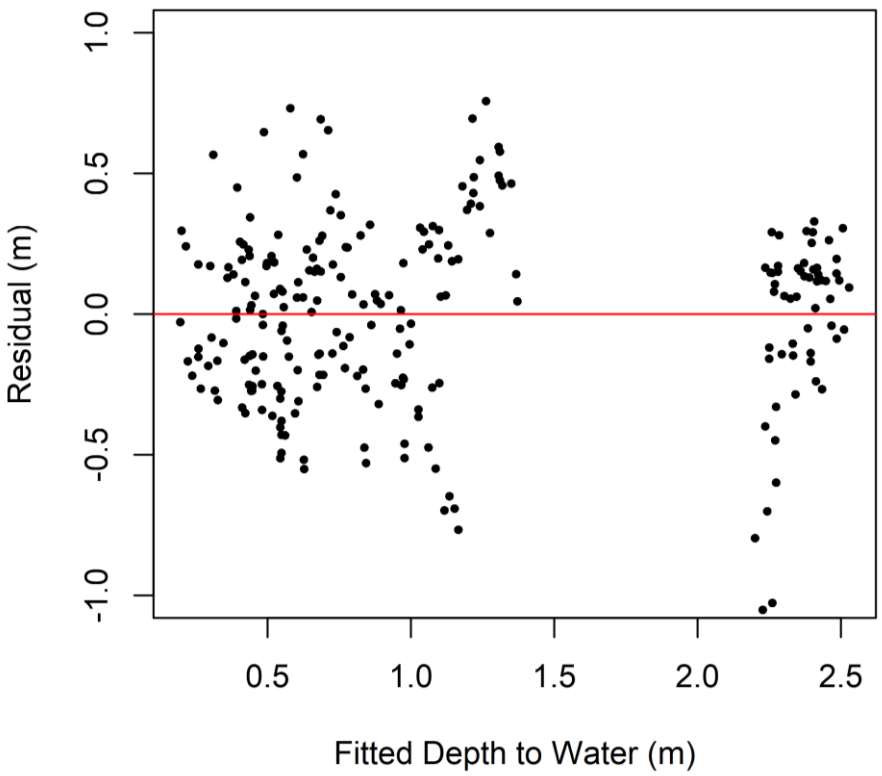

Figure C2. Comparison of depth to groundwater fitted by the overall dataset to the model residuals (observed minus predicted). Residuals were not produced randomly ($p < 0.001$).

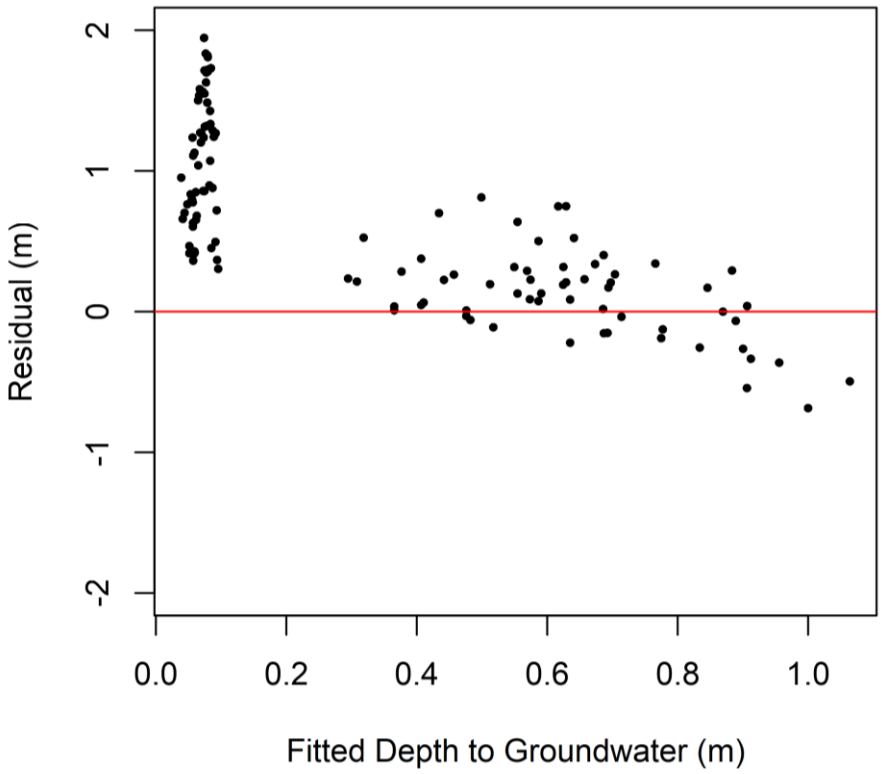

Figure C3. Comparison of depth to groundwater fitted by the dairy farm dataset to the model residuals (observed minus predicted). Residuals were not produced randomly ($p < 0.001$).

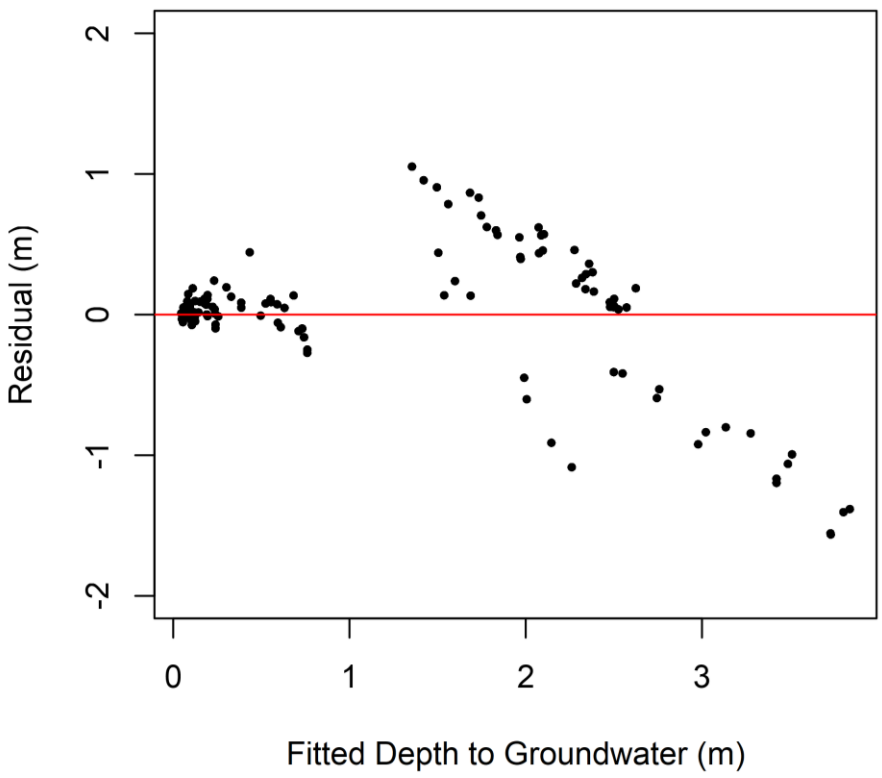

Figure C4. Comparison of depth to groundwater fitted by the McQueen dataset to the model residuals (observed minus predicted). Residuals were not produced randomly ($p < 0.001$).

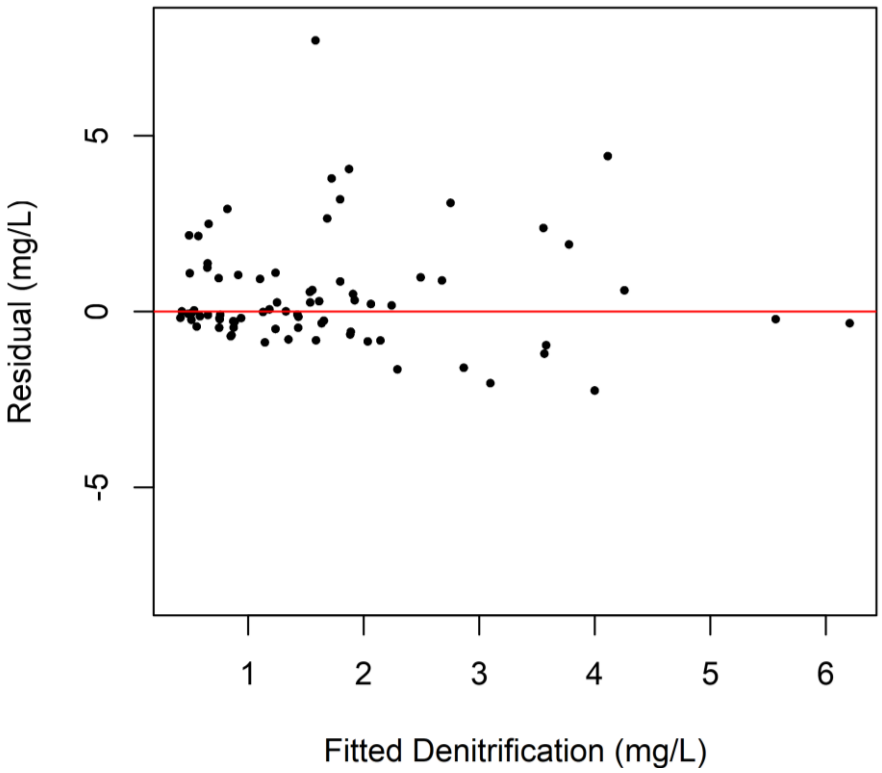

Figure C5. Comparison of denitrification during gaining conditions fitted by the overall dataset to the model residuals (observed minus predicted). Residuals were not produced randomly ($p < 0.001$).

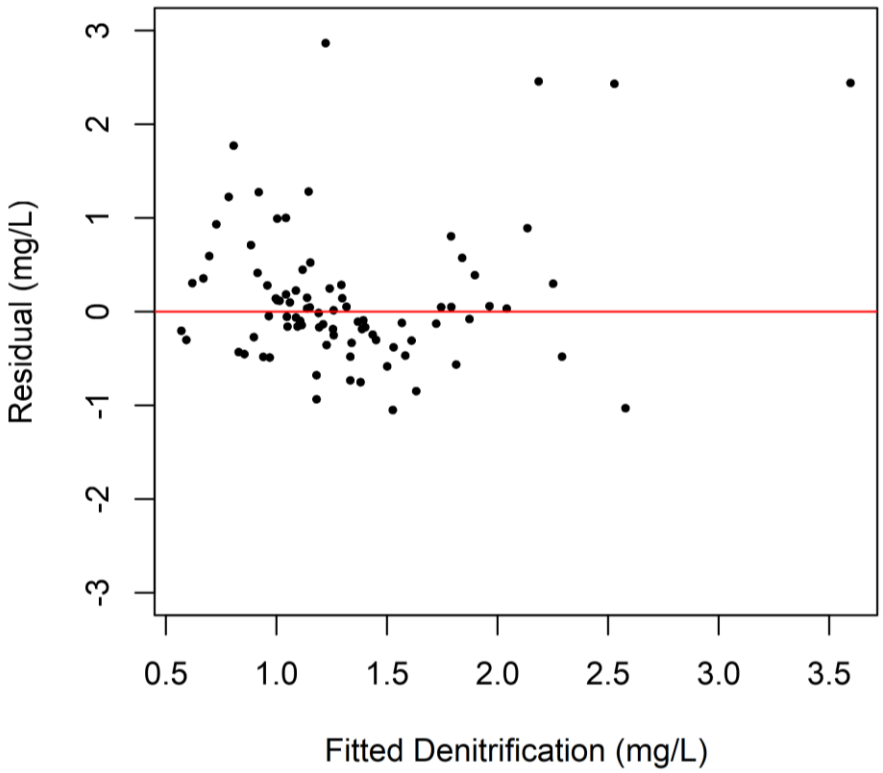

Figure C6. Comparison of denitrification during losing conditions fitted by the overall dataset to the model residuals (observed minus predicted). Residuals were not produced randomly ($p = 0.02$).

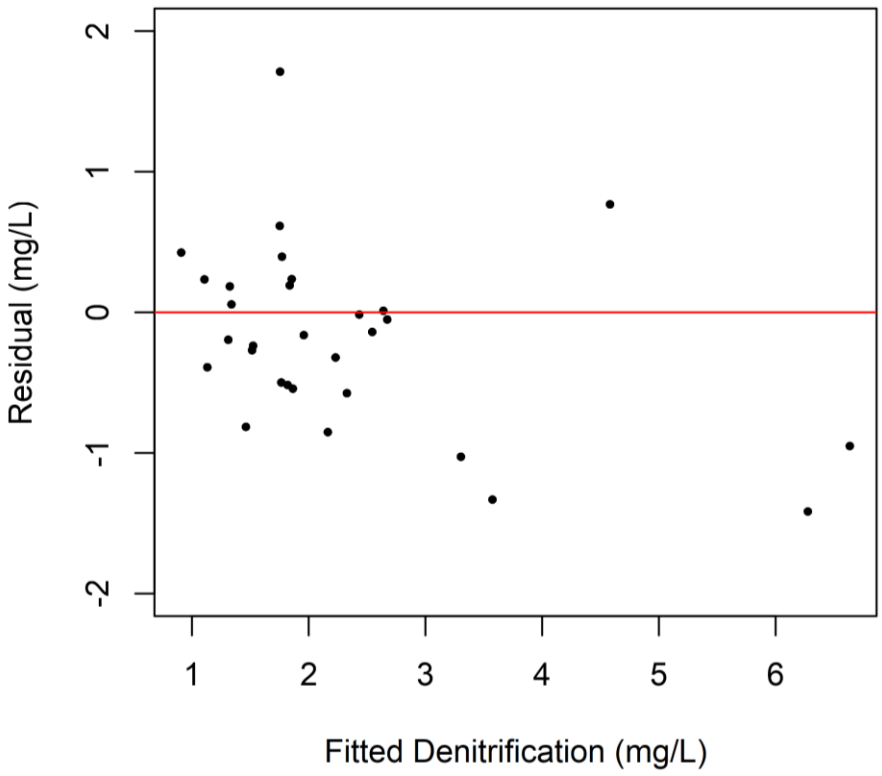

Figure C7. Comparison of denitrification during gaining conditions fitted by the dairy farm dataset to the model residuals (observed minus predicted). Residuals were produced in a random manner ($p = 0.72$).

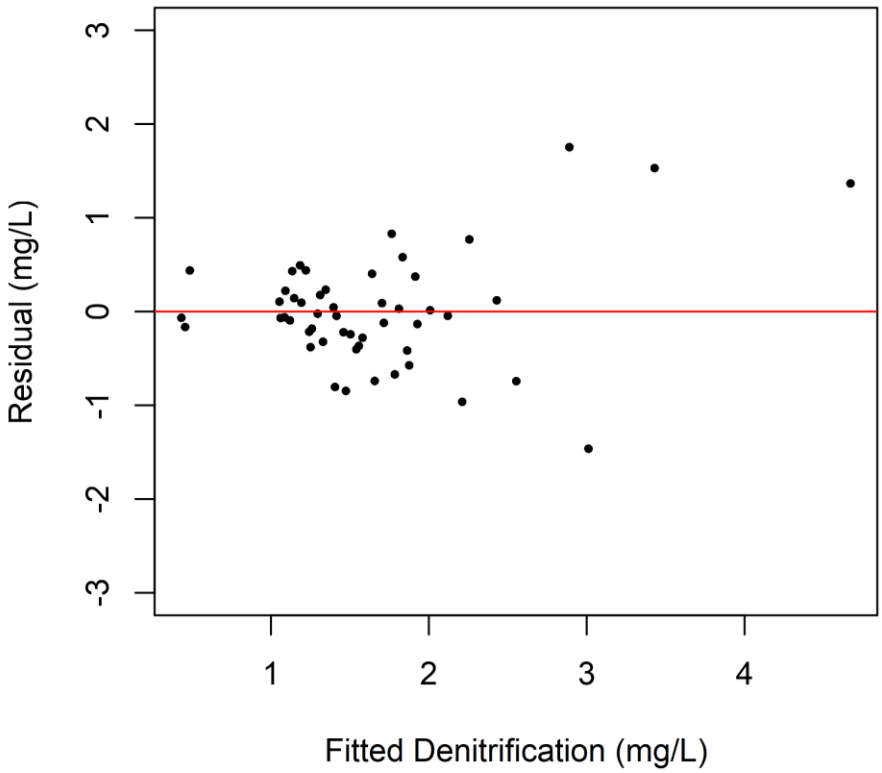

Figure C8. Comparison of denitrification during losing conditions fitted by the dairy farm dataset to the model residuals (observed minus predicted). Residuals were produced in a random manner ($p = 0.78$).

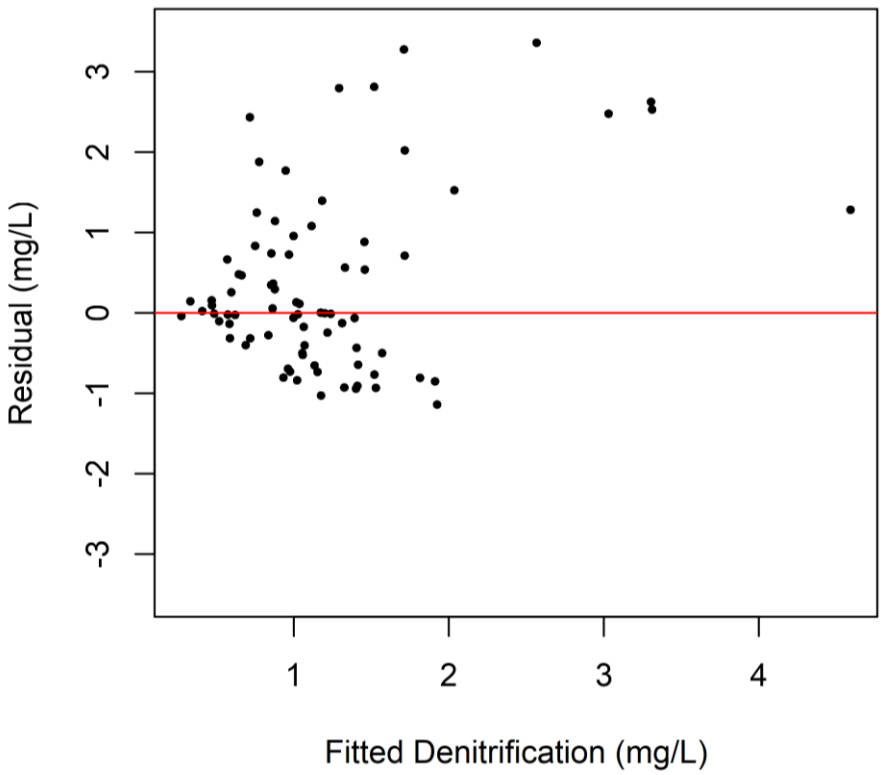

Figure C9. Comparison of denitrification fitted by the McQueen dataset to the model residuals (observed minus predicted). Residuals were not produced randomly ($p = 0.02$).

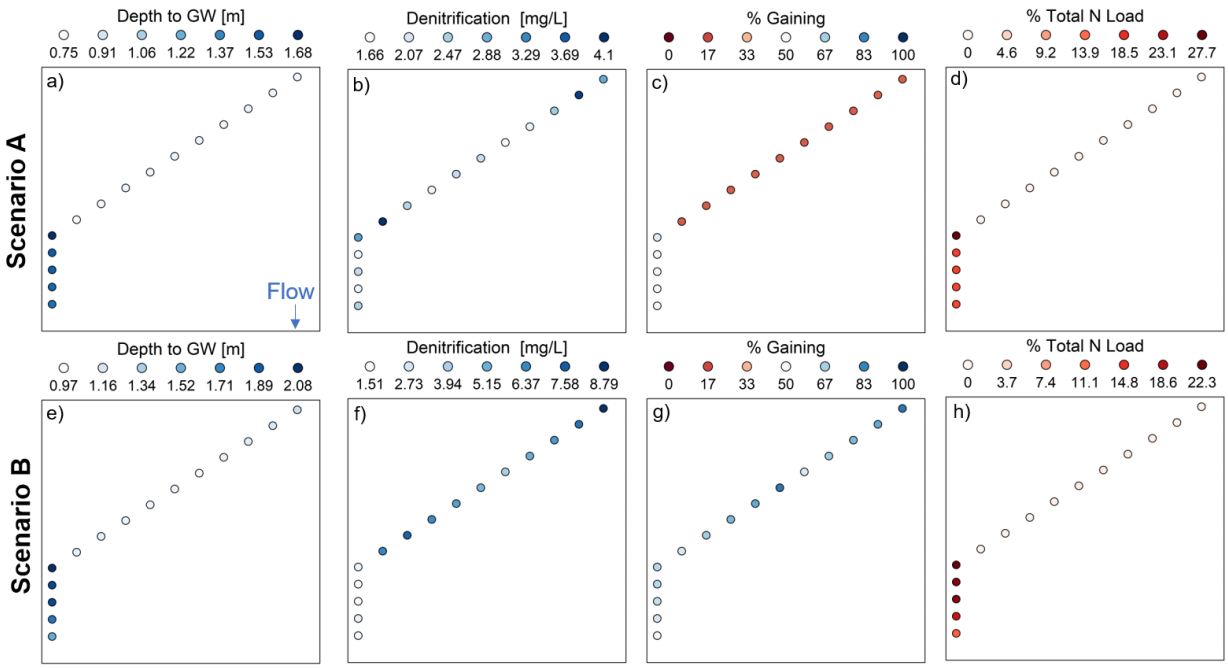

Figure C10. Average groundwater depth (panels a and e) and denitrification (b and f) across the 30-year REM simulation at the dairy farm, plus the percentage of gaining flow (c and g) and stream network nitrogen load from each cross-section (d and h), as predicted by the site-specific models. Scenario A (panels a-c) had less incision than Scenario B (d-f). Each dot is a cross-section, spaced 10 m apart. Flow is moving from top to bottom.

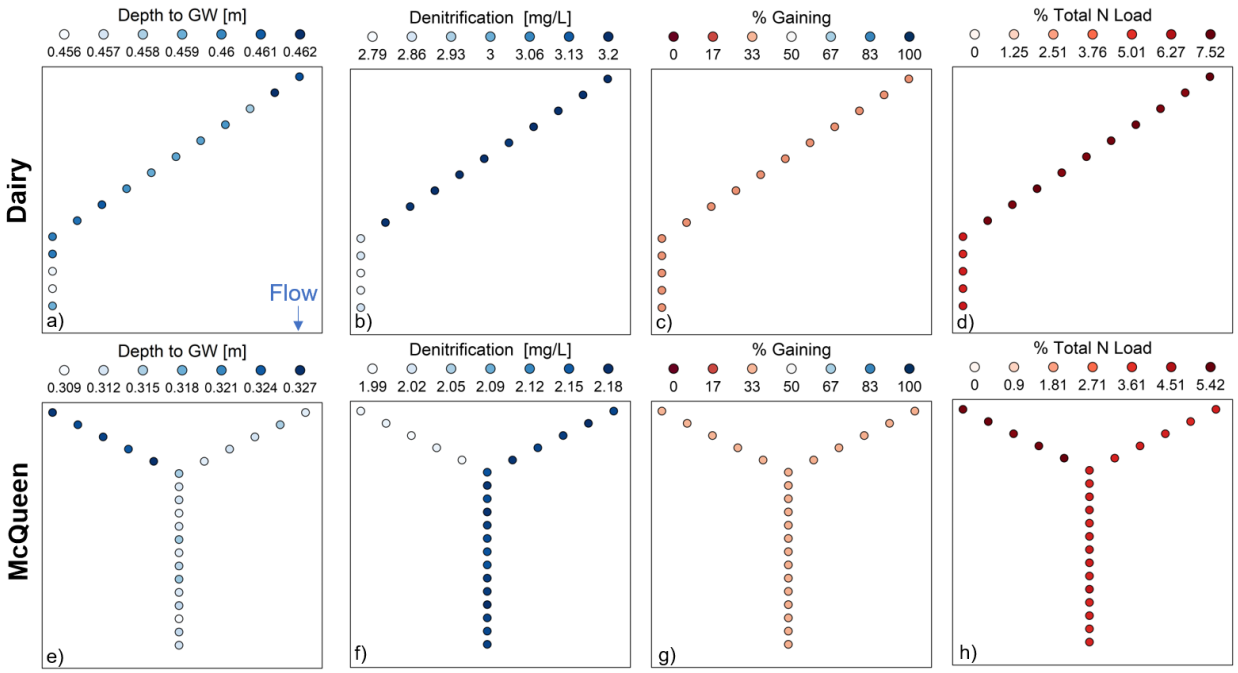

Figure C11. Average groundwater depth (panels a and e) and denitrification (b and f) across 30 years for the unincised, base condition at both locations, plus the percentage of gaining flows (c and g) and stream network nitrogen load from each cross-section (d and h), as predicted by the overall models. Each dot is a cross-section, spaced 10 and 20 m apart for Dairy and McQueen, respectively. Flow is moving from top to bottom.

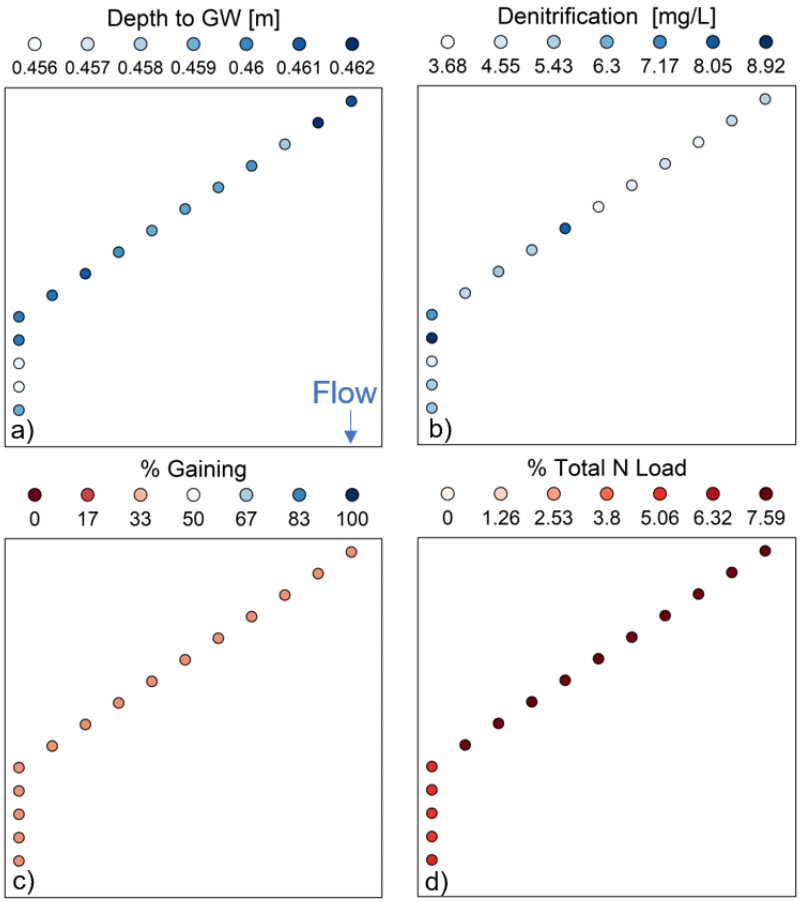

Figure C12. Average groundwater depth (panel a) and denitrification (b) across 30 years for the unincised, base condition at the dairy farm, plus the percentage of gaining flows (c) and stream network nitrogen load from each cross-section (d), as predicted by the site-specific models. Each dot is a cross-section, spaced 10 m apart. Flow is moving from top to bottom.

Table C3. Comparison of changes in total network nitrogen loading, riparian denitrification and reaction progress (RP), and proportion of gaining flows compared to the base condition, for the site-specific model at the dairy farm.

Model	Scenario	% Change in N Load	% Change in Denitrification	% Change in RP	% Change in Gaining
Dairy	Scenario A	22 %	-97 %	-7.8 %	5.7 %
	Scenario B	110 %	-92 %	10 %	130 %

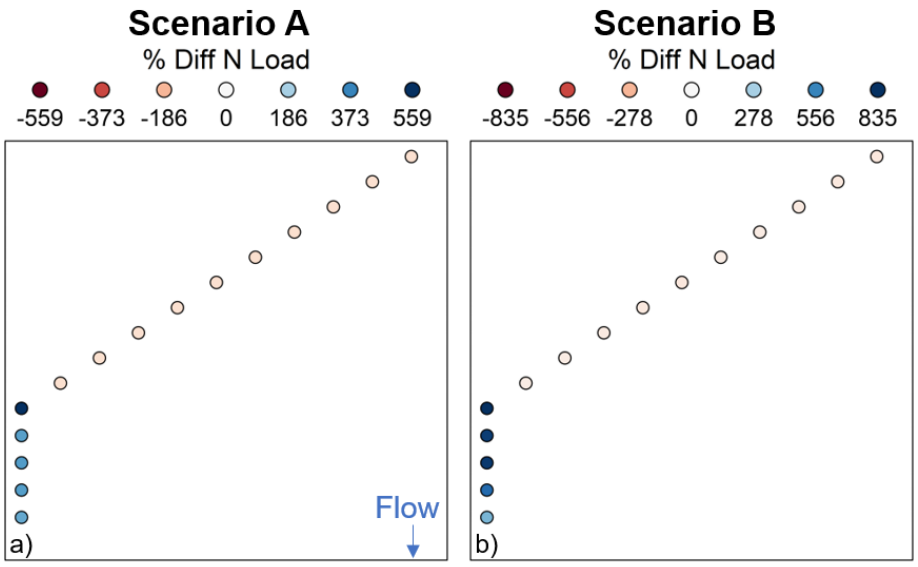

Figure C13. Spatial distribution of percent differences in nitrogen loading between each incision scenario and the base case at the dairy farm, as predicted by the site-specific models. Each dot is a cross-section, spaced 10 m apart. Flow is moving from top to bottom.